ITK IS A CRITICAL REGULATOR OF SPATIOTEMPORAL

LOCALIZATION AT THE IMMUNOLOGICAL SYNAPSE

APPROVED BY SUPERVISORY COMMITTEE

Christoph Wülfing, Ph.D.

J. David Farrar, Ph.D.

Michael Rosen, Ph.D.

Zhijian J. Chen, Ph.D.

ITK IS A CRITICAL REGULATOR OF SPATIOTEMPORAL LOCALIZATION AT THE IMMUNOLOGICAL SYNAPSE

by

KENTNER LEROY SINGLETON

DISSERTATION

Presented to the Faculty of the Graduate School of Biomedical Sciences

The University of Texas Southwestern Medical Center at Dallas

In Partial Fulfillment of the Requirements

For the Degree of

DOCTOR OF PHILOSOPHY

The University of Texas Southwestern Medical Center at Dallas

Dallas, Texas

April, 2010

ITK IS A CRITICAL REGULATOR OF SPATIOTEMPORAL LOCALIZATION AT THE IMMUNOLOGICAL SYNAPSE

KENTNER LEROY SINGLETON, Ph.D.

The University of Texas Southwestern Medical Center at Dallas, 2010

Supervising Professor: Christoph Wülfing Ph.D.

The activation of T cells by antigen presenting cells (APCs) is an important step in the initiation of the adaptive immune response. Itk, a member of the Tec family of non-receptor protein tyrosine kinases, is important for T cell activation – $Itk^{-/-}$ $CD4^{+}$ T cells are hyporesponsive, displaying decreased calcium flux, proliferation, and IL2 production compared to wildtype T cells. The mechanism by which Itk mediates this effect is not fully elucidated. Here we show that Itk is a key regulator of spatiotemporal localization of receptors and proximal signaling intermediates at the T cell / APC

interface. As part of this organizational regulation, we found that Itk, through the recruitment of SLAT, mediates activation of Cdc42 at the center of the interface, which is critically required for actin polymerization. We show that targeting activated Cdc42 to the center of the interface restores actin polymerization in the $Itk^{-/-}$ T cell while the addition of constitutively active Cdc42 to the entirety of the interface cannot. These results provide beginnings of a mechanistic explanation of how Itk both regulates the actin cytoskeleton and acts to amplify T cell signaling. These results further demonstrate that control of protein localization at the immunological synapse can be the critical determinant in protein function and that the center of the interface is a site of active signaling.

TABLE OF CONTENTS

CHAPTER III: RESULTS

LIST OF PUBLICATIONS

1. Lin MT, Gooley T, Hansen JA, Tseng LH, Martin EG, **Singleton KL**, Smith AG, Mickelson EM, Petersdorf EW, Martin PJ. Absence of statistically significant correlation between disparity for the minor histocompatibility antigen-HA-1 and outcome after allogeneic hematopoietic cell transplantation. *Blood*. 2001; 98(10):3172-3

2. Tseng LH, Chen PJ, Lin MT, **Singleton KL**, Martin EG, Yen AH, Martin PJ, Hansen JA. Simultaneous genotyping of single nucleotide polymorphisms in the IL-1 gene complex by multiplex polymerase chain reaction-restriction fragment length polymorphism. *J Immunol Methods*. 2002; 267(2):151-6

3. Tseng LH, Chen PJ, Lin MT, **Singleton KL**, Martin EG, Yen AH, Martin PJ, Hansen JA. Simultaneous genotyping of single nucleotide polymorphisms in the IL-6, IL-10, TNFalpha and TNFbeta genes. *Tissue Antigens*. 2002; 59(4):280-6

4. **Singleton KL***, Parvaze N*, Dama KR, Chen KS, Jennings P, Purtic B, Sjaastad MD, Gilpin C, Davis MM, Wülfing C. A large T cell invagination with CD2 enrichment resets receptor engagement in the immunological synapse. *J Immunol*. 2006; 177(7):4402-13 *Equal contribution

5. **Singleton KL***, Roybal KT*, Sun Y, Fu G, Gascoigne NR, van Oers NS, Wülfing C. Spatiotemporal patterning during T cell activation is highly diverse. Sci Signal. 2009; 2(65):ra15. PMCID: 2694444 *Equal contribution

LIST OF FIGURES

LIST OF TABLES

LIST OF ABBREVIATIONS

Å – Ångström ($1x10^{-10}$ meters)

α- – Anti (e.g. α-CD3)

αPIX - p21-activated kinase-interactive exchange factor

APC – Antigen presenting cell

Arp3 – Actin related protein 3

Btk - Bruton's tyrosine kinase

BSA – Bovine serum albumin

caCofilin – Constitutively active Cofilin

CCD – Charge coupled device

CD – Cluster of differentiation (e.g. CD3)

CD2AP – Cluster of differentiation 2 associated protein

Cdc42 – Cell division control protein 42 homolog

Cdc42ca – Constitutively active cell division control protein 42 homolog

Cin85 – Cbl-interacting protein of 85 kDa

CPα1 – F-Actin capping protein alpha 1

CRAC – Calcium release-activated calcium

CTLA4 – Cytotoxic T-lymphocyte antigen 4

cSMAC – Central supramolecular activation complex

CXCR4 - CXC chemokine receptor 4

DAG – 1,2-diacylglycerol

DIC – Differential interference contrast

DMEM – Dulbecco’s modified Eagle's medium

EBV – Epstein-Barr virus

ELISA – Enzyme-linked immunosorbent assay

ER – Endoplasmic reticulum

FBS – Fetal bovine serum

GEF – Guanine nucleotide-exchange factor

GFP – Green fluorescent protein

HS1 – Hematopoietic lineage cell-specific protein 1

ICAM1 – Inter-cellular adhesion molecule 1

ICOS-L – Inducible T-cell co-stimulator ligand

IgG – Immunoglobulin G

IL – Interleukin (e.g. IL2)

IP_3 – Inositol 1,4,5-trisphosphate

IP_3R – Inostiol 1,4,5-trisphosphate receptor

IPTG – Isopropyl-beta-D-thogalactopyranoside

ITAM – Immunoreceptor tyrosine-based activation motif

ITSN2 – Intersectin 2

Itk – IL2-inducible T-cell kinase

K390R – Itk mutant where the kinase domain is non-functional

kDa – kilo Dalton (also kD)

LAT – Linker of activated T cells

Lck – Leukocyte-specific protein tyrosine kinase

LFA – Lymphocyte function-associated antigen

MAPK – Mitogen-associated protein kinase

MHC – Major histocompatibility complex

MLCK – Myosin light chain kinase

MTOC – Microtubule-organizing center

mRNA – Messenger ribonucleic acid

NF-κB - Nuclear factor kappa-light-chain-enhancer of activated B cells

NFAT – Nuclear factor of activated T cells

PBS – Phosphate buffered saline

PH – Pleckstrin homology

$PI_{(3,4,5)}P_3$ – Phosphatidylinositol (3,4,5) trisphosphate

$PI_{(4,5)}P_2$ – Phosphatidylinositol (4,5) bisphosphate

PI3K – Phosphoinositide 3-kinase

PIP5kγ1 - Phosphatidylinositol 4-phosphate 5-kinase gamma 1

PKC – Protein kinase C

PLC – Phospholipase C

PMA – Phorbol myristate acetate

PRR – Proline rich region

PTEN – Phosphatase and tensin homology

pSMAC – Peripheral supramolecular activation complex

PxxP – Proline-X-X-Proline

R265K – Itk mutant where the SH2 domain is not able to bind targets

Rac1 - Ras-related C3 botulinum toxin substrate 1

RhoA - Ras homolog gene family, member A

Rlk – Resting lymphocyte kinase

RPMI – Roswell Park Memorial Institute medium

SDS-PAGE – Sodium dodecyl sulfate polyacrylamide gel electrophoresis

SH2 – Src homology 2

SH3 – Src homology 3

shRNA – small hairpin RNA

SKAP55 – Src kinase-associated phosphoprotein of 55 kDa

SLAT – SWAP-70-like adaptor protein of T cells

SLP76 – SH2 domain containing leukocyte protein of 76kD

SMAC – Supramolecular activation complex

STIM1 – Stromal interaction molecule 1

TCR – T cell receptor

TH – Tec homology

Th1 – T helper 1

Th2 – T helper 2

TIRF – Total internal reflection fluorescene

WASP – Wiskott-Aldrich syndrome protein

WAVE2 – WASP-family verprolin-homologous protein

Y – Tyrosine (e.g. Y180)

Zap70 – Zeta-chain-associated protein kinase 70

CHAPTER I

INTRODUCTION

The Immunological Synapse

T cell activation by an antigen presenting cell (APC) in response to foreign antigens is critical for the formulation of the adaptive immune response. This activation event occurs by cell-cell contact between the T cell and APC, where a tight interface forms between the two cells. Originally, little consideration was given spatial organization at the interface, as it was assumed that receptor-receptor interactions were freely distributed across the junction. However, in 1997 and 1998 Abraham (Avi) Kupfer showed that the T cell interface was organized in a concentric manner, with the T cell receptor (TCR) and Protein kinase C θ (PKCθ) being clustered at the center of the interface, and Lymphocyte function-associated antigen 1 (LFA-1) and Talin being preferentially recruited in a surrounding ring at the periphery of the interface (1, 2). These patterns of localization were termed supramolecular activation complexes (SMACs), with the central cluster called the central SMAC (cSMAC) and the surrounding peripheral ring called the peripheral SMAC (pSMAC). In its entirety, this structure was later termed the immunological synapse by Michael Dustin (3). Since the original publication the other receptors and signaling intermediates have been individually examined in isolation and have been found to fall within the generalized cSMAC / pSMAC classification; actin is perhaps the most famous and is considered a defining feature of the pSMAC. Formation of the cSMAC is an actin dependent process

as treatment with cytochalasin D, an actin polymerization inhibitor, blocks formation of the cSMAC and inhibits T cell activation (3).

The role of the cSMAC in T cell signaling is an area of open debate. One proposed function is to enhance weak signaling by low-affinity interactions though the concentration of signaling intermediates, promoting efficient signaling by increasing the likelihood of protein-protein interactions occurring (3, 4). In addition to clustering proximal signaling intermediates, the cSMAC may also serve to enhance signaling by promoting the activation of TCRs recognizing endogenous peptide-MHC complexes (5). The cSMAC contains not just antigenic peptide-MHC complexes but includes MHCs bound to self peptides, with a preferential recruitment of endogenous peptides that have a higher avidity for the TCR (6). This may allow for the CD4 dependent formation of 'pseudodimers' of MHCs expressing endogenous and agonist peptides. The pseudodimer model suggests that the TCR engaged with antigenic peptide-MHC complex would recruit Leukocyte-specific protein tyrosine kinase (Lck), allowing for the concurrent phosphorylation of the neighboring TCR. As the half-life of the TCR bound to the endogenous peptide-MHC complex is short, it would allow for the rapid turnover of TCRs, promoting the phosphorylation and activation of numerous TCRs (5, 7). The increased concentration of TCRs clustered at the cSMAC would likely facilitate this process. Experimental support for the idea that the cSMAC supports signaling come with the observation that for low-affinity agonist peptides, cSMAC formation is required for the integration of TCR and CD28 signaling pathways, promoting enhanced interleukin 2 (IL2) production (8).

Another proposed role of the cSMAC is to terminate signaling at the T cell / APC interface. Using total internal reflection fluorescence (TIRF) microscopy to visualize T cells activated on supported bilayers, it has been demonstrated that microclusters of TCR complexes continuously formed in the periphery of the interface and moved in an actin dependent fashion to the center to form the cSMAC (9). Blocking the formation of new microclusters by the addition of a blocking antibody extinguished calcium signaling after the formed microclusters had localized to the cSMAC. It was later shown that phosphorylated Lck and Zeta-chain-associated protein kinase 70 (Zap70) was present in the peripheral microclusters, but not at the cSMAC (9-11). These findings, in conjunction with the observation that formation of the cSMAC is not always required for T cell activation (8), lend to the hypothesis that the role of the cSMAC is to mediate the cessation of signaling.

The two hypotheses, while seemingly in conflict, are likely a product of the experimental system used. Experiments that lend favor to the cSMAC being a site of active signaling tend to use APCs. In contrast, most of the experiments suggesting that the cSMAC is a site of signal termination use supported lipid bilayers. The value of supported lipid bilayers and TIRF microscopy in studying the immunological synapse cannot be understated; however, it's important when evaluating the data to understand the caveats. Supported lipid bilayers are composed of a phospholipid bilayer supported by glass with a 10–20 Å layer of trapped water between the substrate and the bilayer to maintain fluidity of the membrane (12). These bilayers, however, are extremely ridged; lacking the flexibility and three dimensional dynamics of the APC membrane. As a result, certain physical events seen in T cell / APC interactions, such as the T cell

invagination event, have not been reported when using the lipid bilayer system (13). Another caveat is that, being man-made, the ligands presented on the surface of the bilayer tend to consist of either α-CD3 antibody alone (14, 15), MHC and ICAM1 (9-11, 16-18), or the combined set of MHC, CD80 (B7.1), and ICAM1 (19); other costimulatory receptors such as B7.2, ICOS-L, and LFA-3 are notably absent, which could affect the dynamics of the immunological synapse (20, 21). Importantly, CD80 preferentially binds to CTLA-4 (Cytotoxic T-lymphocyte antigen 4) which is an inhibitor to T cell signaling; CD28 binds to CD86 (B7.2) (22). The lack of costimulatory stimulation may account for why recruitment of TCRζ to the center of the interface occurs within 20 seconds when using APCs (Figure 18) (4), but takes over 4 minutes when using the lipid bilayer system (3, 9-11). The final caveat is that the supported lipid bilayers containing MHC are typically seeded at a density of 200 MHC molecules per μm^2 and peptide loaded at a concentration of 100μM agonist peptide (14). In contrast, B cell lymphomas have a surface density of ~300 MHC molecules per μm^2 (calculated from $1.1x10^5$ MHC on a B cell, with an average diameter of 10μm (23)) and, in this study and other studies conducted by the Wülfing lab, are peptide loaded at a concentration of 10μM agonist peptide (4). With virtually all of the MHC peptide loaded with no endogenous peptides expressed on the supported bilayers, or through the use of αCD3 as TCR agonists, the supported bilayers would represent extreme activation of the T cell receptor. It seems unlikely that the T cell would need to enhance signaling and may instead engage in feedback loops to down-regulate signaling; Increasing levels TCR phosphorylation has been shown to enhance TCR down-regulation and degradation (24).

In all likelihood, both hypotheses are correct. The TCR likely engages with peptide-MHC at the periphery of the cell, possibly forming microclusters, and proceeds to migrate to the center of the interface through an actin-dependent process. The cSMAC, in turn, acts as a buffer by either retaining the TCR to help propagate further signaling, or remove it from the interface in an attempt to down-regulate signal strength depending on the current conditions.

IL2-Inducible T-Cell Kinase

IL2-inducible T-cell kinase (Itk) is a non-receptor protein tyrosine kinase that plays an important role in regulation of T cell receptor (TCR) induced signaling and effector function. Itk is a member of the Tec family of non-receptor tyrosine kinases, which includes Tec, Btk, Rlk, and Bmx. Of the Tec family members, only Itk, Tec, and Rlk are expressed in T cells, with Itk being the most prominent member; Rlk mRNA levels are 3 to 10-fold lower than Itk, with Tec being 100-fold lower in naïve T cells (25). Upon T cell activation, Itk and Tec expression levels are increased while Rlk expression is significantly reduced; however upon Th1 polarization, Itk levels drop and Rlk expression is reestablished (26-28). T cells from mice lacking Itk are hyporesponsive, with reduced proliferation, impaired calcium flux, decreased effector cytokine production in response to TCR stimulation (26, 29-36). Treatment with phorbol myristate acetate (PMA) and ionomycin rescues these phenotypes, indicating that the role of Itk primarily resides within the proximal signaling network (32-34). Unlike Lck or Linker of Activated T cells (LAT), which are required for TCR signaling to proceed, Itk instead

acts as an analog regulator that amplifies TCR signaling (36, 37). In accordance with the expression pattern, Itk deficiency more severely affects Th2 polarized T cells and $Itk^{-/-}$ mice are consequentially highly susceptible to pathogens that require Th2 mediated clearance (30, 38, 39). Importantly, however, mice lacking Itk are also highly resistant to both the acute and late phases allergic asthma, prompting the development of Itk inhibitors for possible therapeutic use (40-51). Itk is expressed in humans, with shRNA mediated Itk knockdown of human peripheral blood T cells showing reduced actin polymerization similar to the $Itk^{-/-}$ murine T cells (52); other $Itk^{-/-}$ phenotypes were not examined. Humans with Itk deficiency have been described, with both patients succumbing to EBV-driven lymphoproliferative disease (53). Additionally, a genomic analysis revealed that single nucleotide polymerphisms within *Itk* correlated with patients that experience seasonal allergic rhinitis (54). Together this identifies Itk as an important area of study, both for our understanding of T cell signaling and as significant therapeutic target.

Structurally, Itk is composed of a Pleckstrin homology (PH) domain at the amino-terminus, followed by a Tec homology (TH), Src homology 3 (SH3), Src homology 2 (SH2), and a kinase domain (PH-TH-SH3-SH2-Kinase). The PH domain preferentially binds to phosphatidylinositol (3,4,5) trisphosphate ($PI_{(3,4,5)}P_3$), mediating the Phosphoinositide 3-kinase (PI3K) dependent recruitment of Itk to the cell membrane and activation of Itk (3, 55-59). Accordingly, Itk is also regulated by Phosphatase and tensin homolog (PTEN), which dephosphorylates $PI_{(3,4,5)}P_3$ to phosphatidylinositol (4,5) trisphosphate ($PI_{(4,5)}P_2$); for this reason the Jurkat cell line is a poor model for Itk studies as it is deficient in PTEN, resulting in constitutive membrane association of Itk (60). In

addition to regulating localization, the PH domain also plays an important, though undefined, role in Itk activation. The replacement of the PH domain with an alternate membrane localization motif, such as a myristolyation sequence, results in Itk that is localized at the plasma membrane but cannot be activated (59). The TH domain is only found in the Tec family kinases and features a C-terminal Proline rich region (PRR) which mediates both inter- and intra-molecular protein-protein interactions (61). The Src homology 3 (SH3) domain, which binds to PRRs, can associate intramolecularly with the TH domain, folding Itk to keep it in an inactive state (62-69). The SH3 domain contains a conservied Y180, which upon autophosphorylation disrupts the association with the PRR (63, 70, 71). The SH2 domain mediates the interaction between tyrosine phosphorylated proteins. The kinase domain is activated through phosphorylation of Y512 by Lck (58, 72).

Following TCR recognition of an activating peptide-MHC complex, Lck phosphorylates the CD3 immunoreceptor tyrosine-based activation motifs (ITAM), allowing for the recruitment of Zeta-chain-associated protein kinase 70 (Zap70). Zap70 is phosphorylated and activated by Lck, which in turns phosphorylates LAT and SH2 domain containing leukocyte protein of 76kDa (SLP76) (73, 74). Concurrently, Lck also activates PI3K, allowing for the phosphorylation of $PI_{(4,5)}P_2$ to $PI_{(3,4,5)}P_3$, which recruits Itk to the plasma membrane where it is activated through phosphorylation by Lck. Itk activation by Lck may be assisted by CD28, with Itk binding to the CD28 proximal PxxP motif and Lck recruitment to the CD28 distal PxxP motif (75). Upon Itk activation, the SH2 and SH3 domains bind to SLP76 at tyrosine 145 and the PRR respectively, prolonging the activation state (58, 76-78). Itk, bound to SLP76, acts as an adaptor

protein assisting in the formation and stabilization of the LAT/SLP76/PLCγ1 signalosome (79). Within the signalosome, Itk has been shown to mediate the recruitment of Vav1, which in turn optimizes SLP76 phosphorylation, LAT recruitment, and Itk activation (52, 80, 81). One function of Itk in the signalsome is the activation of PLCγ1 as Itk has been shown to bind to and stabilize PLCγ1 within the signalsome, allowing for Itk mediated activation of PLCγ1 through phosphorylation at Y783 (33, 34, 71). While Itk deficient T cells show reduced PLCγ1 phosphorylation, a review of the raw data presented in the literature shows that the pool of phosphorylated PLCγ1 is still quite large indicating that Itk is not the sole activator of PLCγ1 (33, 34). PLCγ1 hydrolyzes $PI_{(4,5)}P_2$ into the second messengers diacylglycerol (DAG) and inositol triphosphate (IP_3). DAG activates plays an important role the activation of the mitogen-associated protein kinase (MAPK) pathway (Reviewed in (82)). DAG also plays an important role in proximal signaling through the recruitment of Protein kinase C θ (PKCθ) to the plasma membrane and subsequent activation (83). PKCθ activation results in the downstream activation and nuclear import of the NF-κB transcription factor, resulting in transcriptional regulation, including IL2 production. IP_3, in turn, binds to Inositol 1,4,5-trisphosphate receptors (IP_3R) on the endoplasmic reticulum, leading to release of the intracellular calcium stores. This release of calcium activates the Calcium release-activated calcium (CRAC) channels, allowing for the sustained influx of extracellular calcium (reviewed in (84)). Sustained calcium flux leads to the activation of the Nuclear factor of activated T cells (NFAT) family of transcription factors resulting in transcriptional regulation, including the production of IL2. Although $Itk^{-/-}$ T cells show a

substantial reduction in the production of IP_3, the defect in calcium flux is not in the initial release of intracellular calcium stores, which is normal, but in the secondary influx of extracellular calcium via the CRAC channels (34). While the mechanism behind this observation is not known, it has been proposed that the reduced IP_3 levels in the $Itk^{-/-}$ T cell may not be sufficient to maintain depletion of intracellular stores, which is required for prolonged triggering of CRAC channels (85, 86).

In addition to having a direct effect on signaling, Itk has been shown to play a role in actin polymerization at the immunological synapse (52, 87, 88). Jurkat cell lines and primary human peripheral T cells in which Itk was knocked down using shRNA displayed abrogated α-CD3 mediated actin polymerization at the site of stimulation (52). The same observation was noted in fixed cell couples of wildtype and $Itk^{-/-}$ primary $CD4^+$ T cells specific for pigeon cytochrome C (AND TCR transgenic) when stimulated by peptide loaded APCs (88). Actin polymerization was shown to be mediated by the Itk SH2 domain, and not the kinase domain. Over expression of SH2 binding deficient Itk in Jurkat cells resulted in blocking actin polarization in response to α-CD3 stimulation; over expression of kinase-dead Itk had no effect (52, 87). The cessation of actin polymerization in $Itk^{-/-}$ T cells correlated with a failure to activate Cdc42 at the activation interface in response to TCR stimulation. It was further shown that $Itk^{-/-}$ T cells similarly did not recruit Vav1, a GEF that is able to activate Cdc42, to the site of TCR activation (52, 88). Consistent with these results, SLP76 was not efficiently co-immunoprecipitated with Vav1 in Itk specific shRNA knockdown T cells, suggesting that Itk may act as an adaptor to stabilize the localization of Vav1 to the LAT / SLP76 signalosome (52). Together, this suggests that Itk plays an important role in actin polymerization at the

immunological synapse through the recruitment of Vav1, which activates Cdc42, allowing for WASP mediated actin polymerization.

Conclusion

Itk is an integral protein within the T cell proximal signaling network. Others have demonstrated that a significant role of Itk is to act as an analog amplifier for TCR induced signaling, leading to proper T cell effector function. How Itk accomplishes this is not understood. Work presented in this thesis demonstrates that Itk is a critical regulator of the spatiotemporal localization of receptors and proximal signaling intermediates at the T cell / APC interface. We propose that Itk mediated spatial coordination at the immunological synapse, particularly in the formation of the cSMAC, serves as the mechanism by which Itk modulates T cell signaling.

CHAPTER II

METHODS

Cells

Unless otherwise noted, T cells came from 6-8 week old wildtype or $Itk^{-/-}$ BALB/c TCR-$C\alpha^{-/-}$ DO11.10 TCR transgenic mice, which recognize the OVA peptide fragment 323-339 (OVA323-339 – ISQAVHAAHAEINEAGR) in the context of I-A^d (32, 89). Mice were maintained in the pathogen-free animal care facility at the University of Rochester Medical Center (Rochester, NY). $Itk^{-/-}$ and wildtype T cell suspensions were generated by the laboratory of Dr. Deborah Fowell (University of Rochester Medical Center; Rochester, NY), packed on ice, and shipped via Fed Ex Priority Overnight. Upon receipt of the cell suspension, the cells were immediately centrifuged and resuspended to a concentration of $4x10^6$ cells per mL (rounding down to the nearest mL). OVA peptide was added to a concentration of 3μM and the cells were aliquoted at one mL per well on a 24 well plate. The plates were stored in a 37°C humidified incubator until retroviral transduction the next day.

T cells from B10.BR 5C.C7 TCR transgenic mice were used to generate Figures 3B and 4. 5C.C7 T cells recognize the MCC peptide fragment 88-103 (ANERADLIAYLKQATK) in the context of I-E^k. T cells were isolated from the lymph nodes of 6-8 week old mice maintained in the pathogen-free animal care facility at the University of Texas Southwestern Medical Center (Dallas, TX). The use of these mice

has been reviewed and approved by the University of Texas Southwestern Institute Animal Care and Use Committee.

APCs using for imaging were the A20 B cell lymphoma cell line for the DO11.10 T cells and the CH27 B cell lymphoma cell line for the 5C.C7 T cells.

Retroviral Transduction

The 44 different GFP labeled sensors used in this experiment (Table 1) were expressed from a Moloney murine leukemia virus-derived retroviral expression vector (90). Retroviral supernatants for transduction were generated using the Phoenix helper-free retrovirus producer cell line (originally from the Garry Nolan lab). Briefly, the Phoenix cells were transfected with the plasmid of choice by calcium phosphate transfection on day 0. Media was exchanged on day 1 with fresh media (DMEM containing 4.5g/L glucose, L-Glutamine, and sodium pyruvate (Fisher catalog number 10-013-CV); 10% FBS; 100 IU/mL penicillin; 100μg/mL streptomycin; non-essential amino acids). On day 2 the T cells were received and plated as described previous. The T cells were transduced with the retroviral supernatant on day 3 by spinfection (centrifuged at 1000g for 2 hours). On day 4 the retroviral supernatant was removed from the T cells and replaced with fresh media (RPMI, 10% FBS, 0.05μM β-mercaptoethanol, 100 IU/mL penicillin, 100μg/mL streptomycin, 0.05 U/mL IL2). The cells were split as necessary. On day 7 the T cells were sorted based on GFP expression using flow cytometry. Sort gates were set to collect cells with a GFP expression 1 – 1.5

logs above the negative population. The sorted T cells were imaged either that afternoon or the next morning.

Th2 Polarization

T cells were Th2 polarized by the addition of 100 U/mL IL4, 10% R46A2 Hybridoma supernatant (contains α-IFNγ; Gift from Dr. David Farrar), and 10% ToshαmIL12 Hybridoma supernatant (contains α-IL12; Gift from Dr. David Farrar) to the T cell media on day 2 (upon receipt of the T cells) and day 4 (when the retroviral supernatant was exchanged with fresh media).

Image Acquisition

The interaction between primed, primary DO11.10 T cells and 10μM OVA peptide incubated A20s were imaged in PBS containing 10% fetal bovine serum, 1mM calcium, and 0.5mM magnesium at 37°C in 1536 or 384 well glass bottom plates (MatriCal MGB111-1-2 or MGB101-1-2-HG). Imaging experiments ran for 15 minutes, with 1 differential interference contrast (DIC) and 21 fluorescent images acquired every 20 seconds. The 21 fluorescent images were taken at 1μM intervals along the z-plane, for a total height of 20μM, using a 40 x/NA = 1.3 oil objective. Rapid focusing across the z-plane was accomplished using a piezoelectric z-motor. Images were acquired using a MicroMax cooled charge coupled device (CCD) camera (Princeton Instruments) with a 200 millisecond exposure captured at a 1300 x 1030 pixel resolution (6.7 x 6.7 μm pixel

size) using 2 x 2 binning. All 21 images of a z stack were streamed into the computer memory to maximize speed of image acquisition, with a single z stack acquired in 7 seconds.

Imaging Analysis

Cell coupling was defined using the DIC images, without regard for the fluorescent images. The formation of a tight cell couple was defined as either the first time point with a fully spread T cell / APC interface, or 40 seconds after first membrane contact, whichever occurred first. The formation of a tight cell couple was internally referenced as time = 0 seconds for each cell, allowing for the comparison of cell couples that formed at different times throughout the experiment. More than 90% of the cell couples formed a fully spread interface upon first contact or within 20 seconds. Rare T cells that formed interfaces with multiple APCs were excluded from analysis.

Image analysis was executed using the Metamorph software package. Fluorescent images were analyzed at 12 time points, from -40 seconds to 2 minutes at 20 second intervals, and then at 3, 5, and 7 minutes. Pattern analysis was conducted by evaluating the raw 3D stacks and maximum-type three-dimensional reconstructions for each cell at each time point. Fluorescence intensities were displayed as a rainbow false color scale. Accumulation at the interface was defined as a region with an average fluorescence intensity of > 1.35 times the background cellular fluorescence. Areas of interface accumulation that were contiguous with non-interface accumulation were scored as no accumulation, as it was uncertain whether the accumulation was dependent

on receptor engagement at the T cell / APC interface. Interface accumulation was classified into five mutually exclusive patterns: Central, Invagination, Diffuse, Lamellal, and Peripheral (Figure 1). Distal accumulation was scored independently of the interface pattern; a T cell could display one of the five interface patterns together with the distal accumulation. Distal accumulation was not included in the "any accumulation" category. To ensure reliability of the analysis, two investigators routinely independently analyzed the images. Data for each experimental condition were displayed as the percentage of cell couples that showed accumulation of any of the six patterns at each time point. The spatial preference index used in Figure 6 was calculated by the following formula:

$$\text{Spatial preference index} = \log\left[\frac{\%\text{ cell couples with central accumulation} + \%\text{ cell couples with diffuse accumulation}}{\%\text{ cell couples with peripheral accumulation} + \%\text{ cell couples with diffuse accumulation}}\right] \times \%\text{ cell couples with any accumulation}$$

A value of 1 or -1 indicates almost exclusive central or peripheral accumulation, respectively, whereas a value of 0 indicates a balance between central and peripheral accumulation.

STIM1 was defined as having an defined, non-interface accumulation when in a three-dimensional reconstruction, the top 25% of the fluorescence intensity was contained in 25% of the T cell diameter both parallel and perpendicular to the interface. The position of STIM1 was determined by dividing the T cell into three sections of equal length along the cellular axis parallel to T cell / APC interface. Each section was given a numerical value, with 1 being the third of the cell closest to the interface, 2 being the middle third of the cell, and 3 being the third at the distal pole. If STIM1 was fully contained within one of the sections, it was given a score of 1, 2, or 3 depending on

which third STIM1 resided. If STIM1 was positioned on one of the internal section boundaries, it was scored a 1.5 or 2.5.

Tat Fusion Proteins

Tat fusion proteins were expressed in BL21(DE3) Escherichia coli at room temperature in the presence of 0.4mM IPTG (Isopropyl-beta-D-thiogalactopyranoside) and 4% ethanol (to reduce inclusion body formation). Bacteria were lysed under native conditions using a French Press in the presence of Lysis Buffer (4x PBS, 0.01% IGEPAL, 10% Glycerol, 10mM Imidazole, 1mM $MgCl_2$, 0.01% IGEPAL, 0.2mg/mL Lysozyme, 0.14% β-mercaptoethanol, and protease inhibitors). The tat fusion proteins were purified using Nickel-NTA immobilized metal affinity chromatography. After binding to the column, the protein was washed once with Lysis Buffer, twice with Wash Buffer (4x PBS, 20mM Imidazole, 1mM $MgCl_2$, 0.14% β-mercaptoethanol), and removed from the column Imidazole elution (4x PBS, 250mM Imidazole, 1mM $MgCl_2$, 0.14% β-mercaptoethanol). All buffers were 1 pH unite removed from the protein's isoelectric point with a pH or 8 when possible due to maximum His tag binding. Purity and concentration was determined by SDS-PAGE (Figure 2).

To use the tat fusion proteins, T cells were incubated for 30 minutes at 37°C in the presence of the desired concentration of tat-protein prior to being used for imaging. Tat fusion proteins were included in the buffer at the same concentration during image acquisition of T cell / APC interactions.

Activated Cdc42 Pull-down

Cellular levels of activated Cdc42 was determined using the EZ-Detect Cdc42 Activation Kit (Pierce; Catalog number 89857) according to the instructions provided by the manufacturer. T cells were activated using 10μg/mL α-CD3ε (Clone 145-2C11; BD Pharmingen catalog number 553057), 10μg/mL α-CD28 (Clone 37.51; BD Pharmingen catalog number 553295), 5μg/mL α-Syrian Hamster IgG (Clone G94-56; BD Pharmingen catalog number 554006 – cross-links αCD3), and 5μg/mL α-Armenian Hamster IgG (Clone G192-1; BD Pharmingen catalog number 554024 – cross-links αCD28) for 5 minutes at 37°C.

IL2 Production Assay

25,000 primed, primary T cells and 50,000 10μM peptide loaded A20 APCs were cultured in a 96-well round bottom plate for 16 hours at 37°C in a total volume of 200μL. Supernatant was collected and analyzed for IL2 content using BD OptIEA Mouse IL-2 ELISA Assay Kit (BD; Catalog number 555148). Supernatant from $Itk^{-/-}$ T cells were analyzed undiluted while supernatant from wildtype cells were diluted 1:10 to stay within the linear range of the standard curve.

Statistical Analysis

Statistical analysis examining the differences in percent expression of a localization phenotype between experimental conditions was calculated using a 2-sample proportion z-test. Statistical analysis comparing interface intensity was calculated using the Student's *t*-test. Values of $p < 0.05$ were taken as significant.

Signaling Protein	Design
Actin	GFP-Actin
αPIX	GFP-αPIX
Arp3	Arp3-GFP
CD2	CD48-GFP
CD28	B7.2-GFP
CD2AP	GFP-CD2AP
CD3ε	CD3ε-GFP
Active Cdc42	WASP.GBD-GFP-caax
tat-Cdc42ca	tat-GFP-Cdc42ca
Cin85	GFP-Cin85
Cofilin	Cofilin-GFP
Coronin	Coronin-GFP
CPα1	CPα1-GFP
CXCR4	CXCR4-GFP
HS1	HS1-GFP
Itk	Itk.PH.TH.SH3.SH2-GFP
ITSN2	ITSN2-GFP
LAT	LAT-GFP
Lck	Lck-GFP
LFA-1	ICAM1-GFP
Ly108.1	LY108.1-GFP
MLCK	MLCK-YFP-
Myosin1c	Myosin1c-GFP
PI3kinase	PI3k.SH2.interSH2.SH2-GFP
$PI_{(4,5)}P_2$	GFP-PLCδ.PH
$PI_{(3,4,5)}P_2$	GFP-Cytohesin.PH
PIP5kγ1	GFP-PIP5Kγ1
PKCη	PKCη-GFP
PKCθ	PKCθ.GFP
PLCγ1	PLCγ1.PH.SH2.SH2-GFP
Active Rac1	POSH.GBD-GFP-caax
Active RhoA	Rhotekin.GBD-GFP-caax
SKAP55	GFP-SKAP55
SLAT	GFP-SLAT
STIM1	STIM1-YFP-CFP
TCRζ	TCRζ-GFP
Tec	Tec.PH.TH.SH3.SH2-GFP
tat-Tec.PH.TH.SH3	tat-GFP-Tec.PH.TH.SH3
tat-Tec.PH.TH.SH3-Cdc42ca	tat-GFP-Tec.PH.TH.SH3-Cdc42ca
Themis	Themis-GFP
Vav1	Vav1-GFP
WASP	WASP-GFP
WAVE2	WAVE2-GFP
Zap70	Zap70.2SH2-GFP
tat-Zap70.2SH2-Cdc42ca	tat-Zap70.2SH2-GFP-Cdc42ca

Table I: Sensors Used for the Analysis of Spatiotemporal Localization. The left column lists the sensors used in this study. The right hand column lists the design of sensor. GFP positioning indicates whether the sensor is tagged on the c-terminal end, n-terminal end, or internally within the protein. If the full protein is used, no specific domain structure is provided. If a partial protein is used the recruitment domains used are listed.

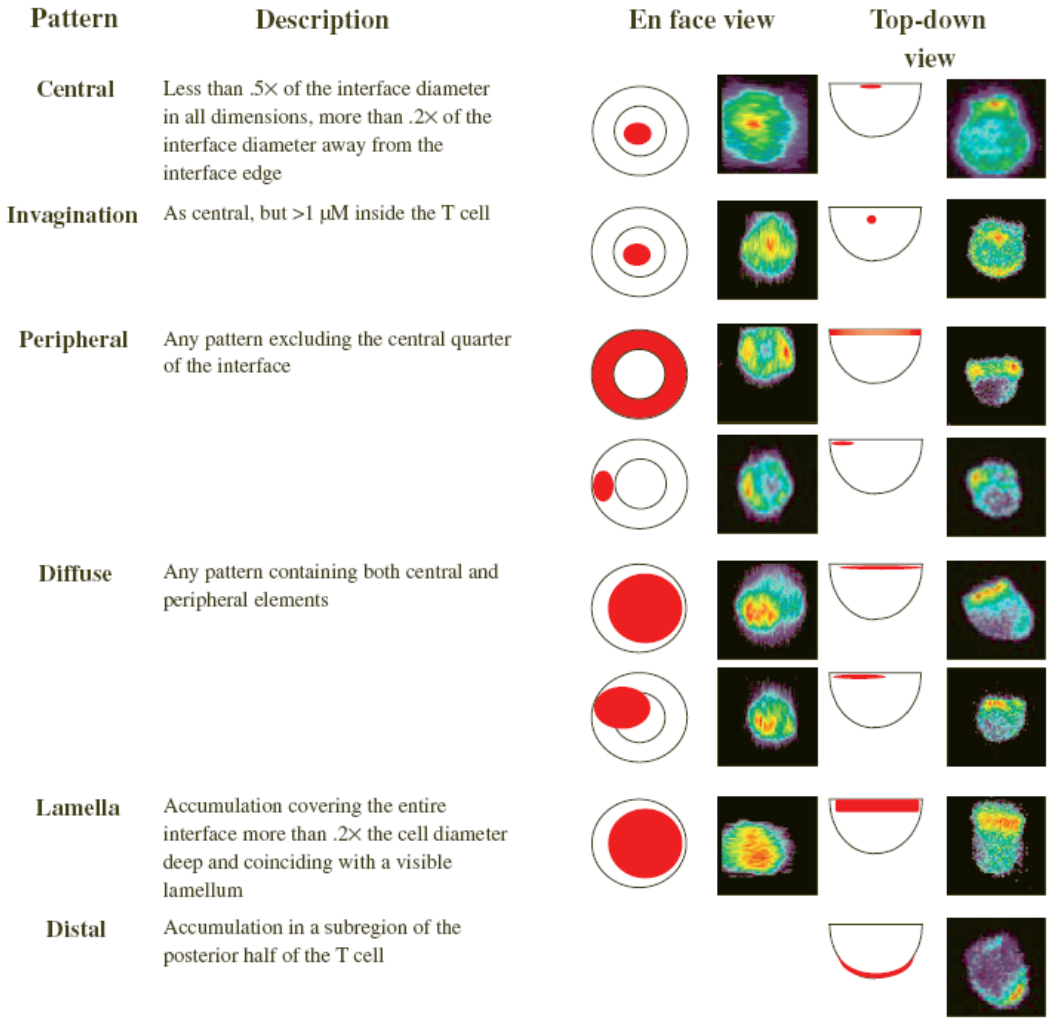

Figure 1: Spatiotemporal Patterns of Accumulation of Sensors. Presented are the definitions of the patterns used for analysis, as well a both a schematic and representative image. The en face view displays the T cell / APC interface as the APC would see it. In the schematics, the inner circle denotes the center of the interface while the outer circle signifies the entirety of the interface. The top-down view provides a bird's eye view of the T cell, with the APC at the top half of the image. In the schematic, the APC is not shown and would be at the top of the T cell, along the flat interface.

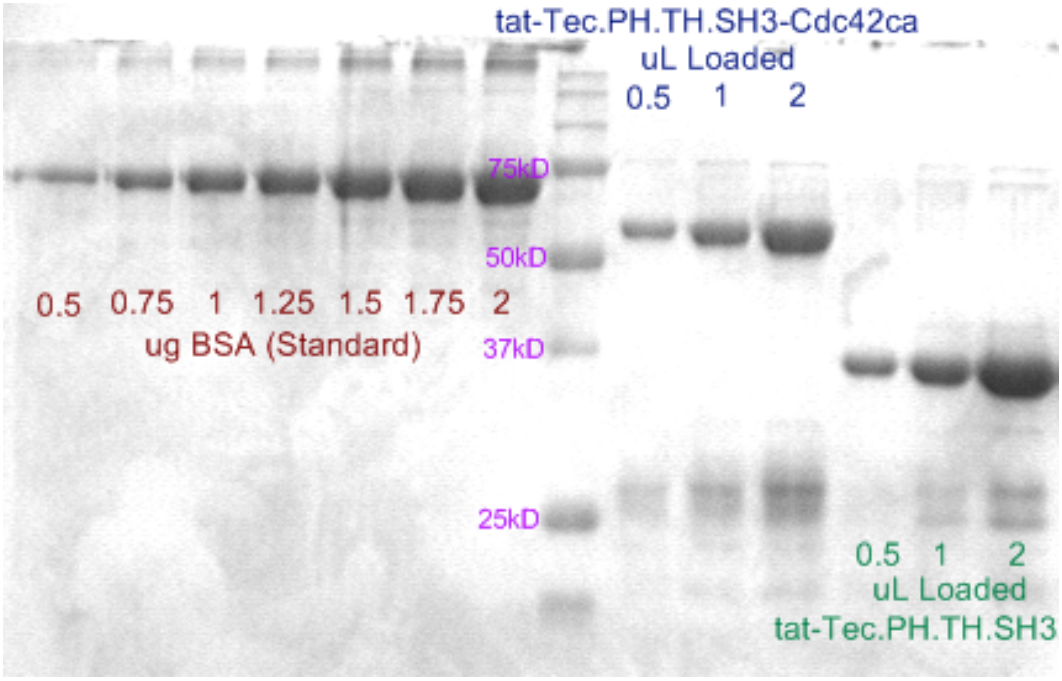

Figure 2: Purification of tat-Proteins Under Native Conditions. tat-Tec.PH.TH.SH3-Cdc42ca (blue) and tat-Tec.PH.TH.SH3 (green) were expressed in BL21(DE3) Escherichia coli, which were lysed under native conditions. The tat-proteins, which contain a 6x His tag, were purified by Nickel-NTA immobilized metal affinity chromatography with Imidazole elution. Protein purity and concentration were determined by SDS-PAGE against a BSA standard (red). The gel was converted to a digital image by scanning, and analyzed for band size and density using Metamorph software.

CHAPTER III

RESULTS

Itk Localizes to the Center of the Immunological Synapse

Itk is recruited to the T cell / APC interface upon T cell activation by an APC (27, 91). The spatial and temporal dynamics of this recruitment, however, are not known. This information would be useful as a guide for determining how to best assess of the role of Itk in T cell signaling – different hypotheses would be generated and strategies taken towards studying Itk if it were recruited to the center of the synapse early and transiently versus if it displayed a late, sustained recruitment at the periphery. To determine the subcellular localization of Itk during T cell reactivation, the Itk PH.TH.SH3.SH2 recruitment domains were fused with GFP and retrovirally transduced into primed, primary T cells isolated from DO11.10 TCR transgenic mice. Fluorescence microcopy was used to image the localization of the Itk-GFP sensor in T cells upon stimulation by A20 B cell lymphoma APCs in the presence of 10μM OVA 323-339 peptide. Itk was recruited to the center of the T cell / APC interface in 80.5% of the cell couples immediately upon formation of a cell-cell couple (designated as t=0 seconds) (Figure 3). Over the next 60 seconds, Itk spread out from the center to cover the entirety of the interface (diffuse phenotype) where it was stably maintained over the next six minutes; on average, 42.0 ± 3.7 percent of the cells displayed a central phenotype and 45.4 ± 8.7 percent of the cells displayed a diffuse phenotype. On a per-cell basis 76% of

the total cell couples switched between the central and diffuse phenotypes suggesting that Itk still maintained an overall central preference.

Itk Associates with the TCR Signaling Complex

Since the value of knowing the spatiotemporal localization of an individual protein is limited without a frame of reference, a cluster analysis was performed to determine how the localization of Itk compared with 40 other sensors. As the other sensors were analyzed in T cells isolated from the 5C.C7 TCR transgenic mouse, the localization of Itk was repeated using 5C.C7 T cells, with similar localization dynamics observed (Figure 3). To date, all sensors analyzed in both the 5C.C7 and DO11.10 TCR transgenic T cells have displayed comparable spatiotemporal localizations (4). The cluster analysis identified two distinct, highly segregated clusters, where one cluster contained proteins that were recruited to the periphery with the other cluster containing proteins that were recruited to the center of the T cell / APC interface (Figure 5). The peripheral cluster could be further broken down into two distinct groups. One group contained $PI_{(4,5)}P_2$ and displayed prominent lamellal / peripheral localization at the interface. The second peripheral cluster contained the actin regulatory proteins and was strongly localized at the periphery of the interface. The cluster containing centrally localized proteins could also be further broken down into two groups. The first of the two groups contained centrally localized proteins that were a bit more diffuse, and included proteins such as Tec, CD2AP, and Cin85. The second centrally localized group was highly central, with many of the proteins recruited to the invagination. This second

group contained the TCR signaling complex and intermediates associated with proximal TCR signaling (79); Itk was localized within this sub-cluster.

Itk displayed distinct hierarchical clustering and interface localization from two proteins of interest, Tec and Vav1. Tec is a close homolog of Itk, sharing an identical domain structure with a 57% amino acid identity and 74% amino acid homology (Figure 5). While both Itk and Tec were rapidly recruited to the center of the interface, in contrast to Itk's sustained central localization, Tec dispersed from the interface (Figure 19). Unlike Itk, Tec did not cluster with the TCR signaling complex, suggesting that the protein plays a unique role in T cell signaling. Vav1, however, displayed a preference to the periphery of the immunological synapse, clustering with the actin regulatory proteins. This was unexpected given that Itk and Vav1 have been suggested to promote the recruitment of the other in the formation of a multiprotein complex in combination with LAT and PLCγ1 (52, 92). Vav1 could still be engaged in this role, as there could be two pools of differentially regulated Vav1, one at the periphery and one at the center, with the more prominent pool being at the periphery with the actin regulatory proteins.

Itk is a Positive Regulator of Central Localization at the Immunological Synapse

To better understand the role of Itk in the T cell signaling network, the spatiotemporal localization of 12 sensors was examined in DO11.10 wildtype and Itk deficient T cells. In the wildtype cells, six were more preferentially localized at the center of the T cell / APC interface (LAT, PKCθ, PLCγ1, active Rac1, SLAT, and

TCRζ), five at periphery (actin, cofilin, myosin1c, $PI_{(4,5)}P_2$, and Vav1), and one (active Cdc42) was neutral (Figure 6).

In the $Itk^{-/-}$ T cells, all six central sensors exhibited a reduced preference for the center of the interface. LAT and PKCθ displayed an overall reduction in central localization in the $Itk^{-/-}$ T cells ($p < 0.05$ at all time points vs. wildtype), with the sensors being distributed more diffusely throughout the entirety of the interface (Figures 11 and 13). PLCγ1 localization was transient in the $Itk^{-/-}$ cells, losing the sustained central localization observed in the wildtype cells (Figure 15). Activated Rac1, which was centrally and transiently recruited to the interface in wildtype cells (87.3% ± 4.5% interface accumulation, 47.3% ± 6.7% central at 60 seconds), was significantly reduced in $Itk^{-/-}$ T cells, with < 30% of the cell couples showing interface accumulation at any time point (25.0% ± 7.2% interface accumulation, 8.3% ± 4.6% central at 60 seconds) (Figure 16). Itk appeared to play a specific role in the establishment of centrality at the interface as SLAT and TCRζ both lost the initial burst of central localization observed in wildtype T cells immediately upon APC coupling (Figures 17 and 18). SLAT and TCRζ instead increased their preference for the center of the interface over time, with TCRζ eventually approximating wildtype cells.

Notably, accumulation in the T cell invagination was mostly lost in the $Itk^{-/-}$ cells (LAT, PKCθ, TCRζ, PLCγ1). Further analysis by transmission electron microscopy of sections of fixed T cell / APC couples show invaginations in $Itk^{-/-}$ cells (3 invaginations out of 55 cell couples in the knockout cells vs. 4 invaginations out of 50 cell couples in the wildtype cells), suggesting that the reduced invagination events seen with the four

sensors lie in the recruitment to the invagination rather than a loss of the invagination event itself.

The five peripheral sensors retained the peripheral spatial preference between the wildtype and Itk$^{-/-}$ T cells (Figures 7, 10, 12, 14, and 20). The localization of actin, cofilin, and Vav1 were indistinguishable between the wildtype and Itk$^{-/-}$ T cells. Actin was immediately recruited to the periphery of the T cell / APC interface throughout the duration of the experiment (51.4% ± 2.2% peripheral localization in wildtype T cells, averaged over seven minutes vs. 53.0% ± 2.3% in Itk$^{-/-}$ cells; 88.9% ± 4.3% of the wildtype cells showed at least one peripheral localization vs. 87.0% ± 4.1% of the knockout cells) (Figure 7). Cofilin was initially recruited to the periphery of the interface (44.6% ± 6.2% peripheral localization in wildtype T cells at 40 seconds vs. 40.5% ± 7.6% in Itk$^{-/-}$ T cells) which then dispersed leaving only 15.5% ± 4.8% of the wildtype T cells and 18.8% ± 6.9% of the knockout T cells showing any recruitment at the interface by three minutes (Figure 10). Vav1 localization was primarily peripheral (45.1% ± 5.2% in the wildtype cells at 40 seconds, 36.6% ± 5.0% in the Itk$^{-/-}$ T cells) with a lamellal component peaking at 60 seconds (26.4% ± 4.6% in the wildtype cells at 60 seconds, 20.4% ± 4.2% in the Itk$^{-/-}$ T cells). Vav1 then gradually dissipated from the interface to where only 41.4% ± 6.8% of the wildtype and 36.6% ± 5.7% of the knockout T cells showed any accumulation at the interface, with the majority of the remaining accumulation being diffuse (Figure 20).

Myosin1c, though showing an initial peripheral preference in the wildtype T cells (28.3% ± 6.6% peripheral localization at 0 seconds in wildtype T cells), the majority of

the accumulation resided in the lamellal, peaking at 1 minute (15.2% ± 5.3% lamallel localization at 1 minute in wildtype T cells) (Figure 12). After 1 minute, myosin1c was removed from the interface, with 12.1% ± 5.7% of the cells showing any accumulation at the interface at 7 minutes. In contrast, the $Itk^{-/-}$ cells lost the lamellal phenotype, with no cells showing lamellal accumulation at any time. Overall accumulation at the interface was less than the wildtype cells (a maximum of 36.0% ± 9.6% of the cells showed accumulation at the interface occurring at 40 seconds), with the localization being almost exclusively peripheral.

PLCδPH displayed an enhanced localization at the periphery of the interface in the $Itk^{-/-}$ T cell (Figure 14). In the wildtype cells, PLCδPH displayed prominent lamallal recruitment within the first two minutes of cell couple formation (60.5% ± 7.5% at 40 seconds) with some peripheral localization (16.3% ± 5.6% at 40 seconds). By three minutes, PLCδPH had dissipated from the interface, with 11.6% ± 4.9% of the cells showing any accumulation at the interface. In contrast, the $Itk^{-/-}$ T cells showed a significant reduction in lamallel accumulation and an increase in peripheral localization within the first two minutes (20.7% ± 7.5% lamallel accumulation at 40 seconds, $p < 0.02$; 27.6% ± 8.3% peripheral accumulation at 40 seconds). In contrast to every other sensor, the knockout cells saw an increase in PLCδPH central localization (20.7% ± 7.5% peripheral in the $Itk^{-/-}$ cells at 40 seconds vs. 0% for wildtype cells; $p < 0.02$), though it retained an overall peripheral preference. PLCδPH was also sustained at the interface in the $Itk^{-/-}$ T cells with 41.7% ± 10.1% of the cells showing accumulation at the interface at 3 minutes (versus 11.6% ± 4.9% of the wildtype cells), where localization was split

between peripheral and diffuse phenotypes (20.8% ± 8.3% peripheral; 20.8% ± 8.3% diffuse); lamellal recruitment was absent from the interface during the sustained localization phase. The sustained $PI_{(4,5)}P_2$ levels may be due to reduced PLCγ1 activation observed in Itk deficient T cells, though this isn't clear as there remains a significant pool of phosphorylated PLCγ1 in the $Itk^{-/-}$ cells (33, 34). The data here suggests that sustained $PI_{(4,5)}P_2$ levels may be due, in part, to the transient localization of PLCγ1 at the interface. $Itk^{-/-}$ T cells contain significant, if reduced, levels of activated PLCγ1 and its removal from the interface would certainly interfere with the ability to hydrolyze $PI_{(4,5)}P_2$.

The localization patterns of the proteins described above show an overall trend of decreased central localization and recruitment to the invagination while retaining localization to the periphery. Together, these data show that Itk was a key regulator of the spatiotemporal patterning at the T cell / APC interface. With this in mind, it was asked how Itk might affect associations between proteins. To examine this, a cluster analysis was performed to determine whether proteins in wildtype cells and $Itk^{-/-}$ T cells would associate similarly (Figure 21). In wildtype T cell, the analysis identified two main association clusters. The first group (composed of actin, αPIX, cofilin, myocin1c, PLCδPH, and Vav1) were the predominantly peripherally localized proteins as shown through the spatial preference index described previous. The second cluster consisted of the more centrally localized proteins Itk, LAT, PKCθ, PLCγ1, SLAT, active Rac1, TCRζ, Tec, and included active Cdc42. When the clustering analysis was performed on the $Itk^{-/-}$ T cells, the same two clusters, with one exception, emerged: actin, cofilin, myosin1c, PLCδPH, Vav1, and activated Cdc42 clustered together in one group; and

LAT, PKCθ, PLCγ1, SLAT, active Rac1, and TCRζ in another (the localization of Tec and αPIX hadn't yet been examined in the $Itk^{-/-}$ cells). Active Cdc42 was the only protein that switched clustering group, identifying it as a protein of interest, which is discussed later. This suggests that Itk plays a more general role in the organization of the immunological synapse rather than specifically driving individual proteins.

All together, Itk is a general regulator of the recruitment of proteins to the center of the T cell / APC interface. As the center of the immunological synapse has been identified as a site of active signaling (4), the failure in central recruitment by the $Itk^{-/-}$ T cells may help to explain why these cells are hyporesponsive.

Localization of the Microtubule-organizing Center to the Interface is Normal in $Itk^{-/-}$ T Cells.

STIM1 is a predominantly endoplasmic reticulum (ER) transmembrane protein that detects depletion of calcium from the ER, prompting it to trigger the opening of Orai1 channels in the cell membrane leading to sustained calcium flux. In T cells STIM1 associates with the microtubule-organizing center (MTOC), which translocates from the distal pole to the immunological synapse upon T cell activation (4). The localization of the MTOC to the interface is calcium dependent and is required for both the formation of an ordered synapse and sustained T cell signaling (93, 94). To test the hypothesis that improper MTOC or STIM1 reorientation may be causing the impaired calcium response, enervated T cell signaling, and perturbed synapse seen in the $Itk^{-/-}$ T cells the translocation of STIM1 to the interface was evaluated in both wildtype and $Itk^{-/-}$ T cells.

There was no defect in the movement of the MTOC from the distal pole to the interface in $Itk^{-/-}$ T cells (Figure 22); both the wildtype and knockout cells had moved the MTOC to the interface by 5 minutes following cell couple formation. The loss of centrality in at the $Itk^{-/-}$ T cell / APC interface and effector hyporesponsiveness does not appear to be caused by improper MTOC orientation and T cell polarization.

Itk is Required for a Burst of Actin Polymerization at the Immunological Synapse

Itk is known to play an important role in actin polymerization upon T cell activation (37, 95). $Itk^{-/-}$ T cells present less actin at the activation interface compared to wildtype T cells (52, 87, 88). As these experiments were conducted in fixed cells, the dynamics of actin accumulation were not analyzed. It's not known, for example, if Itk is required for early actin dynamics, which might be inferred by the impaired initial recruitment of TCRζ to the center of the interface in the knockout T cells, or if Itk plays a role in sustained actin polymerization, as suggested by the stable and sustained late localization patterns of Itk and actin.

To calculate the extent of actin localized at the interface, the ratio of fluorescence at the interface was measured relative to that of the cell background. Wildtype T cells displayed a burst of actin accumulation at the interface immediately upon cell couple formation, with of 3.7 ± 0.1 times the amount of actin at the interface over the background of the cell (averaged over the first 60 seconds) (Figure 23). Actin then dissipated from the interface over the next six minutes, dropping by 42% to 2.2 ± 0.1 times the amount of actin at the interface over the background of the cell. In contrast, the

$Itk^{-/-}$ T cells lacked the burst of actin accumulation at the interface reaching a maximum of 2.6 ± 0.1 times the actin at the interface over the background of the cell at 20 seconds after cell couple formation. The reduction of actin at the interface occurred without the $Itk^{-/-}$ T cells showing an increase in the percentage of cells showing no accumulation, suggesting that Itk regulates the amplitude of the actin recruitment but not the initiation. Itk appears to be a positive regulator of early actin accumulation at the T cell / APC interface without influencing the spatial organization of the recruitment.

Itk Regulates the Localization, but Not the Extent of Cdc42 Activation at the Interface

Activated Cdc42 localized to both the center and periphery of the T cell / APC interface in relatively equal proportions in wildtype T cells ($p > 0.02$ central vs. peripheral localization in wildtype cells for the first five minutes following cell couple formation) (Figure 9). In contrast $Itk^{-/-}$ T cells displayed a 4.4 fold reduction in localization of activated Cdc42 at the center of the interface (34.2% ± 2.4% wildtype vs. 7.7% ± 2.7% $Itk^{-/-}$, averaged from one to five minutes post-cell couple formation; $p < 0.02$), with a corresponding 1.7 fold increase in peripheral localization (36.5% ± 5.2% wildtype vs. 60.2% ± 2.2% $Itk^{-/-}$, averaged from one to five minutes post-cell couple formation; $p < 0.02$).

Four possibilities could explain the observed shift towards peripheral localization of activated of Cdc42 in the $Itk^{-/-}$ T cells: 1) There could be an increase in peripheral activation of Cdc42, masking the central localization and resulting in an overall increase in activated Cdc42 at the interface; 2) Activation of Cdc42 at the interface center could

be selectively reduced, enhancing the relative peripheral localization but reducing overall activated Cdc42 levels; 3) activation of Cdc42 could proceed normally, resulting in normal levels of activated Cdc42, but the mobility at the interface was such that the activated Cdc42 was sequestered at the periphery; or 4) a combination of the previous three possibilities could occur, for example, there could be less central activation and greater peripheral activation of Cdc42 concurrently. To explore these possibilities, the relative amount of active Cdc42 to the interface was calculated by measuring the fluorescence of the Cdc42 Sensor. Wildtype and $Itk^{-/-}$ T cells both had the same ratio of average fluorescent intensity vs. background, indicating that the two cell types had the same levels of activated Cdc42 at the interface (Figure 24). This was confirmed by active Cdc42 pull down followed by immunoblotting; however, as APCs express activated Cdc42, the pull downs had to be conducted on α-CD3 / α-CD28 stimulated T cells, losing the spatial localization patterns that occur at a T cell / APC interface. Together, these data show that wildtype and $Itk^{-/-}$ T cells contained the same cellular level of activated of Cdc42, but differed in how the activated Cdc42 was localized at the immunological synapse.

Centrally Targeted Cdc42 Restores the Actin Burst at the $Itk^{-/-}$ Immunological Synapse

Cdc42 is a critical regulator of actin accumulation at the T cell / APC interface (96, 97). It has been shown that central recruitment of activated Cdc42 correlated with the ability of the T cell to centrally cluster TCRζ and polymerize actin at the synapse (97). The correlation was not formally tested, however, as it was not possible to

selectively inhibit Cdc42 activity at the center of the T cell / APC interface while leaving the periphery unperturbed. This, conversely, is the status quo for the $Itk^{-/-}$ T cell; as the model predicted both actin and the central localization of TCRζ were inhibited. The question was asked, if activated Cdc42 was reintroduced to the center of the synapse would the actin burst and central TCRζ recruitment be restored. To test this, constitutively active Cdc42 (V12 constitutively active mutant (98)) was introduced to the cell in one of three permutations: 1) the constitutively active Cdc42 (Cdc42ca) was attached to the Tec PH-TH-SH3 recruitment domains, allowing for the recruitment of Cdc42ca to the center of the interface (Figure 25); 2) Cdc42ca was attached to the Zap70 double SH2 domain, promoting the diffuse recruitment of Cdc42ca at the interface (Figure 25); and 3) Cdc42ca was introduced without a targeted recruitment domain, allowing for the non-localized increase in total cellular Cdc42 activity (Figure 26). All three protein constructs were introduced into the cell by protein transduction, where the addition of a 10 amino acid peptide from the HIV tat protein conferred membrane-permeability in a dose dependent manner (99).

The addition of 100nM of centrally targeted constitutively active Cdc42 (tat-Tec.PH.TH.SH3-Cdc42ca) was able to restore the actin burst in the $Itk^{-/-}$ T cells, with no statistical difference in actin accumulation when compared to the wildtype T cells (Figure 27). The tat-Tec.PH.TH.SH3-Cdc42ca treated $Itk^{-/-}$ T cells reached 3.6 ± 0.2 times the amount of actin at the interface over the background of the cell at 20 seconds; compared to 3.7 ± 0.1 for the untreated wildtype T cells and 2.6 ± 0.1 for the untreated $Itk^{-/-}$ T cells. The wildtype cells under the same treatment did not show an increase in the actin burst, but instead displayed enhanced dispersion of actin from the interface, stabilizing at 2.2 ±

0.1 times the actin at the interface over the background 2 minutes before the untreated wildtype T cells. Together this shows that restoration of the actin burst in the knockout cells by tat-Tec.PH.TH.SH3-Cdc42ca was specific and not a generalized increase in actin localization at the interface. To rule out the possibility that the actin burst was restored by the recruitment domain and not Cdc42ca both wildtype and $Itk^{-/-}$ T cells were treated with 100μM of the recruitment domain sans the attached Cdc42ca (tat-Tec.PH.TH.SH3). The construct had no effect on the recruitment of actin at the interface in either cell type, ($p > 0.02$ tat-Tec.PH.TH.SH3 treated T cells vs. untreated T cells for both wildtype and $Itk^{-/-}$ cells at all time points), suggesting that centrally targeted Cdc42ca was the mediator of the restoration of the actin burst (Figure 27).

To determine whether the restoration of the actin burst was due to the central targeting of Cdc42ca, wildtype and $Itk^{-/-}$ T cells were treated with Cdc42ca attached to the Zap70 double SH2 domain (tat-Zap70.2SH2-Cdc42ca), which recruits Cdc42 to the entirety of the interface. Treatment of the cells with 100nM tat-Zap70.2SH2-Cdc42ca had no effect on the recruitment of actin to the interface in either the knockout or wildtype T cells (Figure 28). To compensate for the possibility that due to the diffuse recruitment pattern the localized concentration of Cdc42ca might be lower at the interface than the centrally targeted Cdc42ca, the experiments were repeated using 350nM of the tat-Zap70.2SH2-Cdc42ca protein. The higher concentration showed no effect on the relative actin intensity.

The Zap70.2SH2 recruitment domain was not without its caveats as Zap70 may play a role in actin polymerization at the interface (100, 101). It was possible that the Zap70.2SH2 recruitment domain might have acted as a dominant negative, preventing

Cdc42ca rescue of the actin burst in the Itk$^{-/-}$ cells; though this was unlikely given the mild actin defect in Zap70$^{-/-}$ T cells and the wildtype T cells showed no effect when treated with the tat-Zap70.2SH2-Cdc42ca construct. To address this, wildtype and Itk$^{-/-}$ T cells were treated with Cdc42ca with no recruitment domains (tat-Cdc42ca). Neither wildtype T cell nor Itk$^{-/-}$ T cells displayed any changes in the extent of actin at the interface in the presence of 100nM, 350nM, or 1μM tat-Cdc42ca. All together these data show that activated Cdc42 specifically at the center of the interface is required for generation of the actin burst upon engagement with an antigen presenting cell.

Restoration of the actin burst would be more biologically significant if the actin recruitment occurred with undisturbed spatiotemporal patterning. To examine this possibility, the actin localization was evaluated for each of the experimental conditions. Both wildtype and Itk$^{-/-}$ T cells significantly increased the preferential peripheral localization of actin at the interface when treated with 100nM of the centrally targeted Cdc42 (tat-Tec.PH.TH.SH3-Cdc42ca) (Figure 29). The other Cdc42ca localization variants (tec-Zap70.2SH2-Cdc42ca; tat-Cdc42ca; tat-Tec.PH.TH.SH3) had no effect on the spatiotemporal recruitment of actin at all concentrations tested (Figures 30-35). Together these data suggest a novel regulatory mechanism where activated Cdc42 at the center of the interface regulates actin at the periphery.

Centrally Targeted Cdc42 Does Not Restore TCRζ Recruitment to the Center of the Itk$^{-/-}$ Immunological Synapse

The recruitment of the TCRζ to the center of the T cell / APC interface is an actin mediated process that is dependent, in part, on activated Cdc42 (97, 102, 103). Since centrally targeted Cdc42ca rescued the actin burst, it was examined whether central recruitment of TCRζ was also restored. The addition of 100nM tat-Tec.PH.TH.SH3-Cdc42ca was not able to reconstitute TCRζ recruitment to the center of the interface in Itk$^{-/-}$ T cells (Figure 36-37); instead, the centrally targeted Cdc42ca impeded central localization. Treated Itk$^{-/-}$ T cells presented a 50.0% ± 15.8% reduction in central recruitment versus the untreated cells (averaged over all time points after cell couple formation). The TCRζ instead appeared to be trapped at the periphery of the interface as the treated cells displayed sustained peripheral localization. Treatment with tat-Tec.PH.TH.SH3-Cdc42ca also inhibited early central TCRζ accumulation in the wildtype T cells, with TCRζ recruitment to becoming similar to that of the untreated Itk$^{-/-}$ T cells. The reduction in central recruitment concurred with a reduction in the percent of cells that showed any interface recruitment, indicating that perhaps the T cells had difficulty recruiting TCRζ to the synapse. After 40 seconds, the wildtype cells treated with 100nM tat-Tec.PH.TH.SH3-Cdc42ca recruited TCRζ to the center faster than the untreated Itk$^{-/-}$ cells, reaching wildtype levels within five minutes of forming the T cell / APC couple. None of the other treatments (100nM tat-Tec.PH.TH.SH3; 100nM or 350nM tat-

Zap70.2SH2-Cdc42ca; 350nM tat-Cdc42ca) affected TCRζ recruitment in either the wildtype or $Itk^{-/-}$ T cells (Figures 35, 38-41).

Increasing Actin Turnover Does Not Restore TCRζ Recruitment to the Center of the $Itk^{-/-}$ Immunological Synapse

One possible mechanism for the reduced central TCRζ localization by centrally targeted Cdc42ca is that signaling pathways that regulate actin turnover may not have been upregulated or may have been inhibited. As a result, relative actin turnover may have decreased, creating a relatively rigid and less dynamic cytoskeleton that interfered with the central mobilization of TCRζ. Additionally, if Itk is indirectly involved in the promotion of actin turnover, the $Itk^{-/-}$ cells would have been more severely affected by the rigid actin network, further trapping TCRζ at the periphery.

One candidate protein important for cytoskeletal dynamics that is affected by both Cdc42 and Itk, is cofilin (Figure 42). Cofilin is a 19kD protein that binds to F-actin, increasing elasticity, severing, and depolymerization (104-106). The protein plays an important role in T cell activation and the formation of the immunological synapse (107-110). Cdc42 regulates cofilin by activating PAK proteins (PAK1, 2, and 4) and KRCKα (Myotonic Dystrophy Kinase-Related Cdc42-Binding Kinase α), activating LIM kinases, which phosphorylate cofilin at Ser 3, inactivating cofilin and inhibiting binding to F-actin (111, 112). The addition of the centrally targeted Cdc42 may have up-regulated this cascade, promoting the inactivation of cofilin and the rigidity of the actin cytoskeleton.

Cofilin is also indirectly regulated by Itk through the activation of PLCγ1. Dephosphorylated (active) cofilin binds to $PI_{(4,5)}P_2$, sequestering it from actin (113). Active cofilin is released from the membrane by hydrolysis of $PI_{(4,5)}P_2$ into diacylglycerol (DAG) and inositol triphosphate (IP_3) by PLCγ1, allowing for the interaction with actin. $Itk^{-/-}$ T cells showed an increase in sustained $PI_{(4,5)}P_2$ at the interface (Figure 15), which may have enhanced the sequestering of active cofilin resulting in decreased turnover and flexibility in the actin burst generated by centrally localized Cdc42ca.

To test this model, a constitutively active cofilin (caCofilin) was generated by mutating serine 3 to alanine, preventing phosphorylation (114). The 10 amino acid tat peptide was then attached to the constitutively active cofilin (tat-caCofilin), allowing for membrane-permeability in a dose dependent manner. Wildtype and $Itk^{-/-}$ cells were treated concurrently with 100nM tat-Tec.PH.TH.SH3-Cdc42ca and 10nM tat-caCofilin and analyzed for central recruitment of TCRζ.

The addition of 10nM of tat-caCofilin was not able to restore central TCRζ localization to unmanipulated wildtype levels in either 100nM tat-Tec.PH.TH.SH3-Cdc42ca treated wildtype or $Itk^{-/-}$ T cells (Figure 43-44). caCofilin was, however, able to rescue the reduction in central TCRζ localization caused specifically by the centrally targeted Cdc42ca in the $Itk^{-/-}$ T cell ($p > 0.05$ at all time points following cell couple formation; 10nM tat-caCofilin, 100nM tat-Tec.PH.TH.SH3-Cdc42ca $Itk^{-/-}$ T cells vs. untreated $Itk^{-/-}$ T cells). In contrast, caCofilin did not rescue the phenotype in wildtype T cells, with no difference in central TCRζ localization with or without tat-caCofilin for the first two minutes following cell couple formation ($p > 0.05$ at all time points 0 – 120

seconds). After two minutes, the T cells ceased to recruit TCRζ to the center of the interface and the spatiotemporal patterns were essentially frozen.

One possible explanation for wildtype phenotype is that $PI_{(4,5)}P_2$ levels rapidly decreased at the same time that TCRζ stopped being recruited to the interface. Prior to the two minute mark, when $PI_{(4,5)}P_2$ levels were high, the $PI_{(4,5)}P_2$ may have sequestered tat-caCofilin, preventing it from acting on the actin cytoskeleton. After two minutes, when $PI_{(4,5)}P_2$ levels dropped, the sequestered tat-caCofilin may have been released from the membrane, increasing caCofilin levels, resulting in the depolymerization of the actin network. Consequentially, increasing the tat-Cofilin concentration may rescue central TCRζ localization within the first two minutes, while decreasing the concentration may rescue the localization after two minutes. The $Itk^{-/-}$ T cells may not have experienced the biphasic TCRζ recruitment because the $PI_{(4,5)}P_2$ levels were relatively sustained.

Restoring the Actin Burst Does Not Restore IL2 Secretion

It is well established that $Itk^{-/-}$ T cells produce less IL2 than wildtype cells (33). To determine whether restoring the actin burst reconstituted IL2 secretion, T cells were cultured in the presence or absence of 100nM tat-Tec.PH.TH.SH3-Cdc42ca and IL2 levels were measured by ELISA. Unmanipulated $Itk^{-/-}$ T cells produced 90.5% ± 0.4% less IL2 than wildtype cells (Figure 45). Treatment with the centrally targeted Cdc42ca was not able to restore IL2 production in either the wildtype or $Itk^{-/-}$ cells, possibly because restoring the actin burst did not rescue the recruitment of TCRζ to the center of

the interface. On the other hand, IL2 production was not impaired in either cell type by the abatement of central TCRζ localization caused by the centrally targeted Cdc42.

Concurrently, it was examined whether increasing cytoskeletal turnover during the reconstituted actin burst could restore IL2 production. T cells were cultured in the presence of 100nM tat-Tec.PH.TH.SH3-Cdc42ca and either 1nM–100nM tat-caCofilin or 3nM–800nM Latrunculin B. Latrunculin B sequesters actin monomers and, at low concentrations, can enhance actin turnover (115). Neither tat-caCofilin nor Latrunculin B were able to positively affect IL2 production in either the wildtype or $Itk^{-/-}$ T cells (Figures 45-47).

Of particular note, wildtype T cells treated with both centrally targeted Cdc42 and 10nM tat-caCofilin saw no difference in IL2 production compared to untreated cells even though recruitment of TCRζ to the center of the interface was dramatically decreased. These data suggest that central clustering of TCRζ is not required for normal IL2 production in DO11.10 T cells.

SLAT is a Candidate GEF for Activating Cdc42 at the Center of the Interface

$Itk^{-/-}$ T cells lack the early actin burst, which can be restored by introducing active Cdc42 to the center of the interface. How Itk mediates the initial central localization of activated Cdc42 is not known. Since Itk is recruited to the center of the interface at the same time as the initiation of the actin burst, one possibility is that Itk could be involved in the recruitment of a guanine nucleotide-exchange factor (GEF) that activates of Cdc42 at the center of the interface. To test this hypothesis, the

spatiotemporal localization for four GEFs known to activate Cdc42 in T cells (αPIX, Intersectin2, SLAT, and Vav1) was examined to determine if any 1) were immediately recruited to the center of the interface in wildtype T cells and 2) showed reduced early central localization in $Itk^{-/-}$ cells.

Intersectin2 was not recruited to the T cell / APC interface in wildtype T cells and was immediately ruled out as a candidate GEF. Vav1 localized at the periphery of the interface in both the wildtype and $Itk^{-/-}$ T cells, ruling it out as a candidate for central Cdc42 activation (Figure 20). αPIX was prominently recruited in a lamellal (40.7% ± 9.5% at 20 seconds) and peripheral (37.0% ± 9.3% at 20 seconds) localization pattern at the interface of the wildtype cell (Figure 8). The peripheral and lamellal accumulation patterns were sustained over time, with no significant central accumulation. αPIX localization was not determined in $Itk^{-/-}$ T cells, though the spatiotemporal patterning in the wildtype cell ruled αPIX out as a candidate GEF. In contrast, wildtype T cells showed strong central SLAT accumulation immediately upon cell couple formation (53.8% ± 6.9% of the cell couples at 0 seconds) which increased over time to peak at 75.5% ± 6.1% at 100 seconds (Figure 17). SLAT remained at the interface, showing sustained accumulation throughout the duration of the experiment (60.8% ± 0.8% average central accumulation 3 to 7 minutes following cell couple formation). $Itk^{-/-}$ T cells had significantly reduced central SLAT for the first minute following cell couple formation (20.0% ± 5.7% at time 0; $p < 0.02$ vs. wildtype cells), with the majority of the accumulation being diffuse (68.0% ± 6.6% at time 0). Central localization of SLAT increased over time, though it was always less than the wildtype cells.

In addition to the spatiotemporal patterning, the extent of accumulation was evaluated for each GEF (Figures 48-49). Wildtype T cells showed a burst of Vav1 accumulation, reaching 4.25 ± 1.1 times the amount of Vav1.GFP at the interface compared to the background of the cell immediately upon cell couple formation. In contrast, the Vav1 accumulation was completely flat in the $Itk^{-/-}$ cells, with an average of 2.3 ± 0.06 times more accumulation at the interface than the background. The recruitment of αPIX in wildtype T cells peaked at cell couple formation (4.5 ± 0.3 times the accumulation at the interface vs. the background of the cell), which steadily declined over time to 2.48 ± 0.32 times more accumulation at the interface than the background of the cell. SLAT strongly recruited to the interface with 6.8 ± 0.5 times the amount of GFP.SLAT at the interface compared to the background of the cell at 20 seconds following cell couple formation. Over the next three minutes, the intensity of SLAT at the interface faded, reaching a plateau of 4.5 ± 0.4 times the intensity at the interface over background. The dynamics of the intensity of accumulation for SLAT at the interface was strikingly similar to the burst accumulation observed for actin. In the $Itk^{-/-}$ T cell, the recruitment of SLAT was on average 30.5% ± 2.8% less than the recruitment measured in the wildtype T cells.

These data suggest that SLAT is a strong candidate as the GEF regulating Cdc42 activity at the center of the T cell / APC interface. The decreased central localization and overall interface recruitment of SLAT in $Itk^{-/-}$ cells could result in less activated Cdc42 at the center of the synapse, preventing the initiation of the actin burst.

Disrupted TCRζ Spatiotemporal Patterning is Due to the Absence of Itk and Not Altered Differentiation

Knocking out a signaling intermediate, particularly one downstream of the TCR, can have dramatic effects on thymic selection and epistatic programming of the T cell. As Itk plays a role in positive and negative selection (32, 116, 117) the perturbed spatiotemporal organization in $Itk^{-/-}$ T cells may have resulted from altered thymic education and not as an immediate consequence of Itk deficiency. To test this, a retroviral vector containing wildtype Itk and TCRζ.GFP was reintroduced to the mature $Itk^{-/-}$ T cell by retroviral transduction. The spatiotemporal localization of TCRζ in reconstituted T cells was comparable to that of the wildtype T cell, with the central localization showing no significant difference at any time point (Figures 50-52). This indicates that the spatiotemporal phenotypes observed are likely due to the direct effect of Itk and not altered developmental programming.

Itk SH2 Domain Mediates TCRζ Recruitment to the Immunological Synapse

To examine the role of the SH2 and kinase domains in spatiotemporal localization, $Itk^{-/-}$ T cells were reconstituted with SH2 binding deficient (R265K) or kinase dead (K390R) Itk mutants (Figures 50-53). The kinase dead Itk partially restored central TCRζ recruitment with 29.8% ± 6.1% of the kinase dead reconstituted T cells showing central recruitment versus 50.6% ± 5.4% in the wildtype and 10.3% ± 3.1% in the $Itk^{-/-}$ T cells. In contrast, reconstitution with the Itk SH2 binding deficient mutant

greatly reduced central TCRζ recruitment, with no cells showing central recruitment from 1 to 3 minutes following cell couple formation. Cells showed less recruitment to the interface (48.0% ± 4.1% average of the reconstituted cells showing any accumulation at the interface vs. 71.3% ± 3.0% of the $Itk^{-/-}$ T cells), with a dramatic increase in the sequestering of TCRζ at the distal pole.

To assess whether a role in the SH2 domain in Itk localization was consistent with its function in the regulation of TCRζ localization, the spatiotemporal localization of Itk lacking the SH2 domain (Itk.PH.TH.SH3.GFP) was examined. Itk.PH.TH.SH3.GFP was not observed at the distal pole but instead gained a new lamellal recruitment pattern at the T cell / APC interface. The construct, while still showing some early central localization, lacked the sharp early and sustained late central recruitment seen in Itk containing the SH2 domain (Figure 54). To determine if the R265K Itk was acting as a dominant negative, wildtype cells were transduced with the reconstitution vector. The spatiotemporal localization of TCRζ was relatively unchanged, if slightly more diffuse, for the first three minutes following cell couple formation. After three minutes, TCRζ appeared to lose its centrality, showing a steady decrease in central localization and a corresponding increase in diffuse localization; however the data are inconclusive and the n value will have to be increased to be more convincing.

Spatiotemporal Localization in Th2 Polarized T Cells

Itk plays a critical role in the ability of Th2 polarized T cells to initiate an effector response (35, 118). One possible contributing mechanism for this may be the

perturbed organization of the immunological synapse in Itk$^{-/-}$ T cells. Additionally, Th2 polarized cells show reduced central TCRζ recruitment relative to Th1 cells (17). Perhaps the two organizational defects act in synergy, preventing the full activation and effector response. To investigate this possibility, TCRζ localization dynamics were examined in Th2 polarized wildtype and Itk$^{-/-}$ T cells.

Wildtype Th2 T cells showed, on average, 34.0% ± 3.4% less central TCRζ than unpolarized T cells with Th2 polarized Itk$^{-/-}$ cells presenting an average of 44.9% ± 5.6% less central TCRζ than unpolarized Itk$^{-/-}$ T cells (Figures 55-58). Localization to the invagination event was completely absent. Peripheral sequestering was increased, similar to what was observed in the Itk knockout, though overall recruitment to the interface appeared normal. Th2 polarized Itk$^{-/-}$ T cells displayed the lowest extent of central TCRζ recruitment, suggesting that there was a synergist effect in synaptic organization by the Itk deficiency and Th2 polarization.

A.

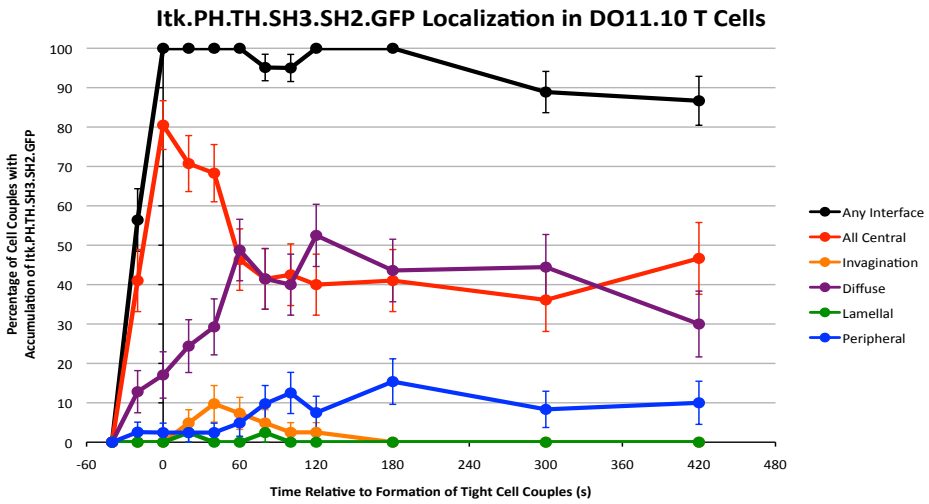

B.

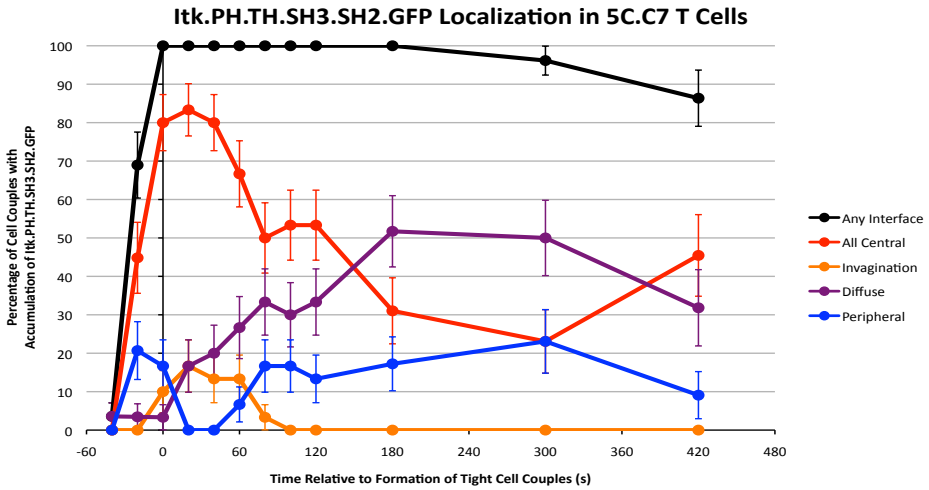

Figure 3: Spatiotemporal Localization of Itk.PH.TH.SH3.SH2.GFP in CD4$^+$ DO11.10 or 5C.C7 TCR Transgenic T Cells. Primed primary (A) DO11.10 or (B) 5C.C7 T cells were transduced with Itk.PH.TH.SH3.SH2.GFP and stimulated with A20 B cell lymphoma APCs in the presence of 10μM OVA antigenic peptide (top) or with CH27 B cell lymphoma in the presence of 10μM MCC antigenic peptide (bottom). Time indicated is relative to the formation of a tight coupling of the T cell with the APC. The graphs display the percentage of cell couples that displayed accumulation of signaling intermediates with the indicated patterns. 41 cell couples were analyzed for the DO11.10 T cells; 30 cell couples for the 5C.C7. Error bars represent standard error.

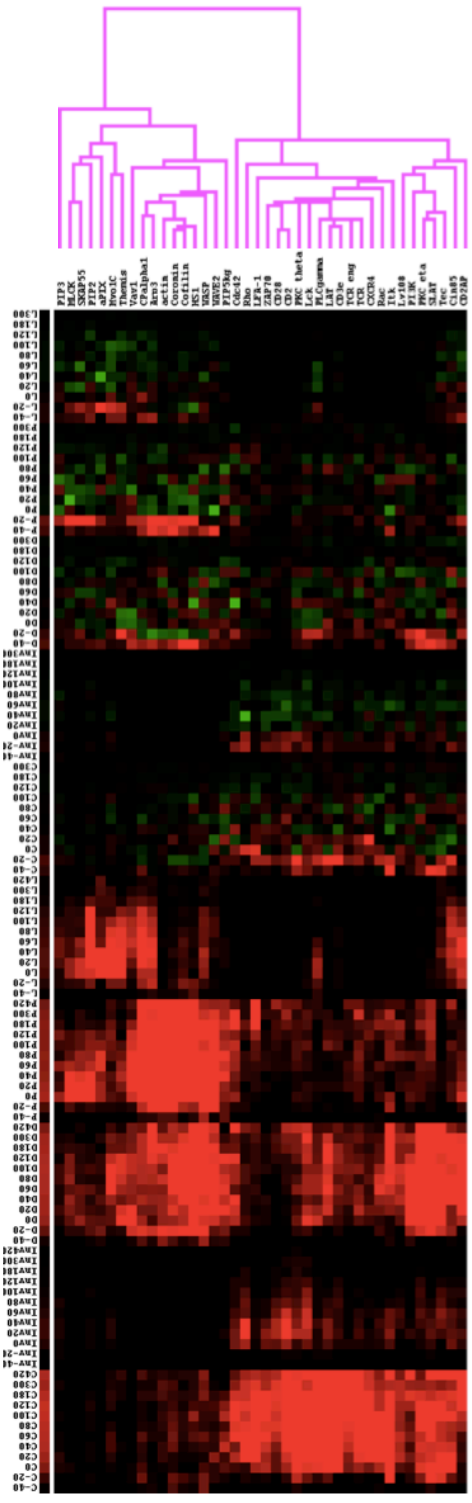

Figure 4: Cluster Analysis of Spatiotemporal Patterning in 5C.C7 TCR Transgenic T Cells. Spatiotemporal patterning of 40 sensors was determined in 5C.C7 TCR transgenic T cells upon stimulation with CH27 B cell lymphoma APCs in the presence of 10μM MCC antigenic peptide. Spatial patterning was categorized into five mutually exclusive phenotypes - Central (C), Invagination (Inv), Diffuse (D), Peripheral (P) or Lamellum (L) – and were evaluated at 12 time points (-40, -20, 0, 20, 40, 60, 80, 100, 120, 180, 300, 420 seconds, with 0 seconds representing tight T cell / APC coupling). The percentage occurrence of each pattern is represented in shades of red (black = 0%, bright red = 100%) (A). To address the pattern dynamics, the percentage change between time points was determined – Red indicates an increase with green being a decrease in percentage occurrence of a particular pattern relative to the previous time point (B). Cluster analysis based on Pearson's correlation was performed on the entire data set, with the dendrogram displayed in pink.

```
 Score =  749 bits (1934),  Expect = 0.0, Method: Compositional matrix adjust.
 Identities = 358/624 (57%), Positives = 463/624 (74%), Gaps = 9/624 (1%)

Query  1    MNFNTILEEILIKRSQQKKKTSPLNYKERLFVLTKSVLSYYEGR-AEKKYRKGVIDISKI  59
            MN   +LEE LIK+SQQK++TSP N+K R FVLTK+ L+Y+E R  +K+  KG I++S+I
Sbjct  1    MNNFILLEEQLIKKSQQKRRTSPSNFKVRFFVLTKASLAYFEDRHGKKRTLKGSIELSRI  60

Query  60   KCVEIVKNDDGVIPCQNKFPFQVVHDANTLYIFAPSPQSRDRWVKKLKEEIKNNNNIMIK  119
            KCVEIVK+D   IPC  K+PFQVVHD   LY+FAP  +SR RWV  LKEE +NNN+++ K
Sbjct  61   KCVEIVKSDIS-IPCHYKYPFQVVHDNYLLYVFAPDCESRQRWVLTLKEETRNNNSLVSK  119

Query  120  YHPKFWADGSYQCCRQTEKLAPGCEKYNLFESSIRKTLPPAPEIKKRRPPPPIPPEEENT  179
            YHP FW DG ++CC Q EK A GC  Y+  +++ +K LPP PE  +R          +E
Sbjct  120  YHPNFWMDGRWRCCSQLEKPAVGCAPYDPSKNASKKPLPPTPEDNRRS-------FQEPE  172

Query  180  EEIVVAMYDFQATEAHDLRLERGQEYIILEKNDLHWWRARDKYGSEGYIPSNYVTGKKSN  239
            E +V+A+YD+Q  +  +L L   +EY +L+ +++HWWR +DK G EGY PS+Y+  K  N
Sbjct  173  ETLVIALYDYQTNDPQELALRCDEEYYLLDSSEIHWWRVQDKNGHEGYAPSSYLVEKSPN  232

Query  240  NLDQYEWYCRNTNRSKAEQLLRTEDKEGGFMVRDSSQPGLYTVSLYTKFGGEGSSGFRHY  299
            NL+ YEWY ++ +R KAE+LL    KEG FMVRDS  PG YTVS++TK     +   +HY
Sbjct  233  NLETYEWYNKSISRDKAEKLLLDTGKEGAFMVRDSRTPGTYTVSVFTKAIISENPCIKHY  292

Query  300  HIKETATSPKKYYLAEKHAFGSIPEIIEYHKHNAAGLVTRLRYPVSTKGKNAPTTAGFSY  359
            HIKET  SPK+YY+AEK+ F SIP +I+YH++N  GLVTRLRYPV +  + AP TAG  Y
Sbjct  293  HIKETNDSPKRYYVAEKYVFDSIPLLIQYHQYNGGGLVTRLRYPVCSWRQKAPVTAGLRY  352

Query  360  DKWEINPSELTFMRELGSGLFGVVRLGKWRAQYKVAIKAIREGAMCEEDFIEEAKVMMKL  419
             KW I PSELTF++E+GSG FG+V LG W  + KVAIK I+EGAM EEDFIEEA+VMMKL
Sbjct  353  GKWVIQPSELTFVQEIGSGQFGLVHLGYWLNKDKVAIKTIQEGAMSEEDFIEEAEVMMKL  412

Query  420  THPKLVQLYGVCTQQKPIYIVTEFMERGCLLNFLRQRQGHFSRDMLLSMCQDVCEGMEYL  479
            +HPKLVQLYGVC +Q PI +V EFME GCL ++LR ++G F+ + LL MC DVCEGM YL
Sbjct  413  SHPKLVQLYGVCLEQAPICLVFEFMEHGCLSDYLRSQRGLFAAETLLGMCLDVCEGMAYL  472

Query  480  ERNSFIHRDLAARNCLVNEAGVVKVSDFGMARYVLDDQYTSSSGAKFPVKWCPPEVFNYS  539
            E+   IHRDLAARNCLV E  V+KVSDFGM R+VLDDQYTSS+G KFPVKW  PEVF++S
Sbjct  473  EKACVIHRDLAARNCLVGENQVIKVSDFGMTRFVLDDQYTSSTGTKFPVKWASPEVFSFS  532

Query  540  RFSSKSDVWSFGVLMWEIFTEGRMPFEKNTNYEVVTMVTRGHRLHRPKLASKYLYEVMLR  599
            R+SSKSDVWSFGVLMWE+F+EG++P+E  +N EVV  ++ G RL++P+LAS ++Y++M
Sbjct  533  RYSSKSDVWSFGVLMWEVFSEGKIPYENRSNSEVVEDISTGFRLYKPRLASCHVYQIMNH  592

Query  600  CWQERPEGRPSFEDLLRTIDELVE  623
            CW+E+PE RP F  LL  + E+ E
Sbjct  593  CWKEKPEDRPPFSQLLSQLAEIAE  616
```

Figure 5: Tec is A Close Homolog of Itk. The protein sequences of Mus Musculus homologs of Itk (gi:56207147) and Tec (gi:164698396) were aligned and evaluated for homology using the National Center for Biotechnology Information's (NCBI) MEGABLAST (MEGA Basic Local Alignment Search Tool).

A.

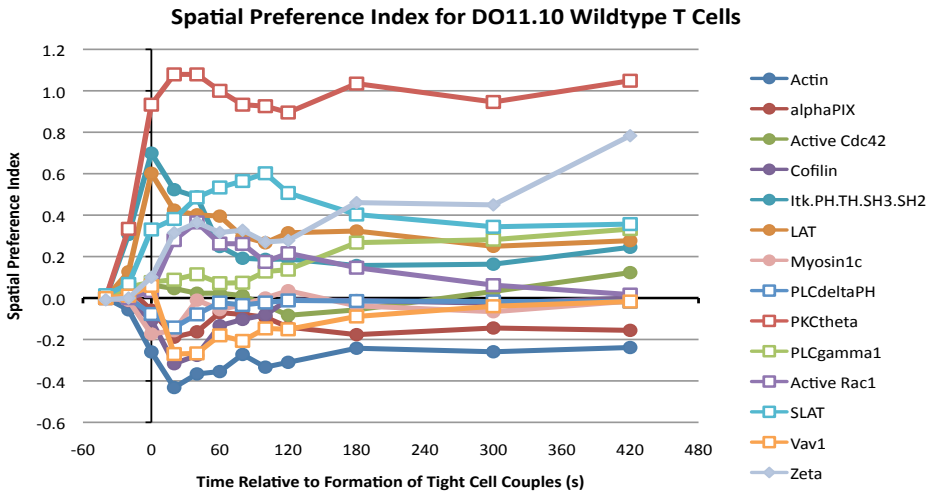

B.

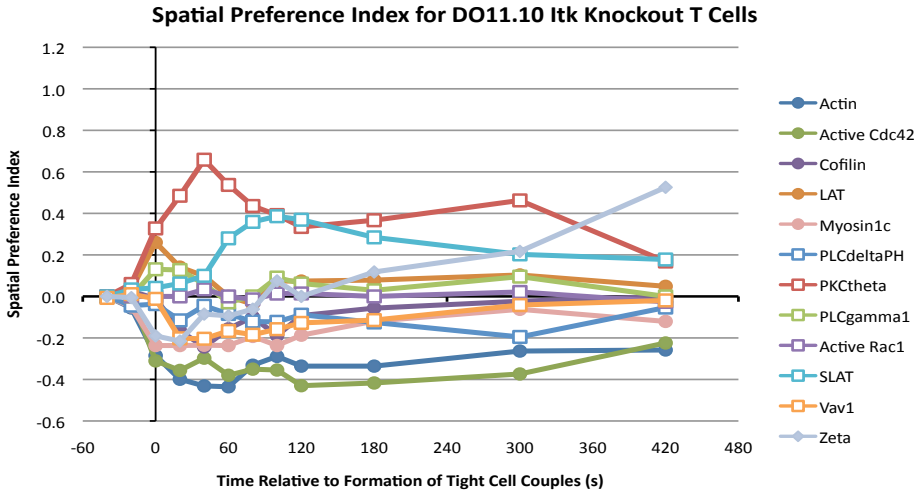

Figure 6: Spatial Preference Index for CD4^{+} DO11.10 TCR Transgenic Wildtype or Itk$^{-/-}$ T Cells. Primed primary DO11.10 (A) wildtype or (B) Itk$^{-/-}$ T cells were transduced with GFP tagged localization sensors and stimulated with A20 B cell lymphoma APCs in the presence of 10μM OVA antigenic peptide. Time indicated is relative to the formation of a tight cell coupling of the T cell with the APC. The equation for the Spatial Preference Index calculation is defined in the Methods. Positive values indicate a central preference, with larger values illustrating a stronger central preference. Negative values indicate a peripheral preference, with more negative values illustrating a stronger peripheral preference. 13 constructs, representing 846 cell couples were analyzed for the wildtype T cells; 11 constructs, representing 584 cell couples were analyzed for the Itk$^{-/-}$ T cells.

A.

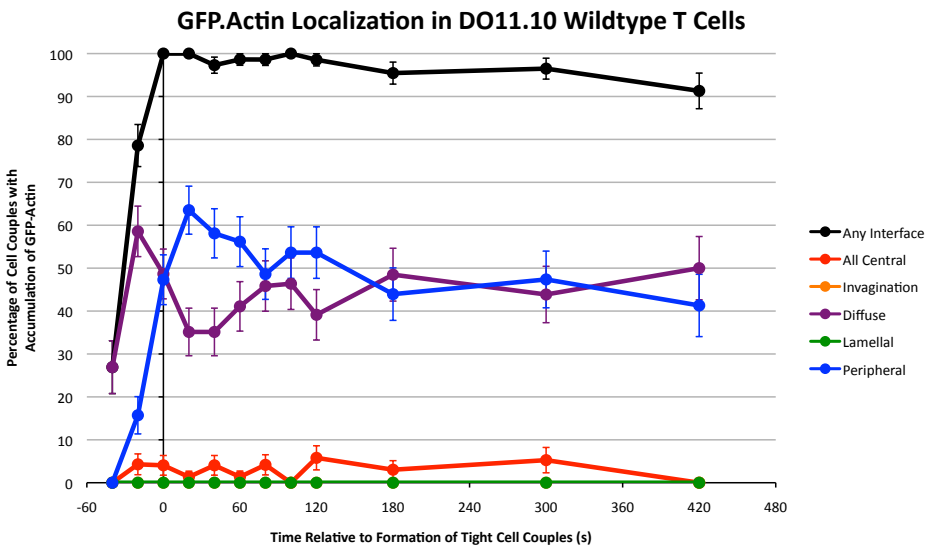

B.

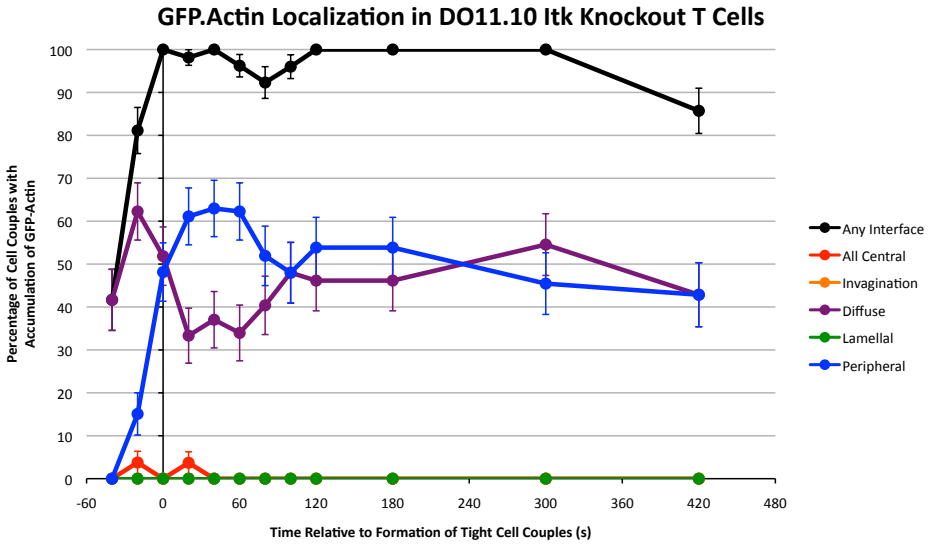

Figure 7: Spatiotemporal Localization of GFP.Actin in CD4$^+$ DO11.10 TCR Transgenic Wildtype or Itk$^{-/-}$ T Cells. Primed primary DO11.10 (A) wildtype or (B) Itk$^{-/-}$ T cells were transduced with GFP.Actin and stimulated with A20 B cell lymphoma APCs in the presence of 10μM OVA antigenic peptide. Time indicated is relative to the formation of a tight coupling of the T cell with the APC. The graphs display the percentage of cell couples that displayed accumulation of signaling intermediates with the indicated patterns. 74 cell couples were analyzed for the wildtype T cells; 54 cell couples for the Itk$^{-/-}$ T cells. Error bars represent standard error.

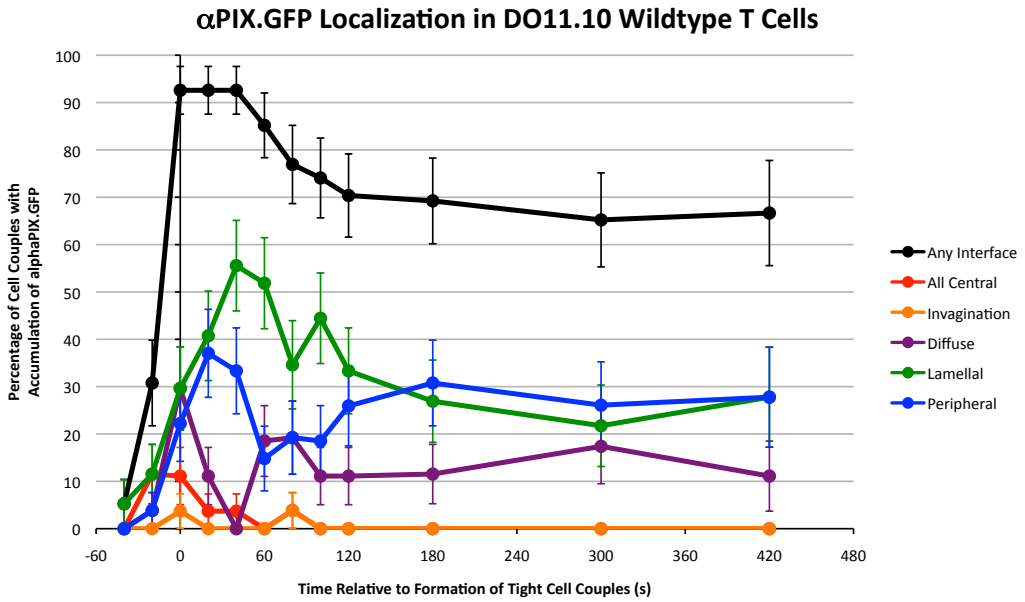

Figure 8: Spatiotemporal Localization of αPIX.GFP in CD4$^+$ DO11.10 TCR Transgenic Wildtype T Cells. Primed primary DO11.10 wildtype T cells were transduced with αPIX.GFP and stimulated with A20 B cell lymphoma APCs in the presence of 10μM OVA antigenic peptide. Time indicated is relative to the formation of a tight coupling of the T cell with the APC. The graphs display the percentage of cell couples that displayed accumulation of signaling intermediates with the indicated patterns. 27 cell couples were analyzed. Error bars represent standard error.

A.

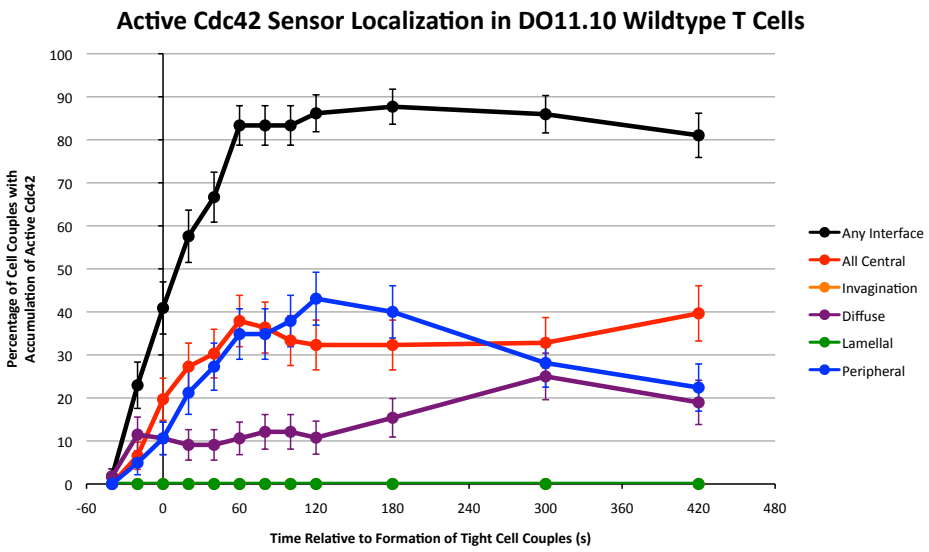

B.

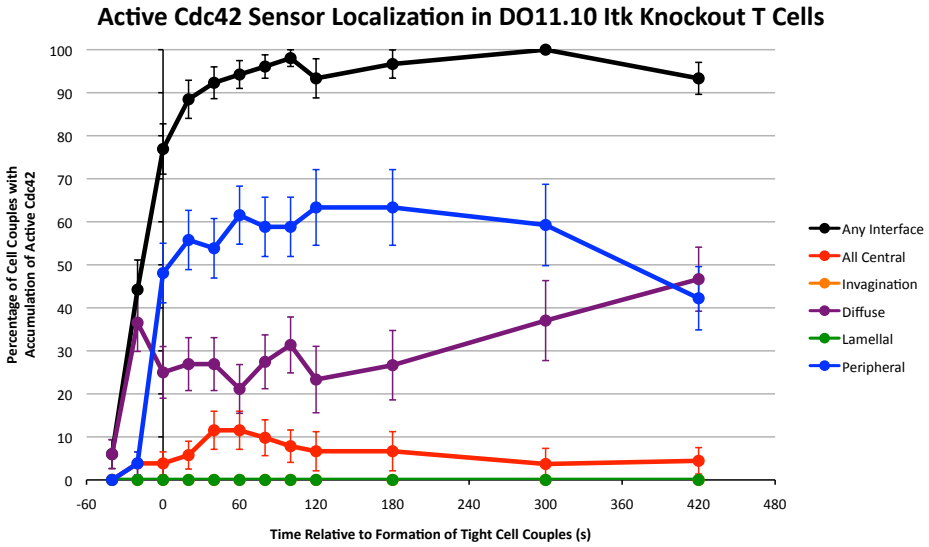

Figure 9: Spatiotemporal Localization of Active Cdc42 Sensor in CD4$^+$ DO11.10 TCR Transgenic Wildtype or Itk$^{-/-}$ T Cells. Primed primary DO11.10 (A) wildtype or (B) Itk$^{-/-}$ T cells were transduced with Active Cdc42 Sensor and stimulated with A20 B cell lymphoma APCs in the presence of 10μM OVA antigenic peptide. Time indicated is relative to the formation of a tight coupling of the T cell with the APC. The graphs display the percentage of cell couples that displayed accumulation of signaling intermediates with the indicated patterns. 66 cell couples were analyzed for the wildtype T cells; 52 cell couples for the Itk$^{-/-}$ T cells. Error bars represent standard error.

A.

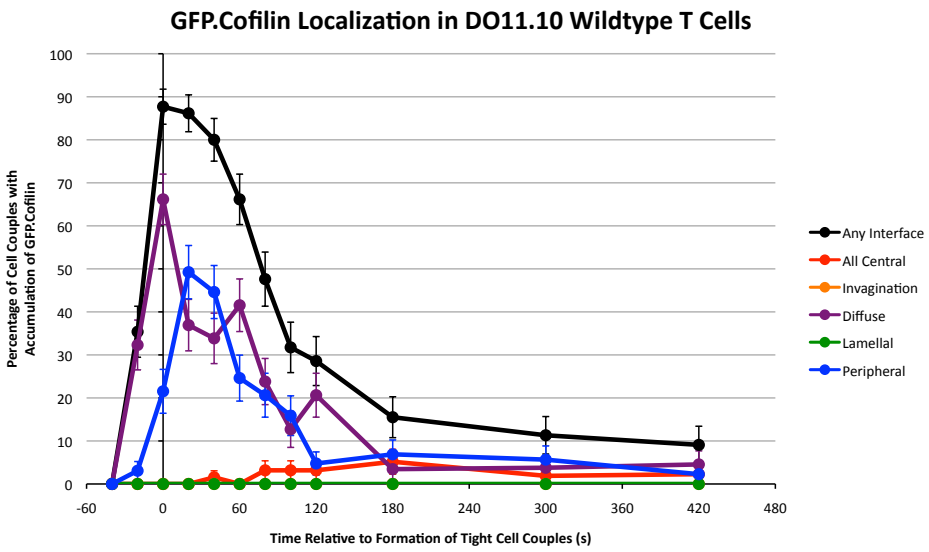

B.

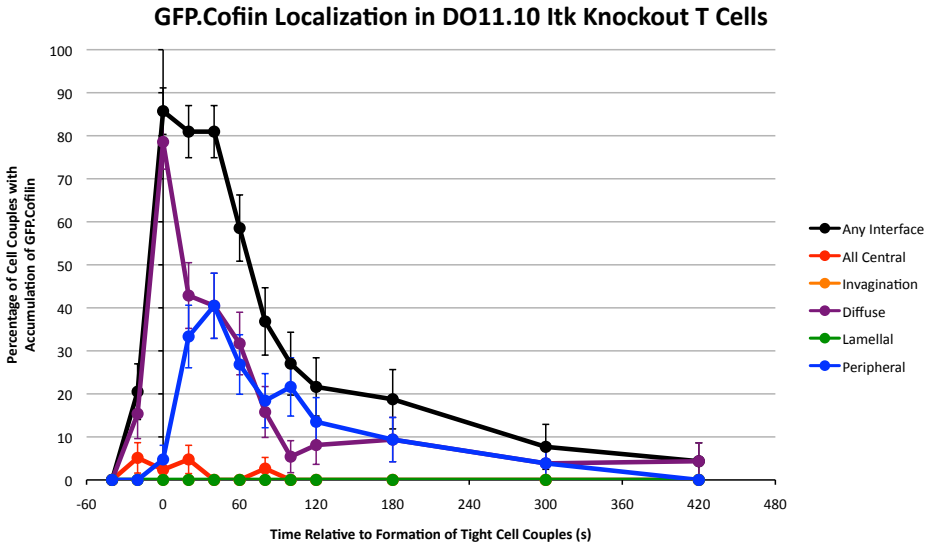

Figure 10: Spatiotemporal Localization of GFP.Cofilin in CD4$^+$ DO11.10 TCR Transgenic Wildtype or Itk$^{-/-}$ T Cells. Primed primary DO11.10 (A) wildtype or (B) Itk$^{-/-}$ T cells were transduced with GFP.Cofilin and stimulated with A20 B cell lymphoma APCs in the presence of 10μM OVA antigenic peptide. Time indicated is relative to the formation of a tight coupling of the T cell with the APC. The graphs display the percentage of cell couples that displayed accumulation of signaling intermediates with the indicated patterns. 65 cell couples were analyzed for the wildtype T cells; 42 cell couples for the Itk$^{-/-}$ T cells. Error bars represent standard error.

A.

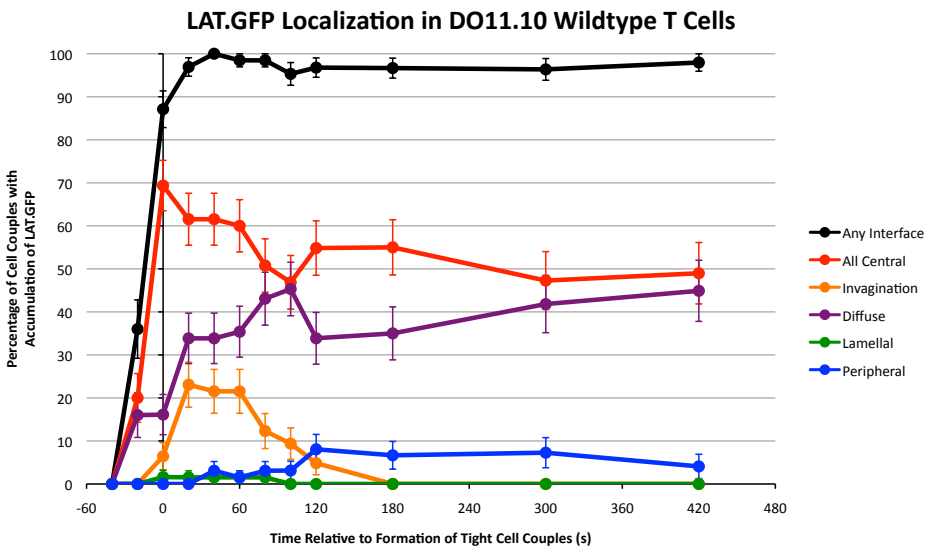

B.

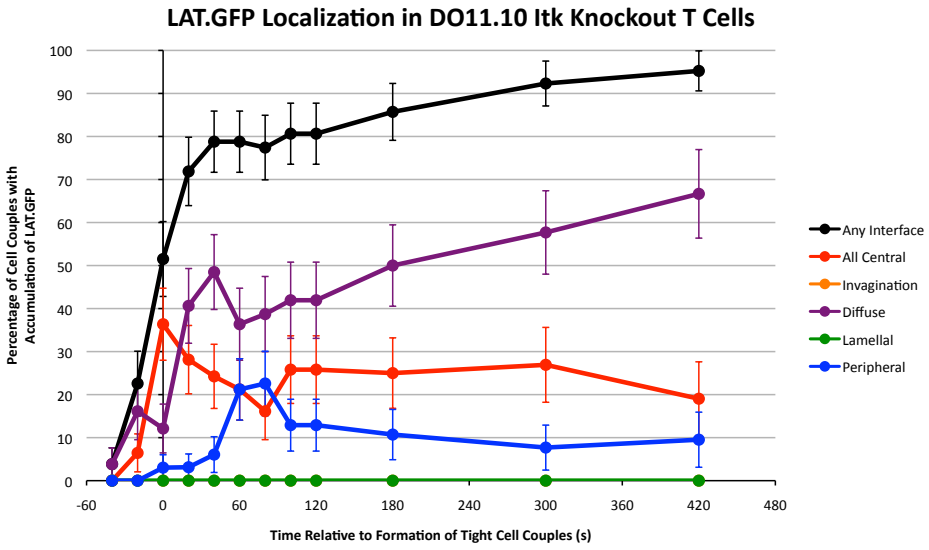

Figure 11: Spatiotemporal Localization of LAT.GFP in CD4$^+$ DO11.10 TCR Transgenic Wildtype or Itk$^{-/-}$ T Cells. Primed primary DO11.10 (A) wildtype or (B) Itk$^{-/-}$ T cells were transduced with LAT.GFP and stimulated with A20 B cell lymphoma APCs in the presence of 10μM OVA antigenic peptide. Time indicated is relative to the formation of a tight coupling of the T cell with the APC. The graphs display the percentage of cell couples that displayed accumulation of signaling intermediates with the indicated patterns. 65 cell couples were analyzed for the wildtype T cells; 33 cell couples for the Itk$^{-/-}$ T cells. Error bars represent standard error.

A.

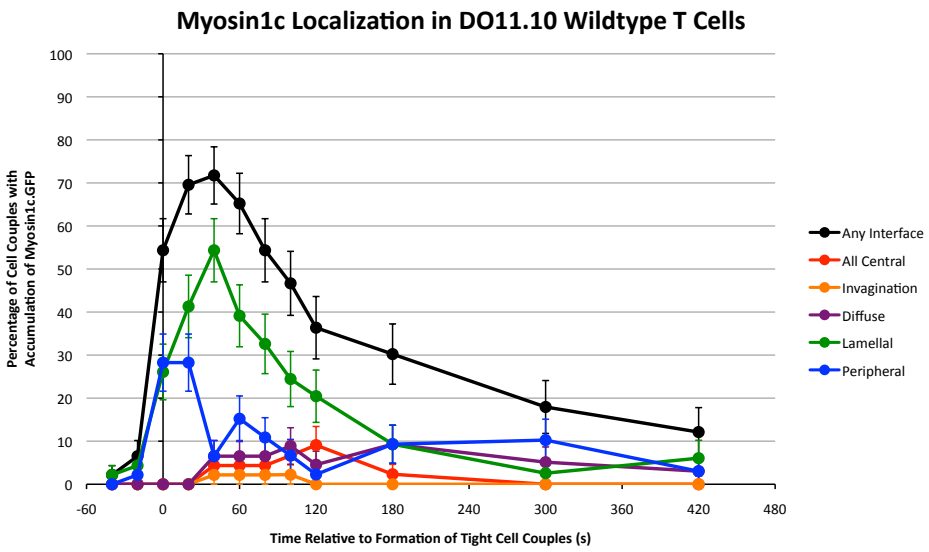

B.

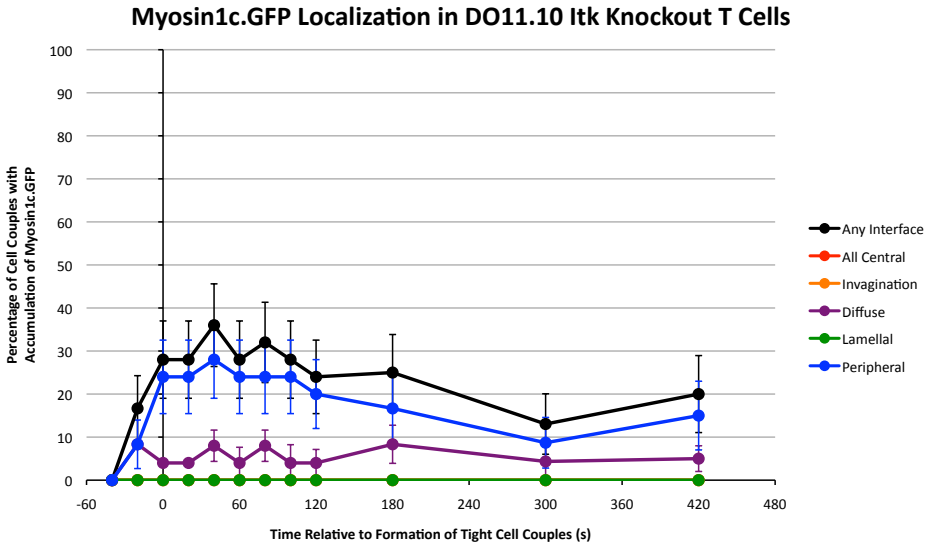

Figure 12: Spatiotemporal Localization of Myosin1c.GFP in CD4$^+$ DO11.10 TCR Transgenic Wildtype or Itk$^{-/-}$ T Cells. Primed primary DO11.10 (A) wildtype or (B) Itk$^{-/-}$ T cells were transduced with Myosin1c.GFP and stimulated with A20 B cell lymphoma APCs in the presence of 10μM OVA antigenic peptide. Time indicated is relative to the formation of a tight coupling of the T cell with the APC. The graphs display the percentage of cell couples that displayed accumulation of signaling intermediates with the indicated patterns. 46 cell couples were analyzed for the wildtype T cells; 25 cell couples for the Itk$^{-/-}$ T cells. Error bars represent standard error.

A.

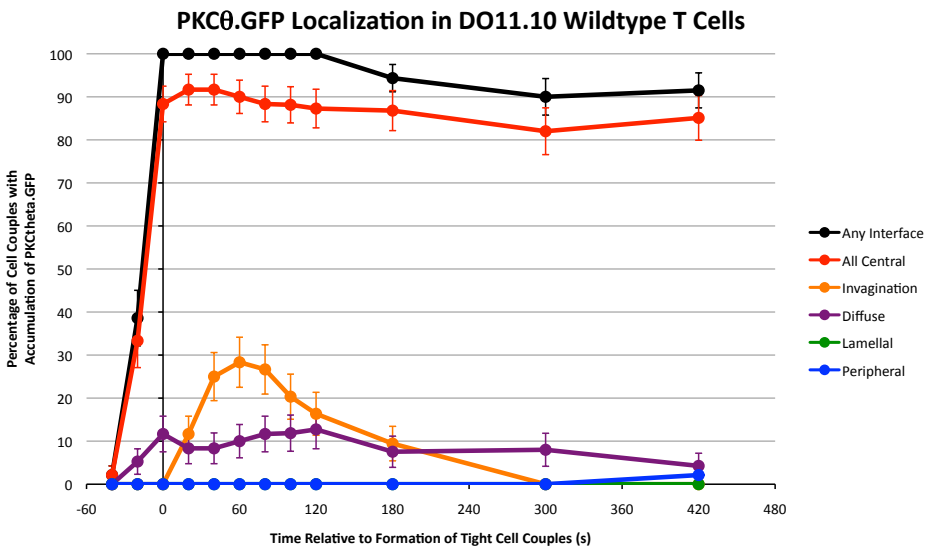

B.

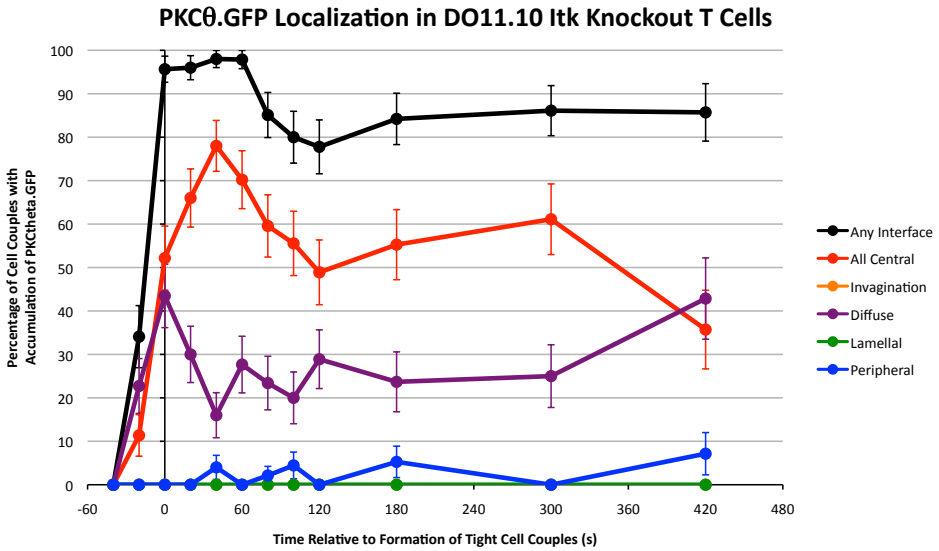

Figure 13: Spatiotemporal Localization of PKCθ.GFP in CD4$^+$ DO11.10 TCR Transgenic Wildtype or Itk$^{-/-}$ T Cells. Primed primary DO11.10 (A) wildtype or (B) Itk$^{-/-}$ T cells were transduced with PKCθ.GFP and stimulated with A20 B cell lymphoma APCs in the presence of 10μM OVA antigenic peptide. Time indicated is relative to the formation of a tight coupling of the T cell with the APC. The graphs display the percentage of cell couples that displayed accumulation of signaling intermediates with the indicated patterns. 60 cell couples were analyzed for the wildtype T cells; 50 cell couples for the Itk$^{-/-}$ T cells. Error bars represent standard error.

A.

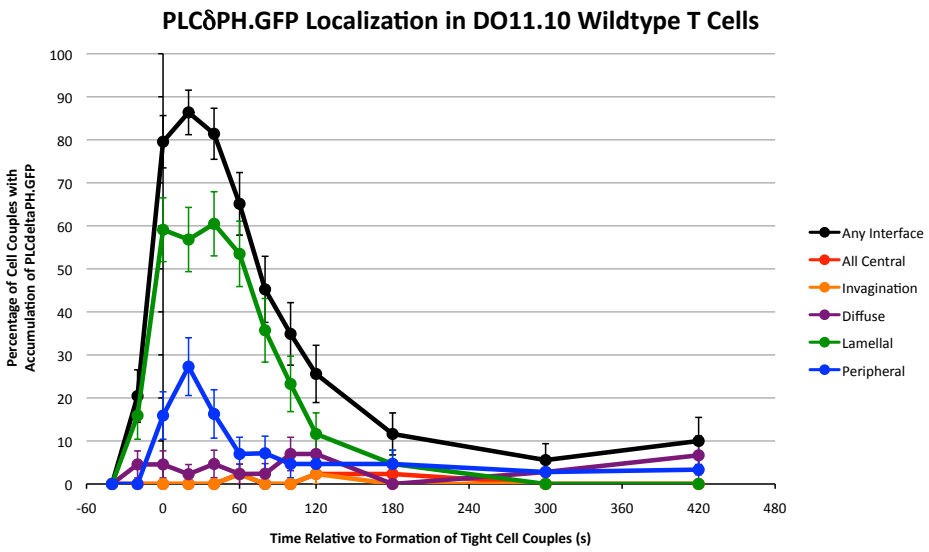

B.

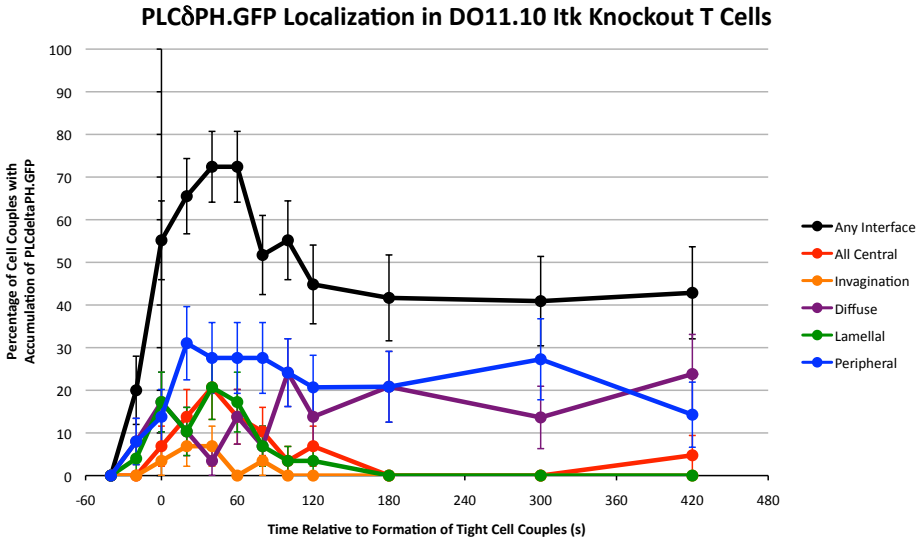

Figure 14: Spatiotemporal Localization of PLCδPH.GFP in CD4^{+} DO11.10 TCR Transgenic Wildtype or Itk$^{-/-}$ T Cells. Primed primary DO11.10 (A) wildtype or (B) Itk$^{-/-}$ T cells were transduced with PLCδPH.GFP and stimulated with A20 B cell lymphoma APCs in the presence of 10μM OVA antigenic peptide. Time indicated is relative to the formation of a tight coupling of the T cell with the APC. The graphs display the percentage of cell couples that displayed accumulation of signaling intermediates with the indicated patterns. 44 cell couples were analyzed for the wildtype T cells; 29 cell couples for the Itk$^{-/-}$ T cells. Error bars represent standard error.

A.

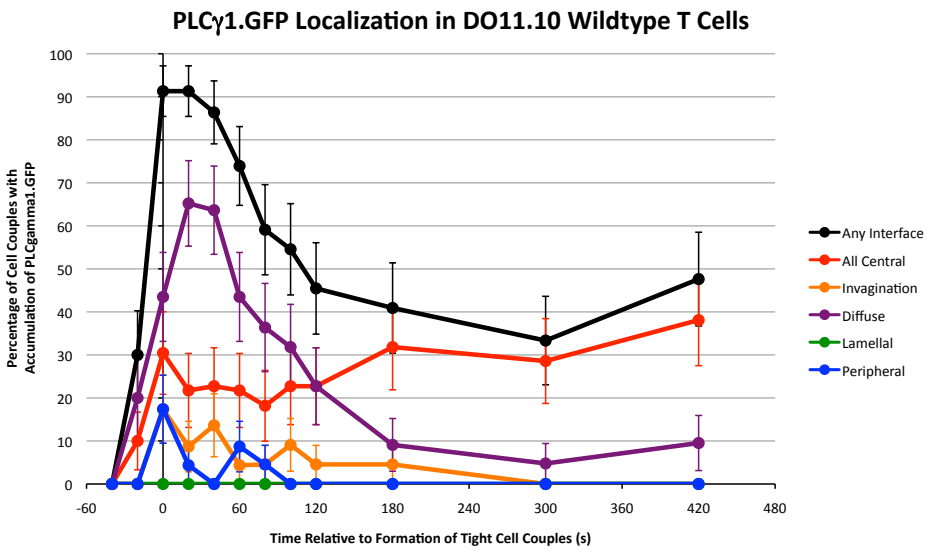

B.

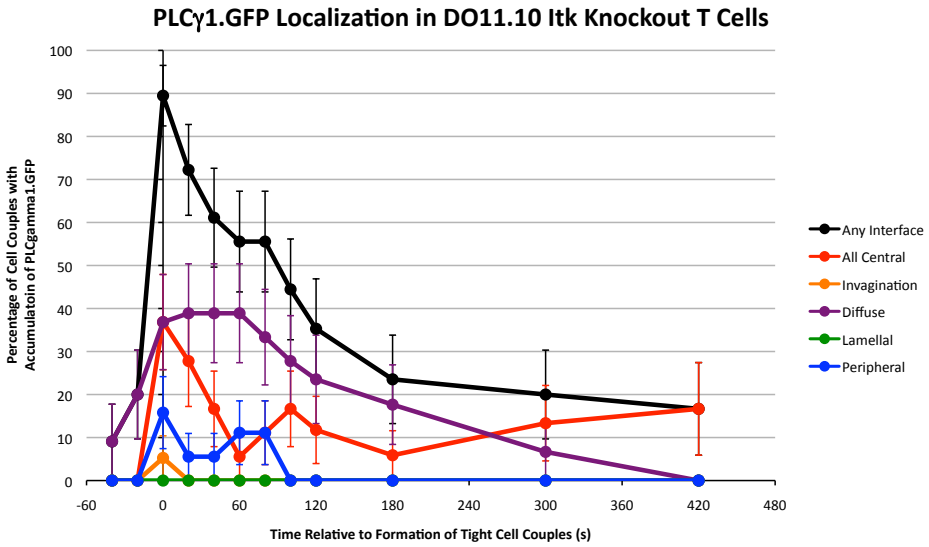

Figure 15: Spatiotemporal Localization of PLCγ1.GFP in CD4$^+$ DO11.10 TCR Transgenic Wildtype or Itk$^{-/-}$ T Cells. Primed primary DO11.10 (A) wildtype or (B) Itk$^{-/-}$ T cells were transduced with PLCγ1.GFP and stimulated with A20 B cell lymphoma APCs in the presence of 10μM OVA antigenic peptide. Time indicated is relative to the formation of a tight coupling of the T cell with the APC. The graphs display the percentage of cell couples that displayed accumulation of signaling intermediates with the indicated patterns. 23 cell couples were analyzed for the wildtype T cells; 18 cell couples for the Itk$^{-/-}$ T cells. Error bars represent standard error.

A.

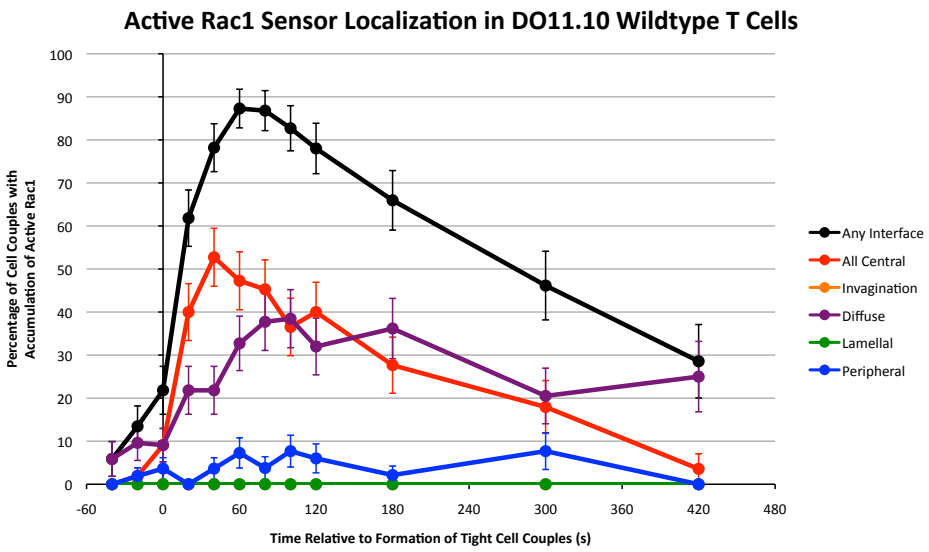

B.

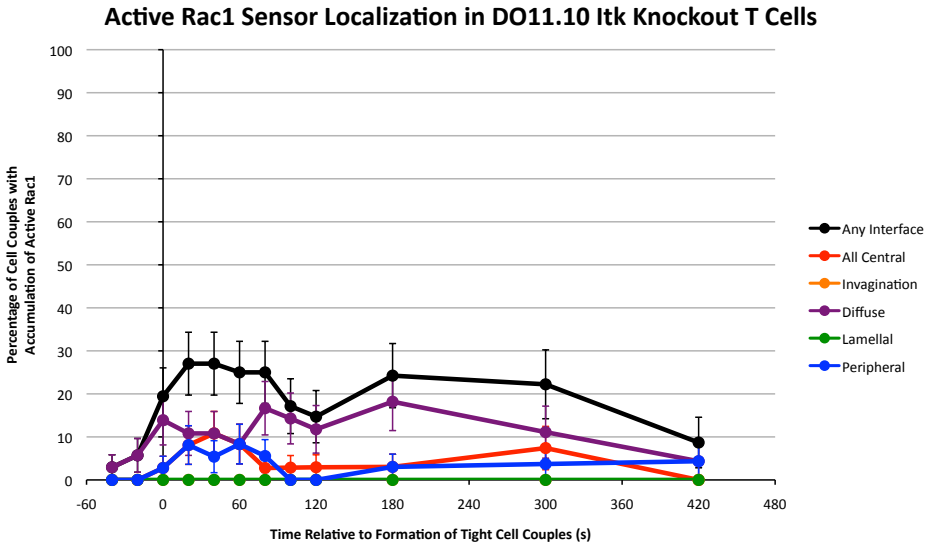

Figure 16: Spatiotemporal Localization of Active Rac1 Sensor in CD4$^+$ DO11.10 TCR Transgenic Wildtype or Itk$^{-/-}$ T Cells. Primed primary DO11.10 (A) wildtype or (B) Itk$^{-/-}$ T cells were transduced with Active Rac1 Sensor and stimulated with A20 B cell lymphoma APCs in the presence of 10μM OVA antigenic peptide. Time indicated is relative to the formation of a tight coupling of the T cell with the APC. The graphs display the percentage of cell couples that displayed accumulation of signaling intermediates with the indicated patterns. 55 cell couples were analyzed for the wildtype T cells; 37 cell couples for the Itk$^{-/-}$ T cells. Error bars represent standard error.

A.

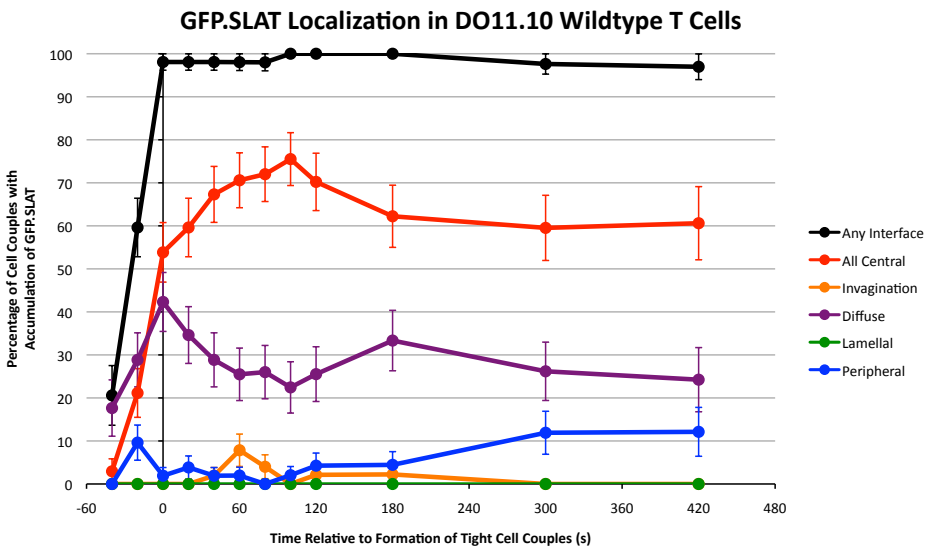

B.

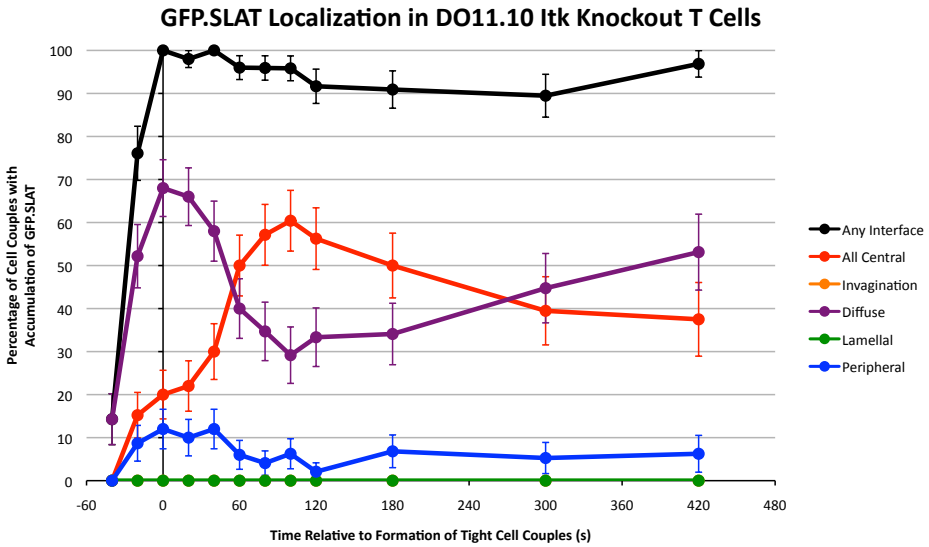

Figure 17: Spatiotemporal Localization of GFP.SLAT in CD4$^+$ DO11.10 TCR Transgenic Wildtype or Itk$^{-/-}$ T Cells. Primed primary DO11.10 (A) wildtype or (B) Itk$^{-/-}$ T cells were transduced with GFP.SLAT and stimulated with A20 B cell lymphoma APCs in the presence of 10μM OVA antigenic peptide. Time indicated is relative to the formation of a tight coupling of the T cell with the APC. The graphs display the percentage of cell couples that displayed accumulation of signaling intermediates with the indicated patterns. 52 cell couples were analyzed for the wildtype T cells; 50 cell couples for the Itk$^{-/-}$ T cells. Error bars represent standard error.

A.

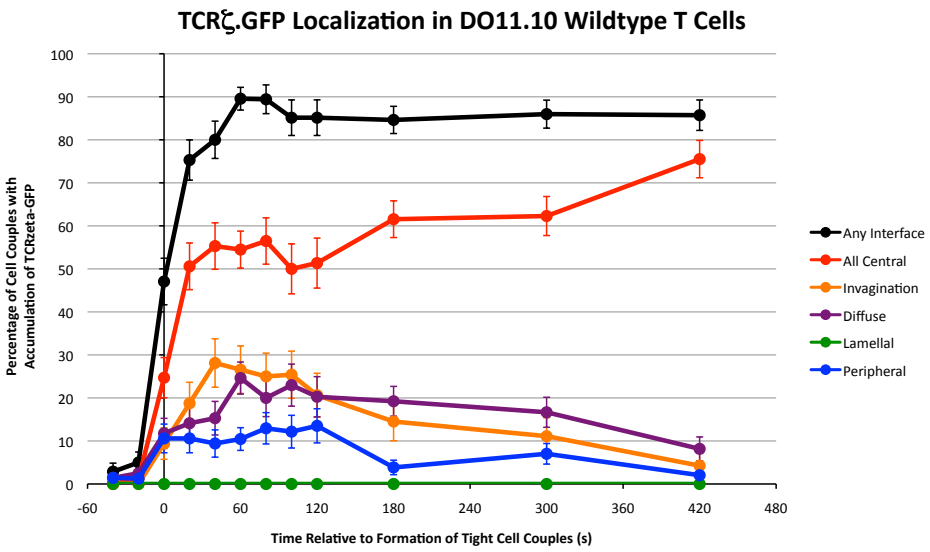

B.

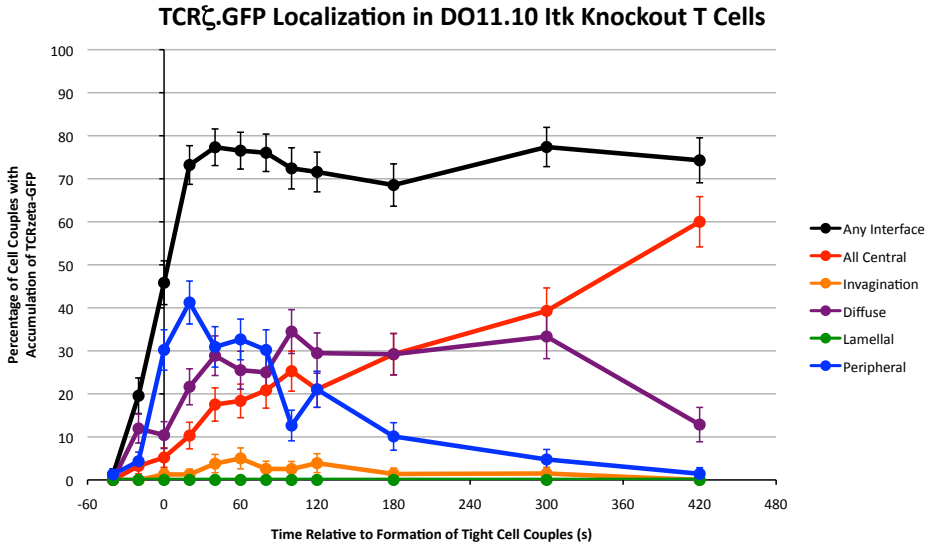

Figure 18: Spatiotemporal Localization of TCRζ.GFP in CD4$^+$ DO11.10 TCR Transgenic Wildtype or Itk$^{-/-}$ T Cells. Primed primary DO11.10 (A) wildtype or (B) Itk$^{-/-}$ T cells were transduced with TCRζ.GFP and stimulated with A20 B cell lymphoma APCs in the presence of 10μM OVA antigenic peptide. Time indicated is relative to the formation of a tight coupling of the T cell with the APC. The graphs display the percentage of cell couples that displayed accumulation of signaling intermediates with the indicated patterns. 134 cell couples were analyzed for the wildtype T cells; 97 cell couples for the Itk$^{-/-}$ T cells. Error bars represent standard error.

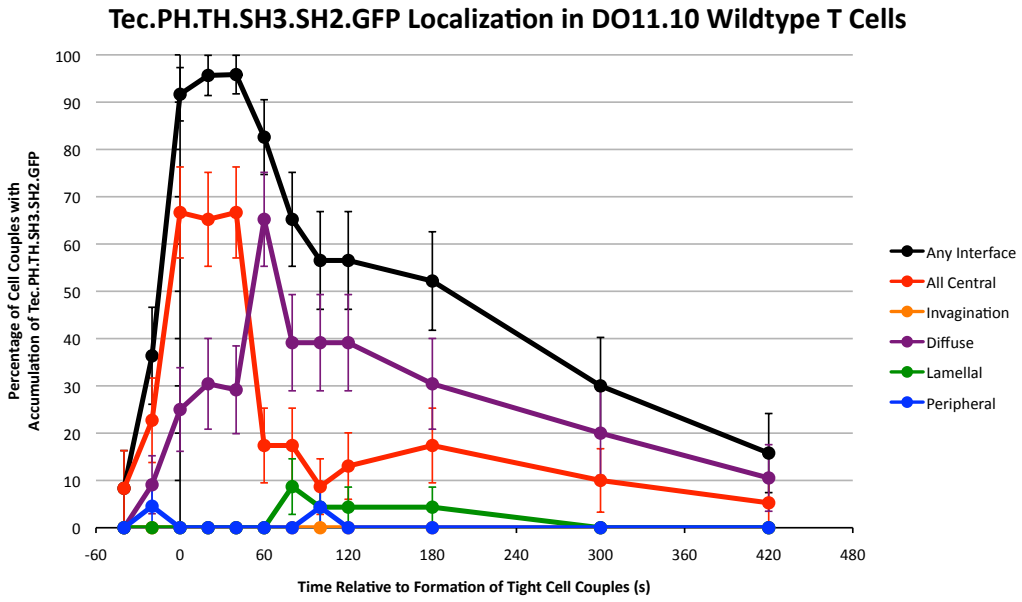

Figure 19: Spatiotemporal Localization of Tec.PH.TH.SH3.SH2.GFP in CD4$^+$ DO11.10 TCR Transgenic Wildtype T Cells. Primed primary DO11.10 (A) wildtype T cells were transduced with Tec.PH.TH.SH3.SH2.GFP and stimulated with A20 B cell lymphoma APCs in the presence of 10μM OVA antigenic peptide. Time indicated is relative to the formation of a tight coupling of the T cell with the APC. The graphs display the percentage of cell couples that displayed accumulation of signaling intermediates with the indicated patterns. 24 cell couples were analyzed. Error bars represent standard error.

A.

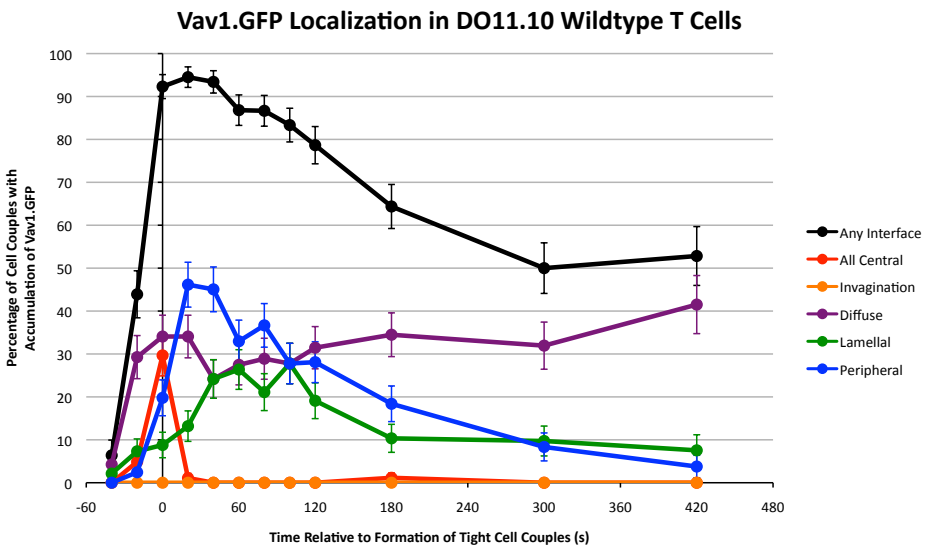

B.

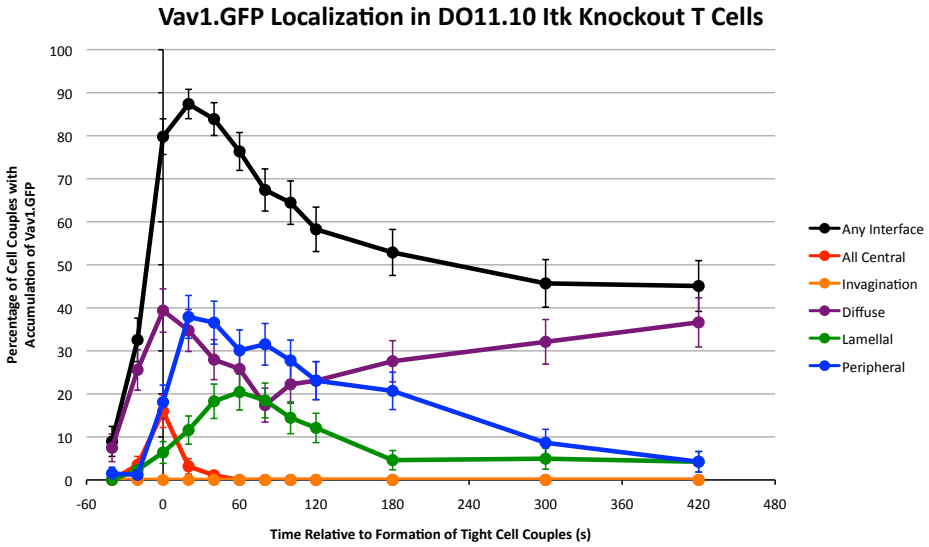

Figure 20: Spatiotemporal Localization of Vav1.GFP in CD4$^+$ DO11.10 TCR Transgenic Wildtype or Itk$^{-/-}$ T Cells. Primed primary DO11.10 (A) wildtype or (B) Itk$^{-/-}$ T cells were transduced with Vav1.GFP and stimulated with A20 B cell lymphoma APCs in the presence of 10μM OVA antigenic peptide. Time indicated is relative to the formation of a tight coupling of the T cell with the APC. The graphs display the percentage of cell couples that displayed accumulation of signaling intermediates with the indicated patterns. 91 cell couples were analyzed for the wildtype T cells; 95 cell couples for the Itk$^{-/-}$ T cells. Error bars represent standard error.

A. Wildtype

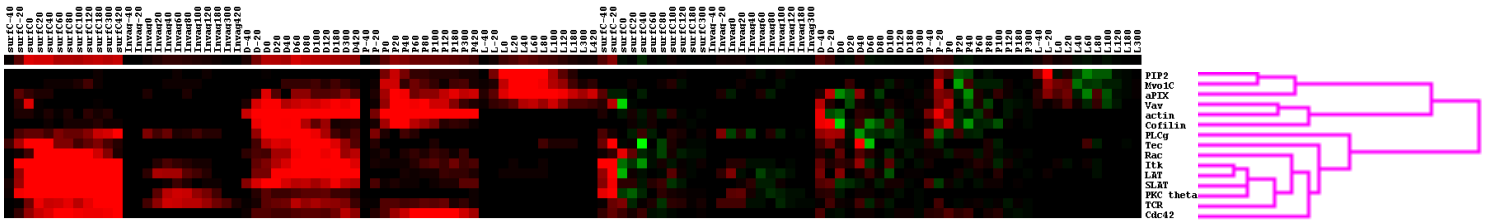

B. Itk$^{-/-}$

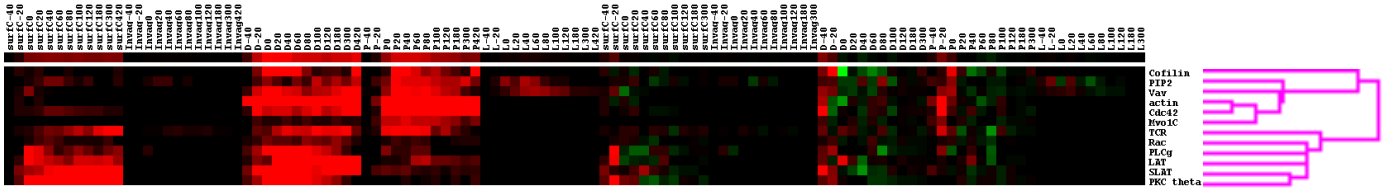

Figure 21: Cluster Analysis of Spatiotemporal Patterning in DO11.10 TCR Transgenic Wildtype and Itk$^{-/-}$ T Cells. Spatiotemporal patterning of sensors was determined in DO11.10 TCR transgenic (A) wildtype and (B) Itk$^{-/-}$ T cells upon stimulation with A20 B cell lymphoma APCs in the presence of 10μM OVA antigenic peptide. Spatial patterning was categorized into five mutually exclusive phenotypes – Surface Central (SurfC), Invagination (Inv), Diffuse (D), Peripheral (P) or Lamellum (L) – and were evaluated at 12 time points (-40, -20, 0, 20, 40, 60, 80, 100, 120, 180, 300, 420 seconds, with 0 seconds representing tight T cell / APC coupling). The percentage occurrence of each pattern is represented in shades of red (black = 0%, bright red = 100%). To address the pattern dynamics, the percentage change between time points was determined – Red indicates an increase with green being a decrease in percentage occurrence of a particular pattern relative to the previous time point. Cluster analysis based on Pearson's correlation was performed on the entire data set, with the dendrogram displayed in pink.

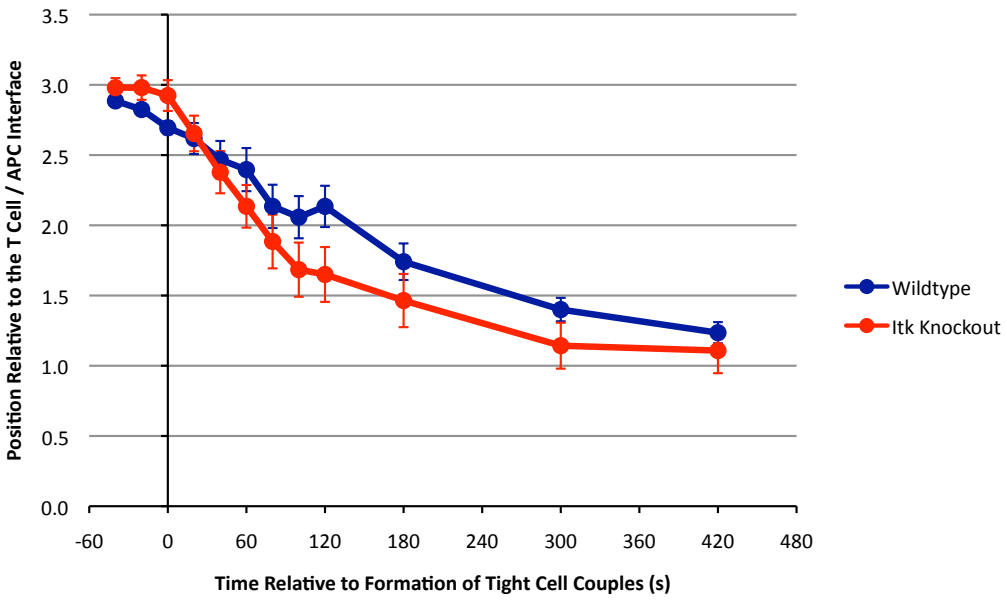

Figure 22: **Translocation of STIM1.GFP in CD4^{+} DO11.10 TCR Transgenic Wildtype or Itk$^{-/-}$ T Cells.** Primed primary DO11.10 wildtype (blue) or Itk$^{-/-}$ (red) T cells were transduced with STIM1.GFP and stimulated with A20 B cell lymphoma APCs in the presence of 10μM OVA antigenic peptide. The graph displays the average position of the peak fluorescent intensity of STIM1.GFP as it moves from the distal pole to the T cell interface. A position of 1 is closest to the interface, whereas a position of 3 is furthest from the interface. Time indicated is relative to the formation of a tight coupling of the T cell with the APC. 37 cell couples were analyzed for the wildtype T cells; 51 cell couples for the Itk$^{-/-}$ T cells. Error bars represent standard error.

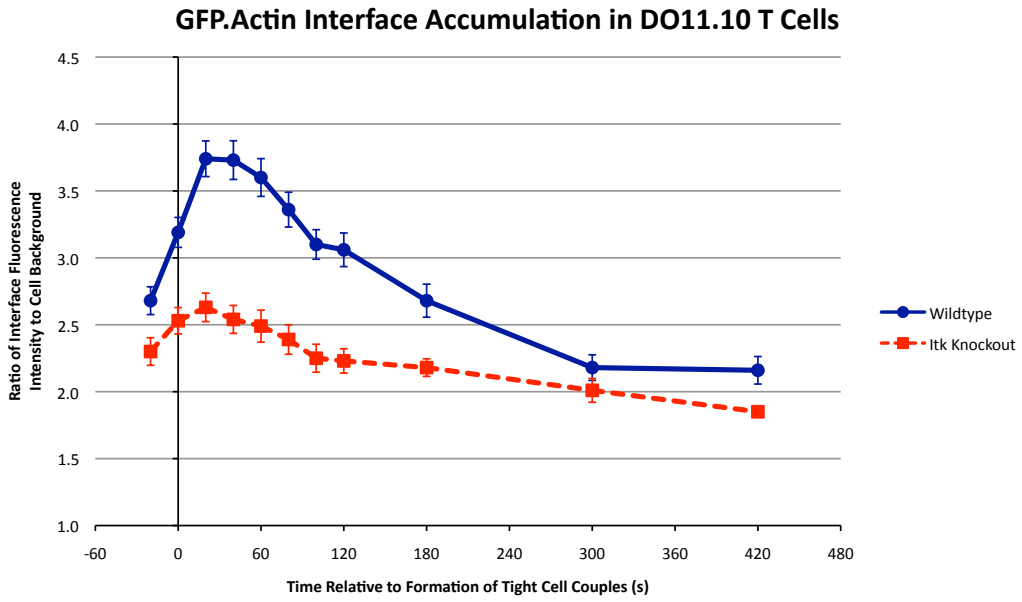

Figure 23: Interface Accumulation of GFP.Actin in $CD4^+$ DO11.10 TCR Transgenic Wildtype or $Itk^{-/-}$ T Cells. Primed primary DO11.10 (A) wildtype or (B) $Itk^{-/-}$ T cells were transduced with GFP.Actin and stimulated with A20 B cell lymphoma APCs in the presence of 10μM OVA antigenic peptide. Time indicated is relative to the formation of a tight coupling of the T cell with the APC. The graphs display the ratio of the fluorescence intensity at the T cell / APC interface to the cell background. A measure of 3, for example, would mean that fluorescence at the interface was three times as bright (three times as much GFP.Actin) as the background of the cell. 70 cell couples were analyzed for the wildtype T cells; 49 cell couples for the $Itk^{-/-}$ T cells. Error bars represent standard error.

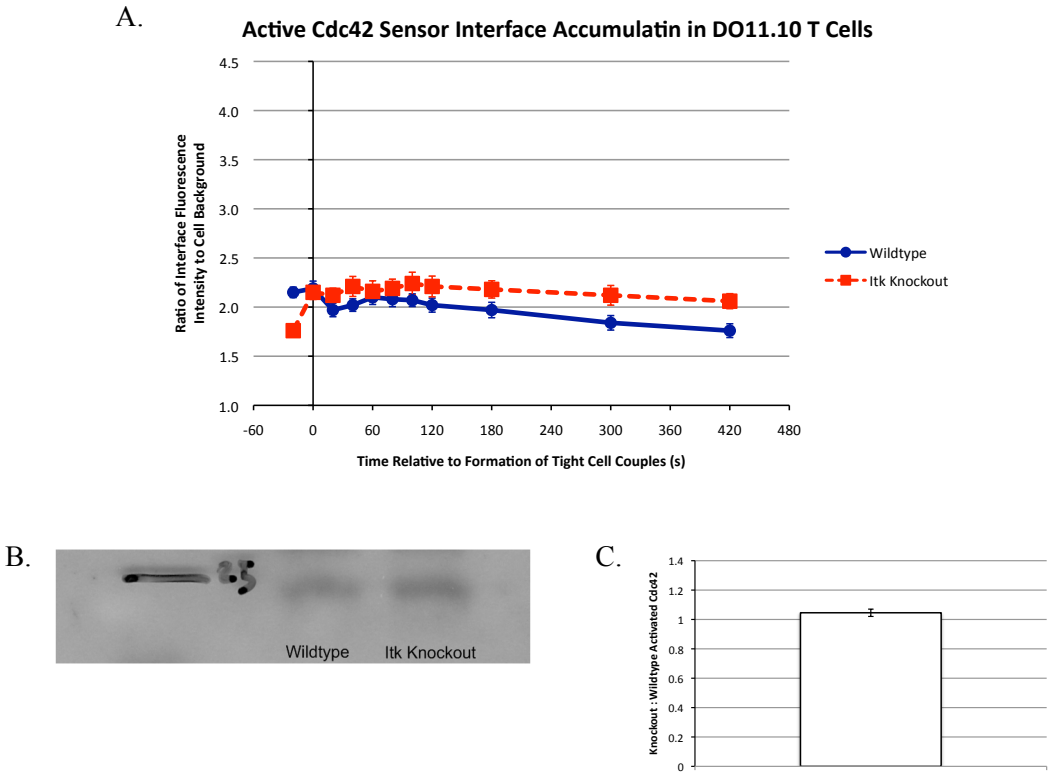

Figure 24: Cdc42 Activation in CD4^{+} DO11.10 TCR Transgenic Wildtype or Itk$^{-/-}$ T Cells. (A) Primed primary DO11.10 wildtype or Itk$^{-/-}$ T cells were transduced with Activated Cdc42 Sensor and stimulated with A20 B cell lymphoma APCs in the presence of 10μM OVA antigenic peptide. Time indicated is relative to the formation of a tight coupling of the T cell with the APC. The graphs display the ratio of the fluorescence intensity at the T cell / APC interface to the cell background. Activated Cdc42 Sensor consists of a GFP fused to the GTPase binding domain of WASP (Wiskott-Aldrich Syndrome Protein), which binds to GTP-bound Cdc42 (activated Cdc42). 38 cell couples were analyzed for the wildtype T cells; 37 cell couples for the Itk$^{-/-}$ T cells. Error bars represent standard error. (B) To corroborate the intensity analysis, activated Cdc42 was pulled down and detected by immunoblot using the Active Cdc42 Pull-Down and Detection Kit (Thermo Scientific; Catalog number 89857). Pull downs were conducted on 2.5x10^{6} million wildtype or Itk$^{-/-}$ T cells stimulated with 10μM α-CD3 and 10μM α-CD28 for 5 minutes at 37°C. (C) The calculated ratio of Wildtype : Knockout band intensity was plotted. Wildtype and Itk$^{-/-}$ samples were treated concurrently. The graph represents the mean of three independently collected and treated sample pairs. Error bars represent standard error.

A.

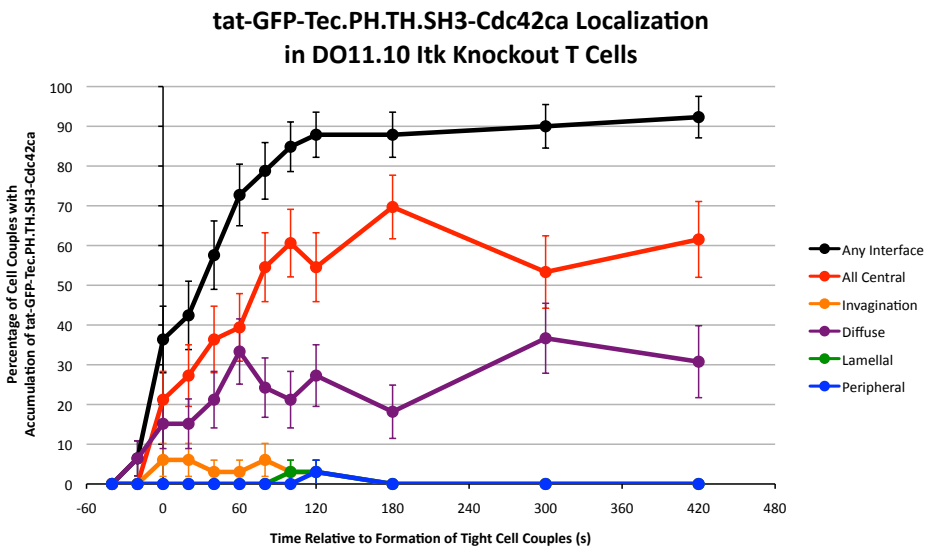

B.

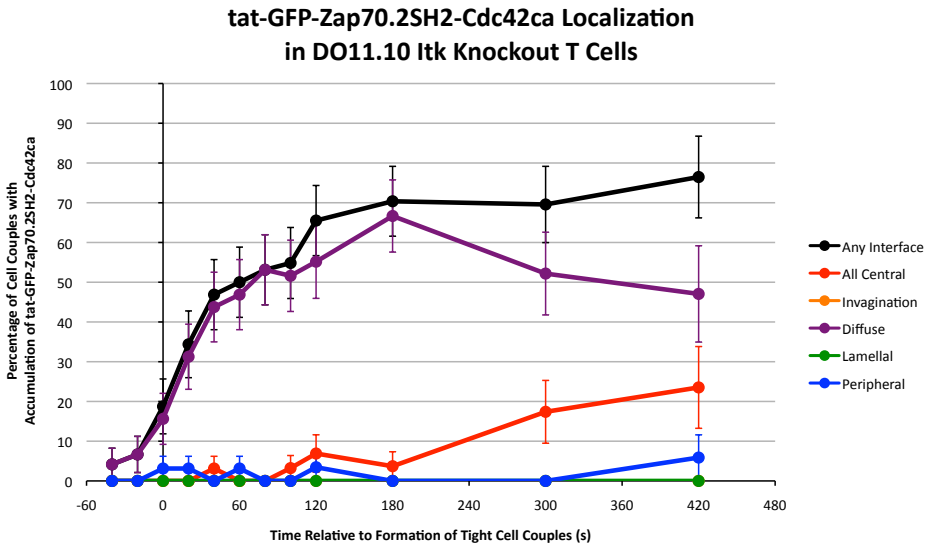

Figure 25: Spatiotemporal Localization of tat-GFP-Tec.PH.TH.SH3-Cdc42ca and tat-GFP-Zap70.2SH2-Cdc42ca in $CD4^+$ DO11.10 TCR Transgenic $Itk^{-/-}$ T Cells. Primed primary DO11.10 (A) wildtype or (B) $Itk^{-/-}$ T cells were transduced with either tat-GFP-Tec.PH.TH.SH3-Cdc42ca or tat-GFP-Zap70.2SH2-Cdc42ca and stimulated with A20 B cell lymphoma APCs in the presence of 10μM OVA antigenic peptide. Time indicated is relative to the formation of a tight coupling of the T cell with the APC. The graphs display the percentage of cell couples that displayed accumulation of signaling intermediates with the indicated patterns. 33 cell couples were analyzed for the tat-GFP-Tec.PH.TH.SH3-Cdc42ca construct; 32 cell couples for the tat-GFP-Zap70.2SH2 construct. Error bars represent standard error.

A.

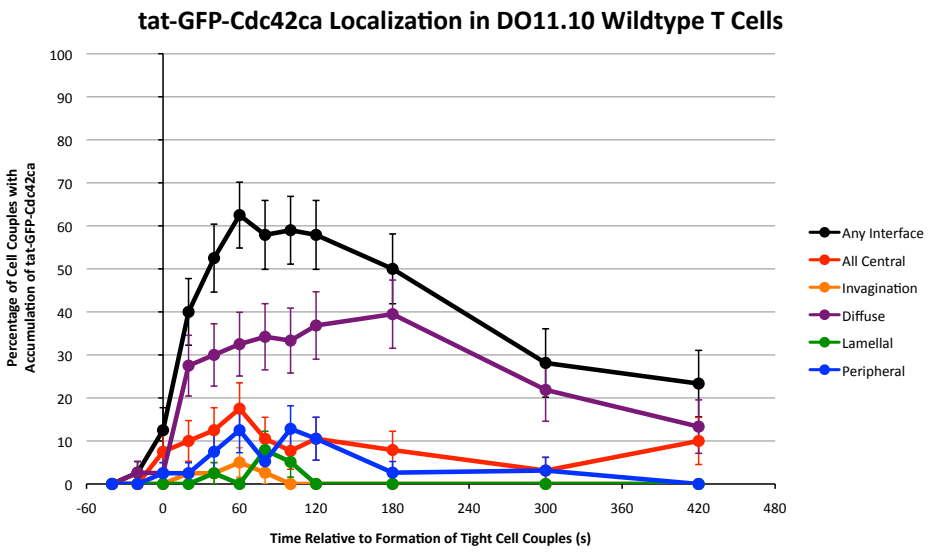

B.

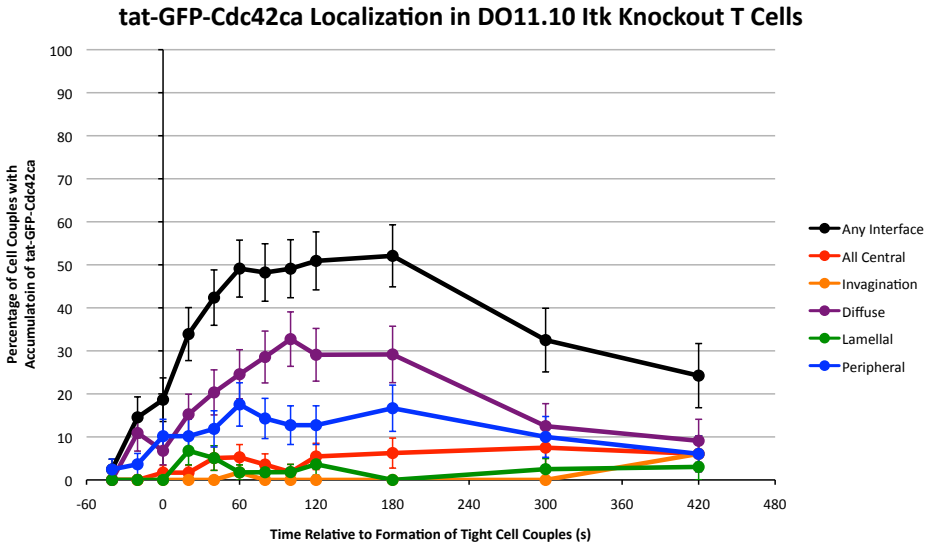

Figure 26: Spatiotemporal Localization of tat-GFP-Cdc42ca in CD4$^+$ DO11.10 TCR Transgenic Wildtype or Itk$^{-/-}$ T Cells. Primed primary DO11.10 (A) wildtype or (B) Itk$^{-/-}$ T cells were transduced with tat-GFP-Cdc42ca and stimulated with A20 B cell lymphoma APCs in the presence of 10μM OVA antigenic peptide. Time indicated is relative to the formation of a tight coupling of the T cell with the APC. The graphs display the percentage of cell couples that displayed accumulation of signaling intermediates with the indicated patterns. 40 cell couples were analyzed for the wildtype T cells; 59 cell couples for the Itk$^{-/-}$ T cells. Error bars represent standard error.

A.

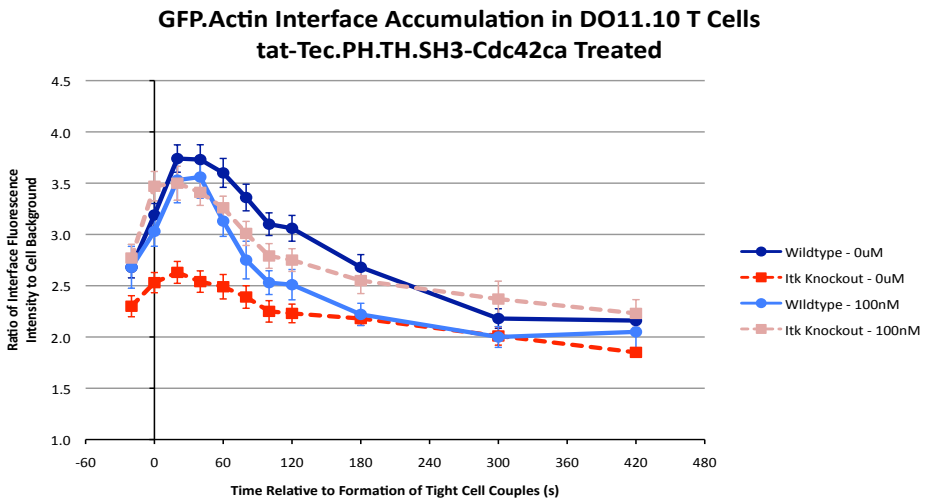

B.

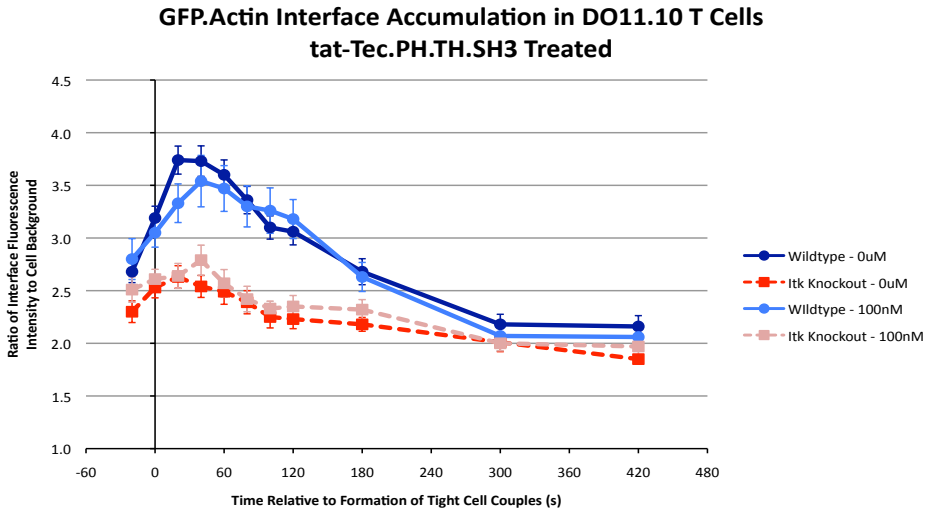

Figure 27: Centrally Targeted Constitutively Active Cdc42 Restores Actin Polymerization at the Immunological Synapse of Itk$^{-/-}$ T Cells. Primed primary DO11.10 wildtype or Itk$^{-/-}$ T cells were transduced with GFP.Actin and stimulated with A20 B cell lymphoma APCs in the presence of 10μM OVA antigenic peptide and (A) 0-100nM tat-Tec.PH.TH.SH3-Cdc42ca or (B) tat-Tec.PH.TH.SH3. Time indicated is relative to the formation of a tight coupling of the T cell with the APC. The graphs display the ratio of the fluorescence intensity at the T cell / APC interface to the cell background. A total of 207 cell couples were analyzed for the tat-Tec.PH.TH.SH3-Cdc42ca treated T cells; 213 cell couples for the tat-Tec.PH.TH.SH3 treated cells. Error bars represent standard error.

A.

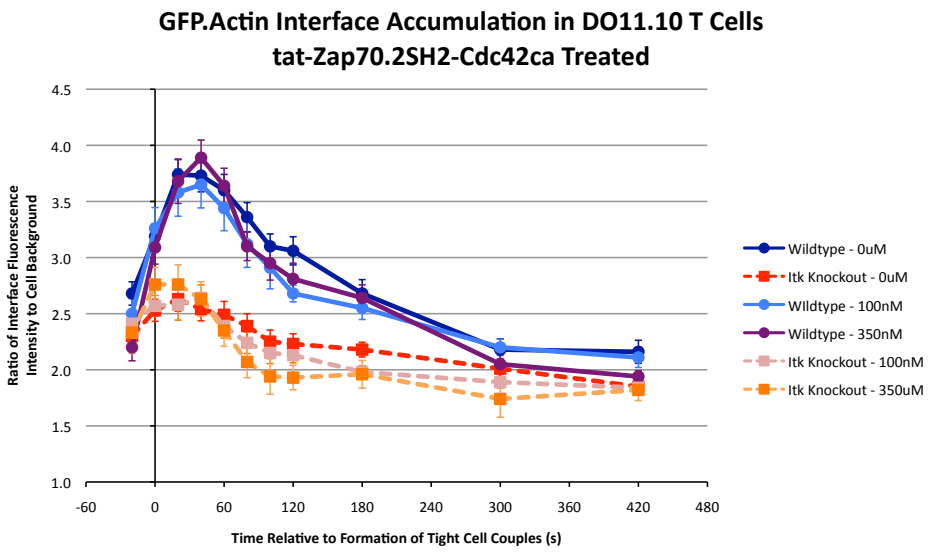

B.

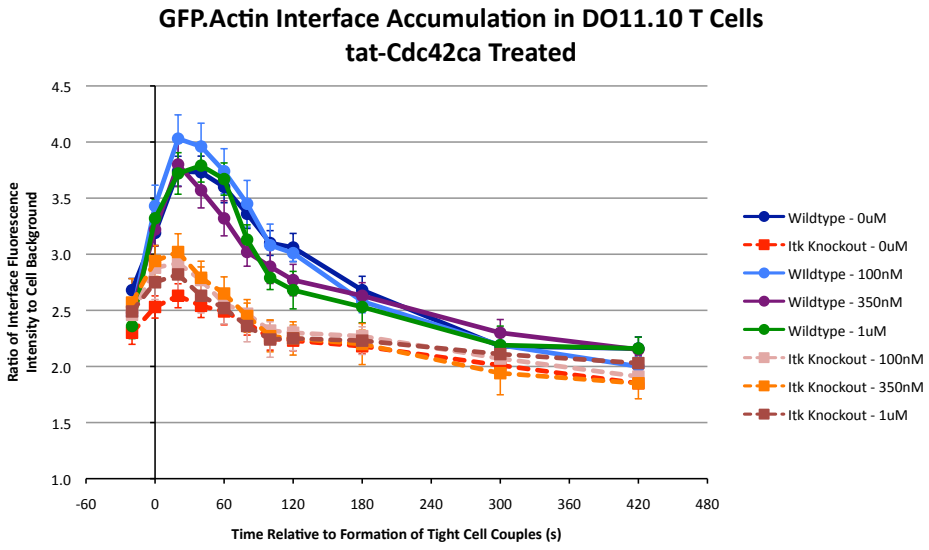

Figure 28: Untargeted Constitutively Active Cdc42 Does Not Restore Actin Polymerization at the Interface in Itk$^{-/-}$ T Cells. Primed primary DO11.10 wildtype or Itk$^{-/-}$ T cells were transduced with GFP.Actin and stimulated with A20 B cell lymphoma APCs in the presence of 10μM OVA antigenic peptide and (A) 0-350nM tat-Zap70.2SH2-Cdc42ca or (B) 0-1μM tat-Cdc42ca. Time indicated is relative to the formation of a tight coupling of the T cell with the APC. The graphs display the ratio of the fluorescence intensity at the T cell / APC interface to the cell background. A total of 246 cell couples were analyzed for the tat-Zap70.2SH2-Cdc42ca treated T cells; 303 cell couples for the tat-Cdc42ca treated cells. Error bars represent standard error.

A.

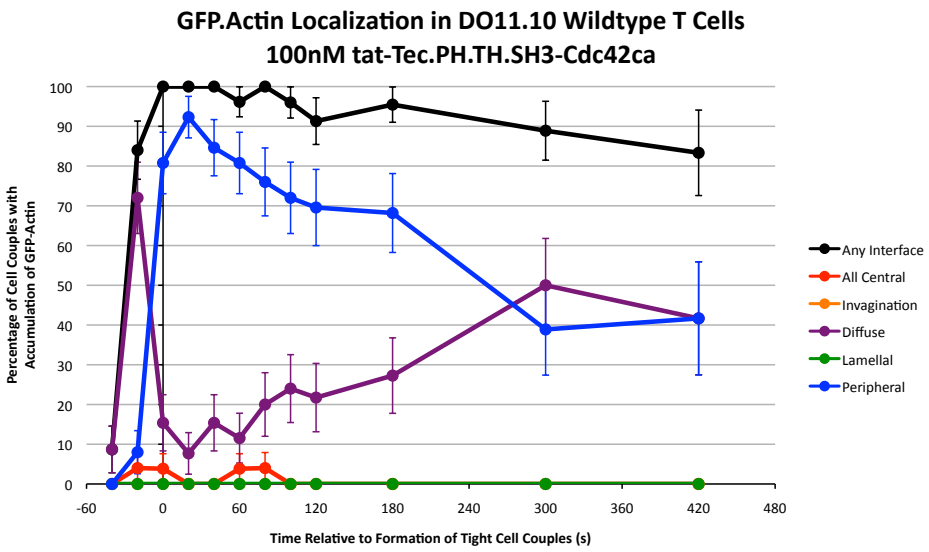

B.

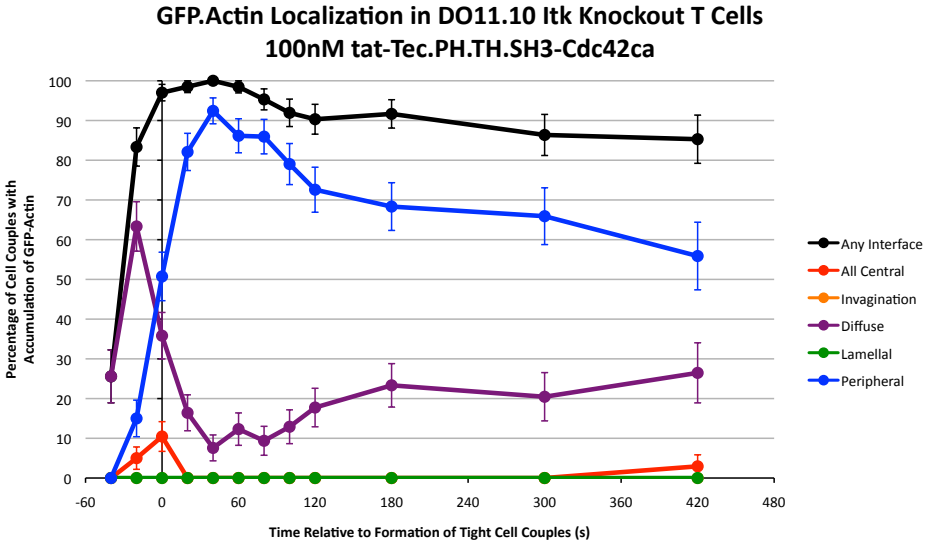

Figure 29: Spatiotemporal Localization of GFP.Actin in CD4$^+$ DO11.10 TCR Transgenic Wildtype or Itk$^{-/-}$ T Cells Treated with 100nM tat-Tec.PH.TH.SH3-Cdc42ca. Primed primary DO11.10 (A) wildtype or (B) Itk$^{-/-}$ T cells were transduced with GFP.Actin and stimulated with A20 B cell lymphoma APCs in the presence of 10μM OVA antigenic peptide and 100nM tat-Tec.PH.TH.SH3-Cdc42ca. Time indicated is relative to the formation of a tight coupling of the T cell with the APC. The graphs display the percentage of cell couples that displayed accumulation of signaling intermediates with the indicated patterns. 26 cell couples were analyzed for the wildtype T cells; 67 cell couples for the Itk$^{-/-}$ T cells. Error bars represent standard error.

A.

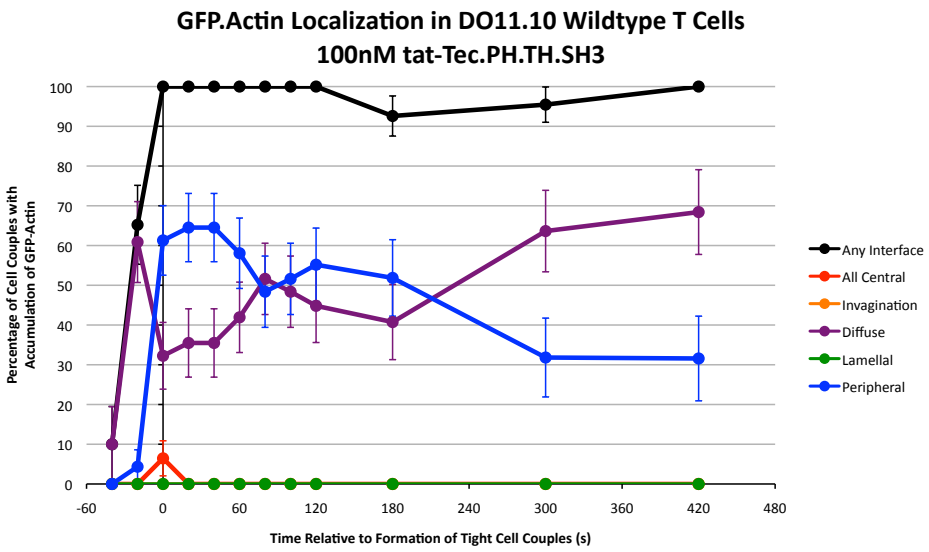

B.

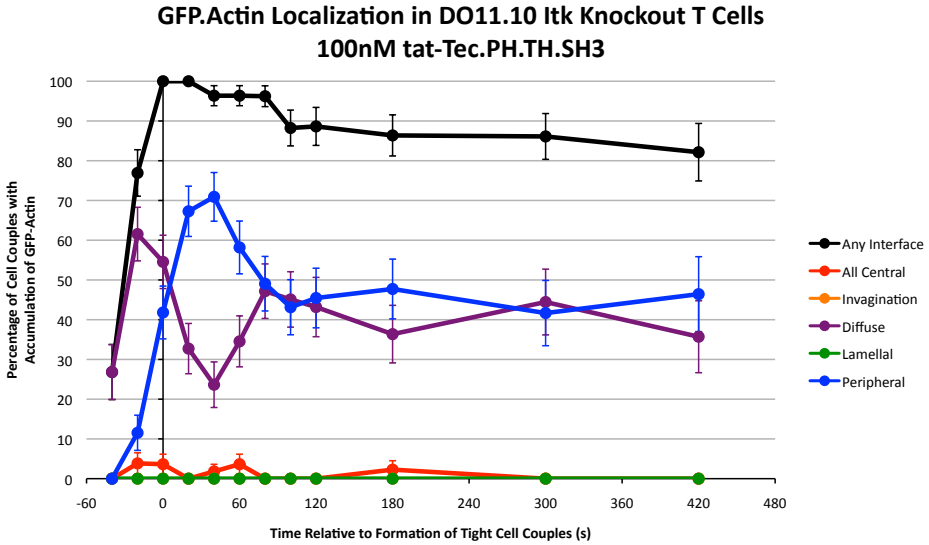

Figure 30: Spatiotemporal Localization of GFP.Actin in CD4$^+$ DO11.10 TCR Transgenic Wildtype or Itk$^{-/-}$ T Cells Treated with 100nM tat-Tec.PH.TH.SH3. Primed primary DO11.10 (A) wildtype or (B) Itk$^{-/-}$ T cells were transduced with GFP.Actin and stimulated with A20 B cell lymphoma APCs in the presence of 10μM OVA antigenic peptide and 100nM tat-Tec.PH.TH.SH3. Time indicated is relative to the formation of a tight coupling of the T cell with the APC. The graphs display the percentage of cell couples that displayed accumulation of signaling intermediates with the indicated patterns. 31 cell couples were analyzed for the wildtype T cells; 55 cell couples for the Itk$^{-/-}$ T cells. Error bars represent standard error.

A.

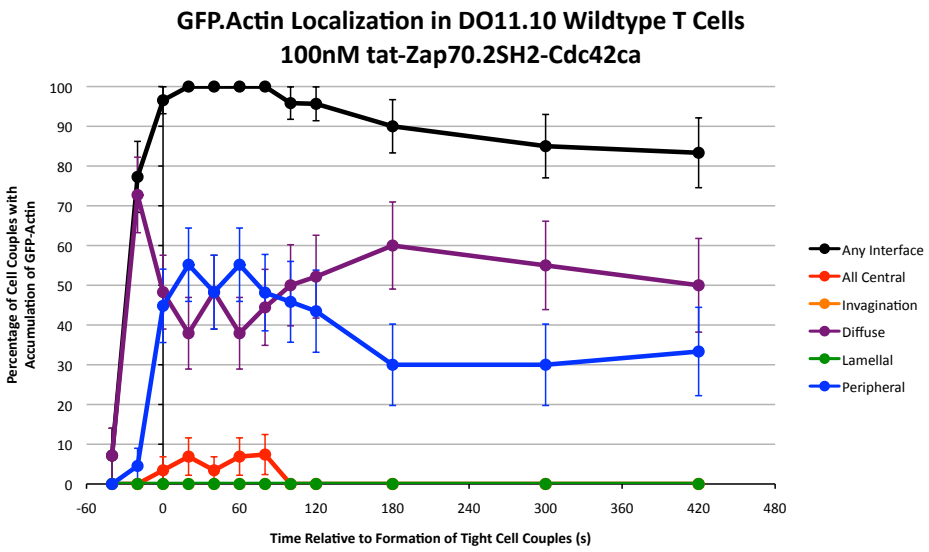

B.

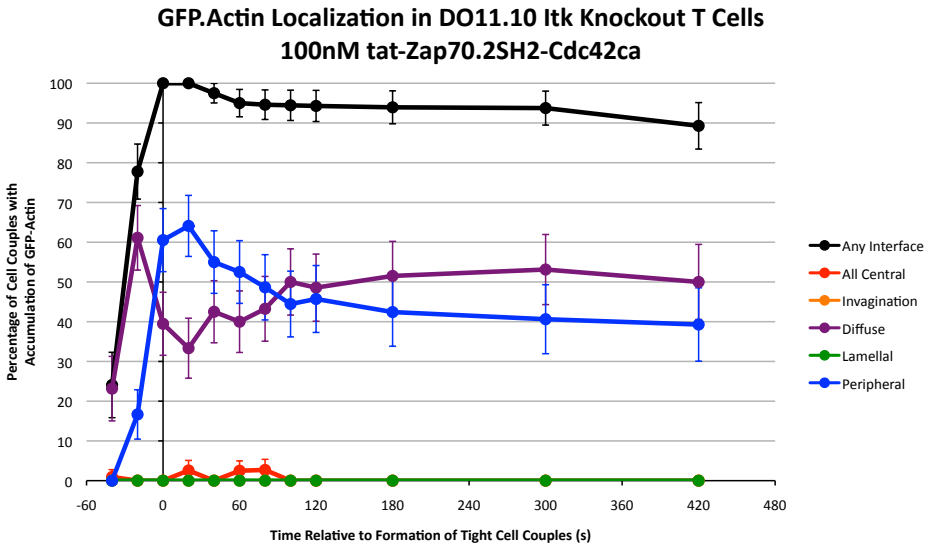

Figure 31: Spatiotemporal Localization of GFP.Actin in CD4$^+$ DO11.10 TCR Transgenic Wildtype or Itk$^{-/-}$ T Cells Treated with 100nM tat-Zap70.2SH2-Cdc42ca. Primed primary DO11.10 (A) wildtype or (B) Itk$^{-/-}$ T cells were transduced with GFP.Actin and stimulated with A20 B cell lymphoma APCs in the presence of 10μM OVA antigenic peptide and 100nM tat-Zap70.2SH2-Cdc42ca. Time indicated is relative to the formation of a tight coupling of the T cell with the APC. The graphs display the percentage of cell couples that displayed accumulation of signaling intermediates with the indicated patterns. 29 cell couples were analyzed for the wildtype T cells; 40 cell couples for the Itk$^{-/-}$ T cells. Error bars represent standard error.

A.

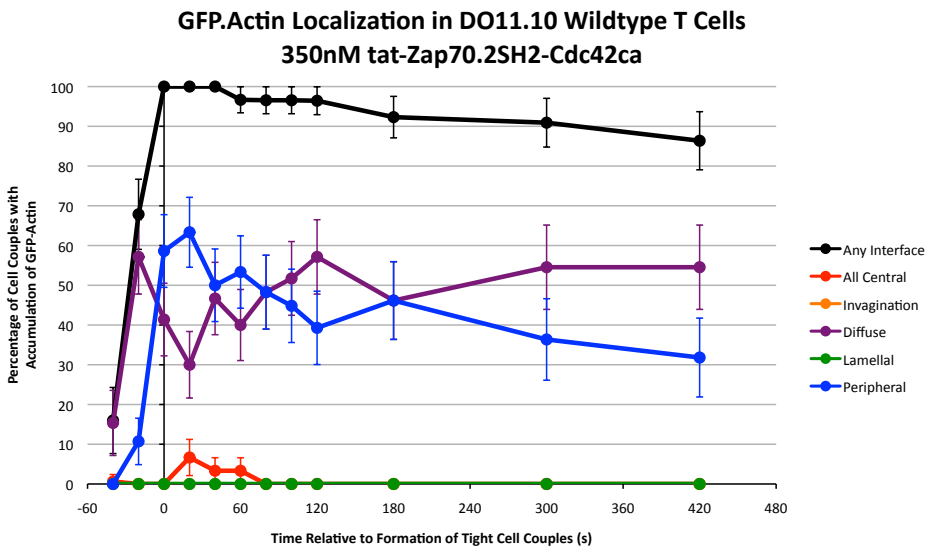

B.

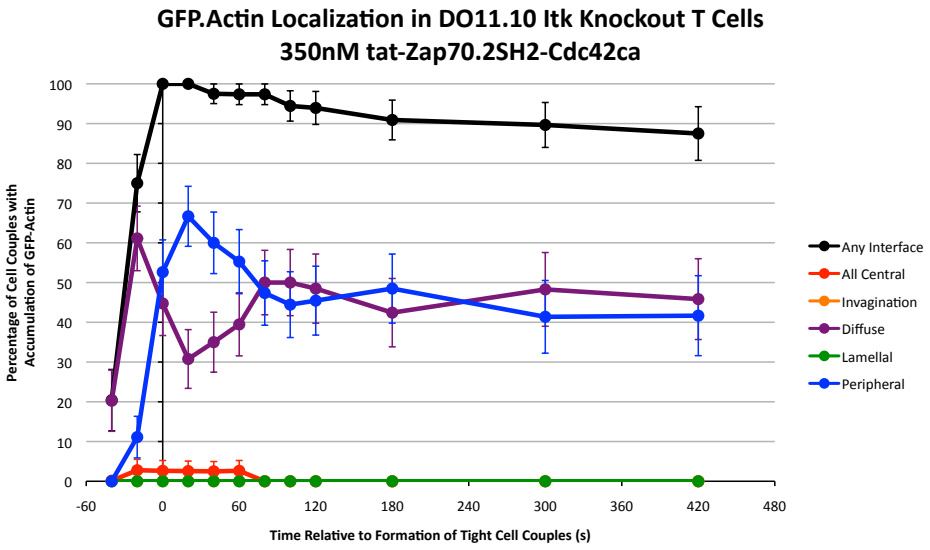

Figure 32: Spatiotemporal Localization of GFP.Actin in CD4$^+$ DO11.10 TCR Transgenic Wildtype or Itk$^{-/-}$ T Cells Treated with 350nM tat-Zap70.2SH2-Cdc42ca. Primed primary DO11.10 (A) wildtype or (B) Itk$^{-/-}$ T cells were transduced with GFP.Actin and stimulated with A20 B cell lymphoma APCs in the presence of 10μM OVA antigenic peptide and 350nM tat-Zap70.2SH2-Cdc42ca. Time indicated is relative to the formation of a tight coupling of the T cell with the APC. The graphs display the percentage of cell couples that displayed accumulation of signaling intermediates with the indicated patterns. 30 cell couples were analyzed for the wildtype T cells; 40 cell couples for the Itk$^{-/-}$ T cells. Error bars represent standard error.

A.

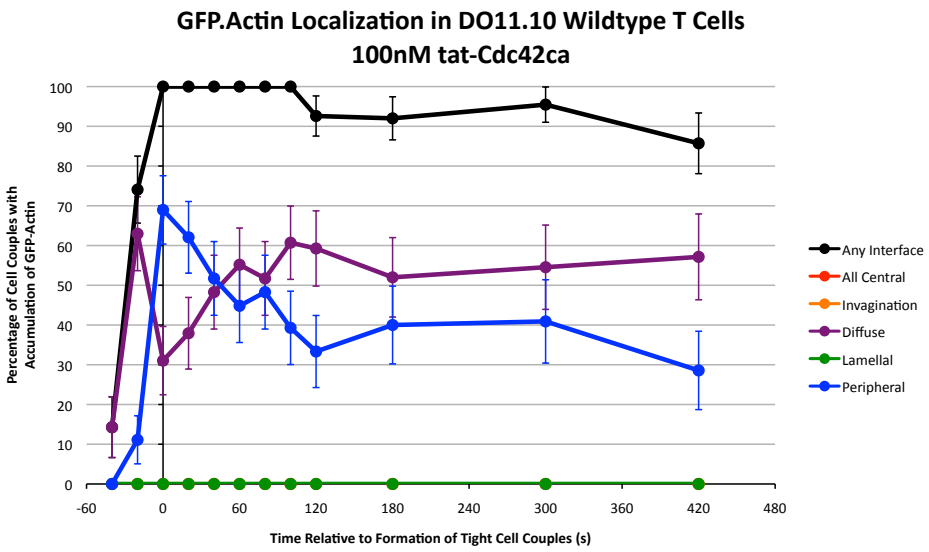

B.

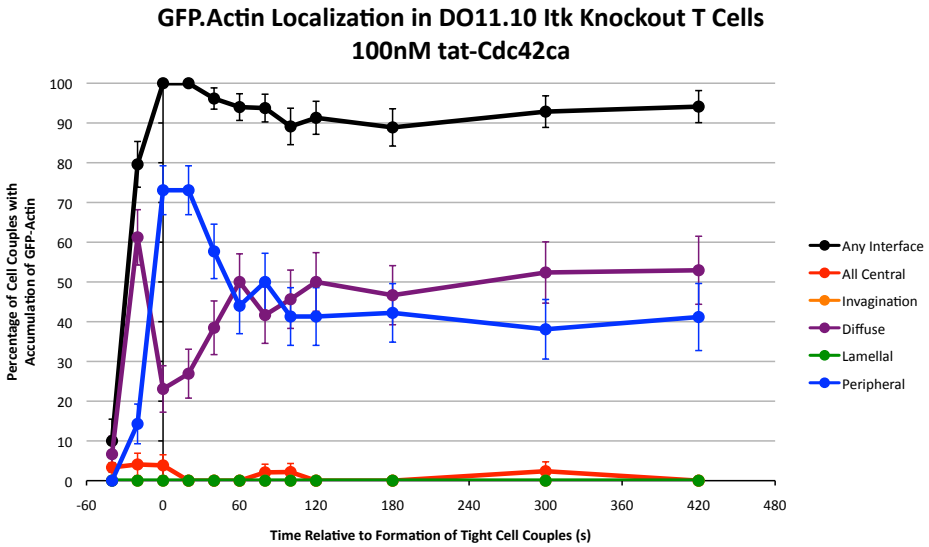

Figure 33: Spatiotemporal Localization of GFP.Actin in CD4$^+$ DO11.10 TCR Transgenic Wildtype or Itk$^{-/-}$ T Cells Treated with 100nM tat-Cdc42ca. Primed primary DO11.10 (A) wildtype or (B) Itk$^{-/-}$ T cells were transduced with GFP.Actin and stimulated with A20 B cell lymphoma APCs in the presence of 10μM OVA antigenic peptide and 100nM tat-Cdc42ca. Time indicated is relative to the formation of a tight coupling of the T cell with the APC. The graphs display the percentage of cell couples that displayed accumulation of signaling intermediates with the indicated patterns. 29 cell couples were analyzed for the wildtype T cells; 52 cell couples for the Itk$^{-/-}$ T cells. Error bars represent standard error.

A.

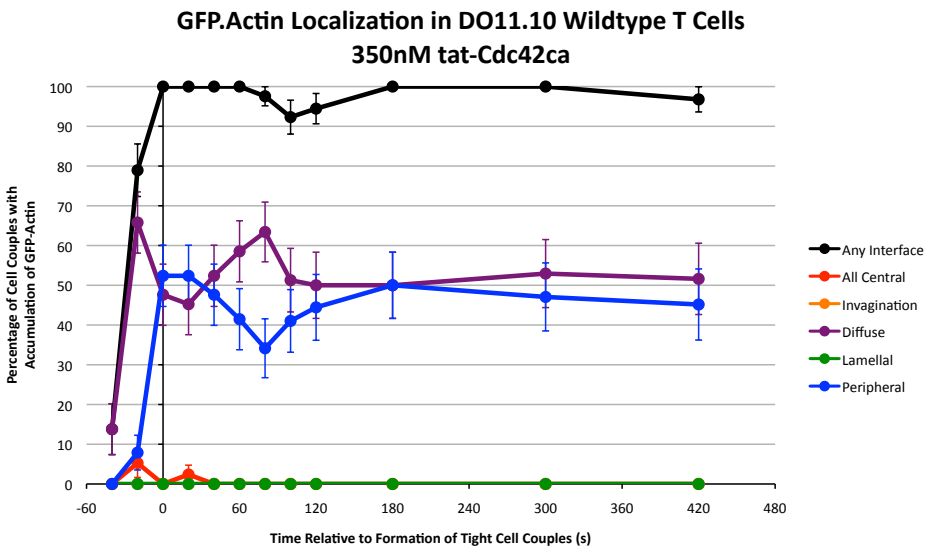

B.

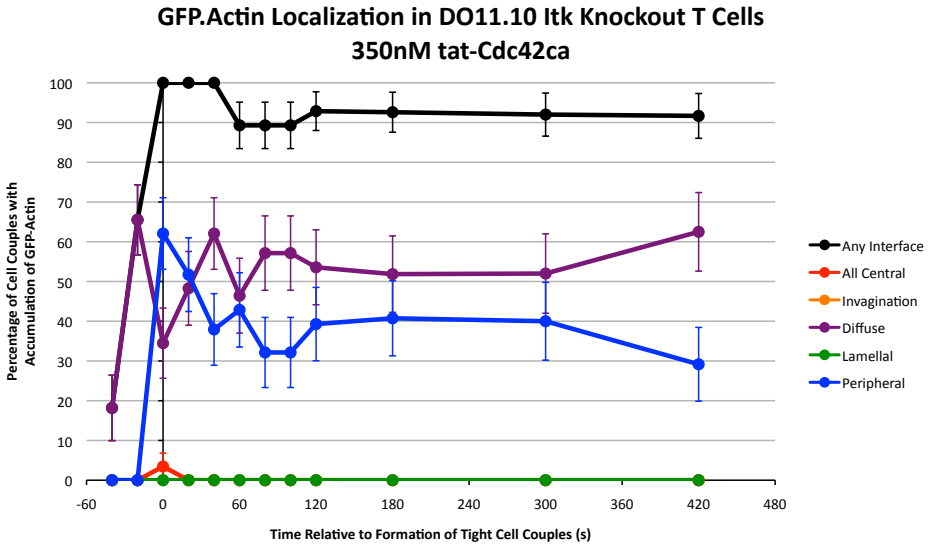

Figure 34: Spatiotemporal Localization of GFP.Actin in CD4$^+$ DO11.10 TCR Transgenic Wildtype or Itk$^{-/-}$ T Cells Treated with 350nM tat-Cdc42ca. Primed primary DO11.10 (A) wildtype or (B) Itk$^{-/-}$ T cells were transduced with GFP.Actin and stimulated with A20 B cell lymphoma APCs in the presence of 10μM OVA antigenic peptide and 350nM tat-Cdc42ca. Time indicated is relative to the formation of a tight coupling of the T cell with the APC. The graphs display the percentage of cell couples that displayed accumulation of signaling intermediates with the indicated patterns. 42 cell couples were analyzed for the wildtype T cells; 29 cell couples for the Itk$^{-/-}$ T cells. Error bars represent standard error.

A.

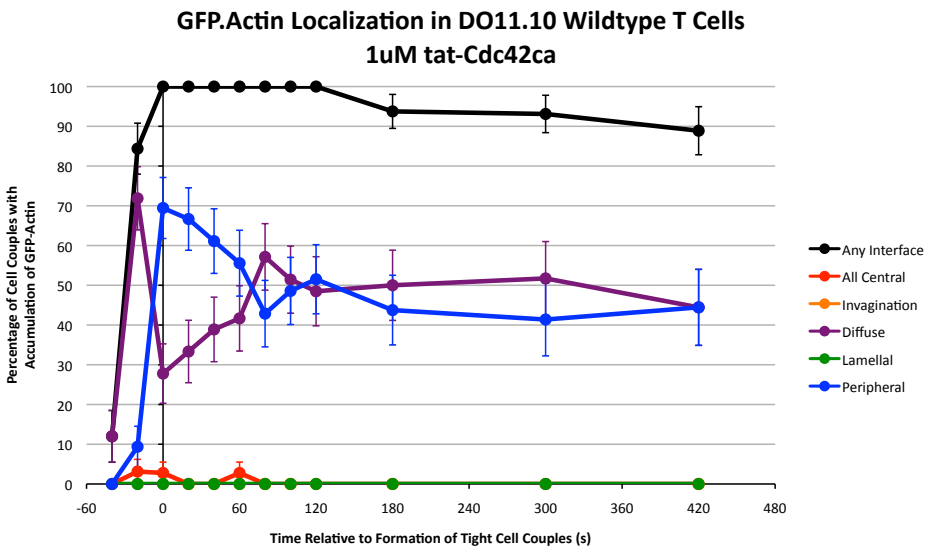

B.

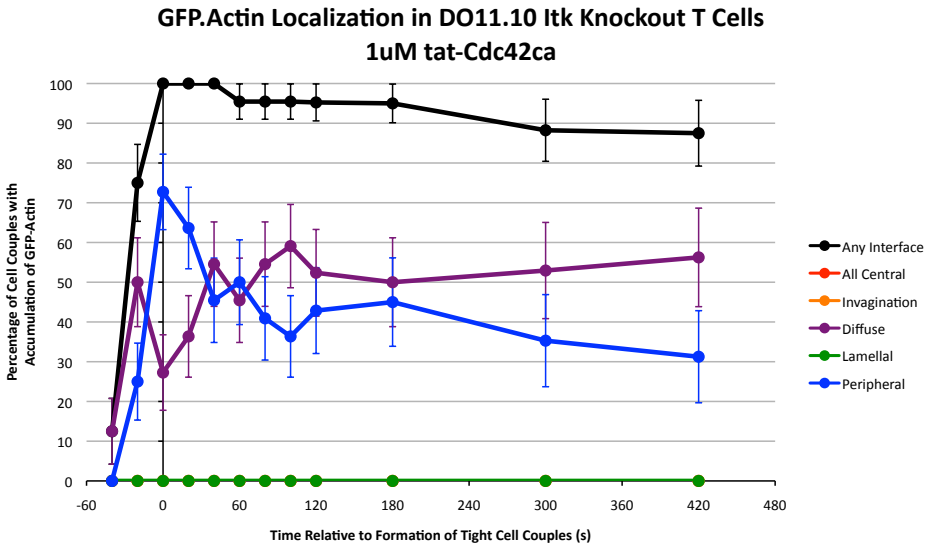

Figure 35: Spatiotemporal Localization of GFP.Actin in CD4$^+$ DO11.10 TCR Transgenic Wildtype or Itk$^{-/-}$ T Cells Treated with 1μM tat-Cdc42ca. Primed primary DO11.10 (A) wildtype or (B) Itk$^{-/-}$ T cells were transduced with GFP.Actin and stimulated with A20 B cell lymphoma APCs in the presence of 10μM OVA antigenic peptide and 1μM tat-Cdc42ca. Time indicated is relative to the formation of a tight coupling of the T cell with the APC. The graphs display the percentage of cell couples that displayed accumulation of signaling intermediates with the indicated patterns. 36 cell couples were analyzed for the wildtype T cells; 22 cell couples for the Itk$^{-/-}$ T cells. Error bars represent standard error.

A.

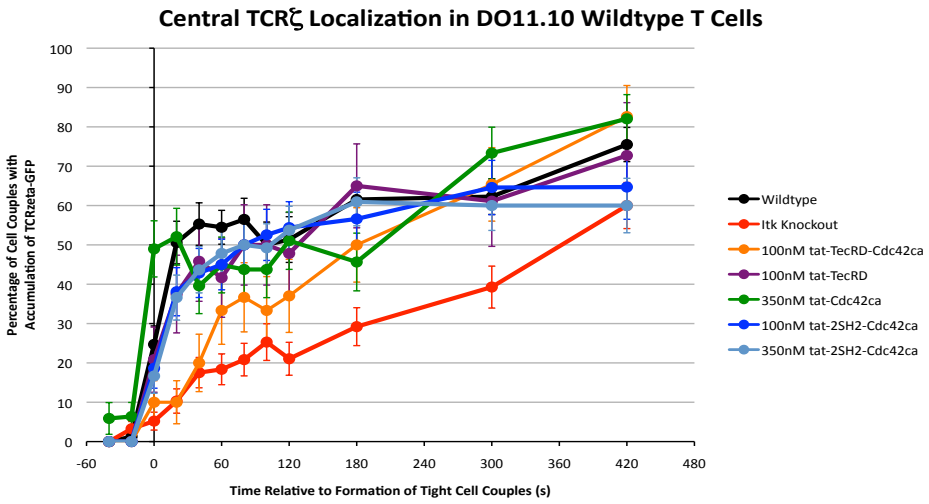

B.

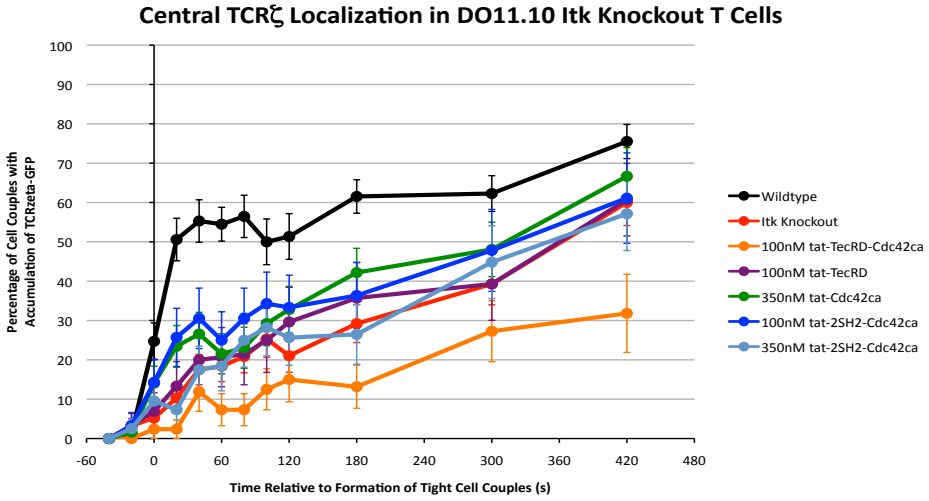

Figure 36: Central Localization of TCRζ in CD4$^+$ DO11.10 TCR Transgenic Wildtype or Itk$^{-/-}$ T Cells Treated with Various tat- Proteins. Primed primary DO11.10 (A) wildtype or (B) Itk$^{-/-}$ T cells were transduced with GFP.Actin and stimulated with A20 B cell lymphoma APCs in the presence of 10μM OVA antigenic peptide and various tat- proteins as indicated in the legend. TecRD indicates the Tec.PH.TH.SH3 recruitment domain. Time indicated is relative to the formation of a tight coupling of the T cell with the APC. The graphs display the percentage of cell couples that displayed accumulation of signaling intermediates with the indicated patterns. A total of 372 cell couples were analyzed for the wildtype T cells; 312 cell couples for the Itk$^{-/-}$ T cells. Error bars represent standard error.

A.

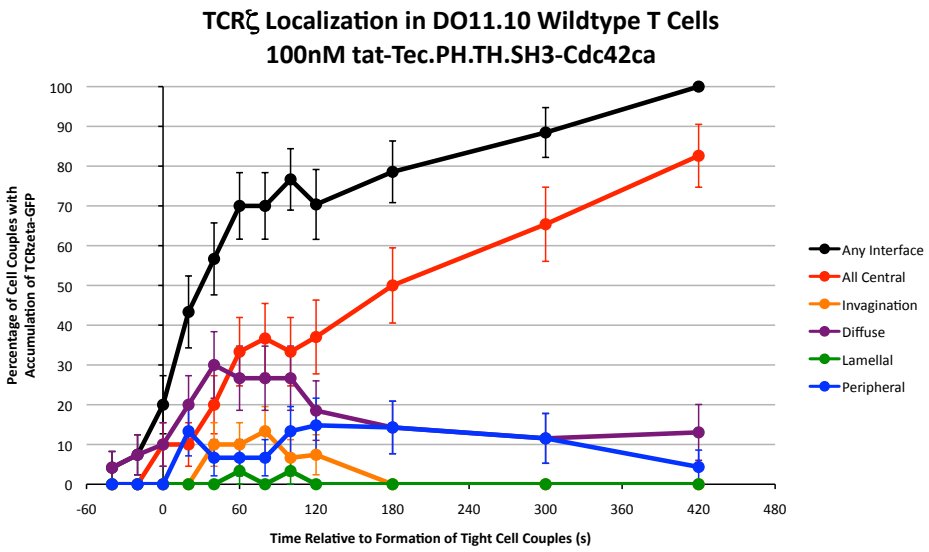

B.

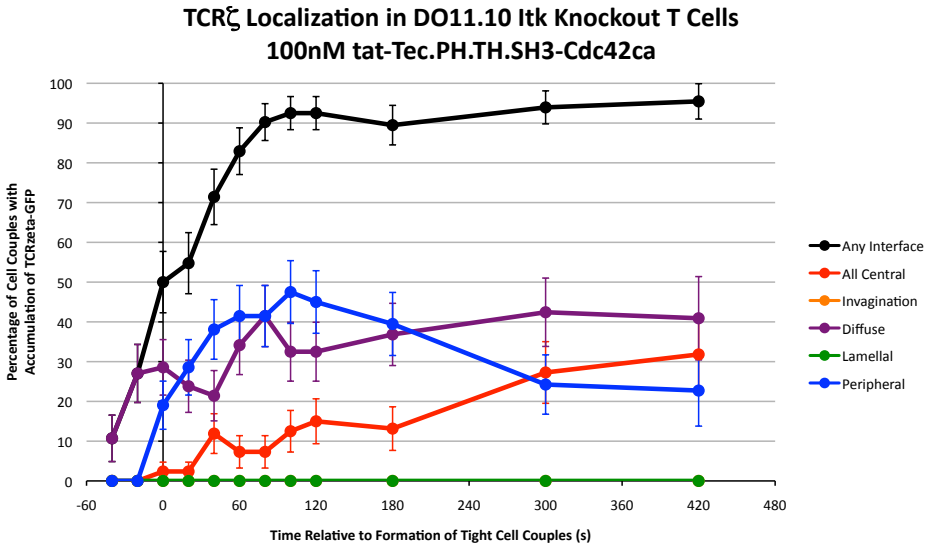

Figure 37: Spatiotemporal Localization of TCRζ.GFP in CD4^{+} DO11.10 TCR Transgenic Wildtype or Itk$^{-/-}$ T Cells Treated with 100nM tat-Tec.PH.TH.SH3-Cdc42ca. Primed primary DO11.10 (A) wildtype or (B) Itk$^{-/-}$ T cells were transduced with TCRζ.GFP and stimulated with A20 B cell lymphoma APCs in the presence of 10μM OVA antigenic peptide and 100nM tat-Tec.PH.TH.SH3-Cdc42ca. Time indicated is relative to the formation of a tight coupling of the T cell with the APC. The graphs display the percentage of cell couples that displayed accumulation of signaling intermediates with the indicated patterns. 30 cell couples were analyzed for the wildtype T cells; 42 cell couples for the Itk$^{-/-}$ T cells. Error bars represent standard error.

A.

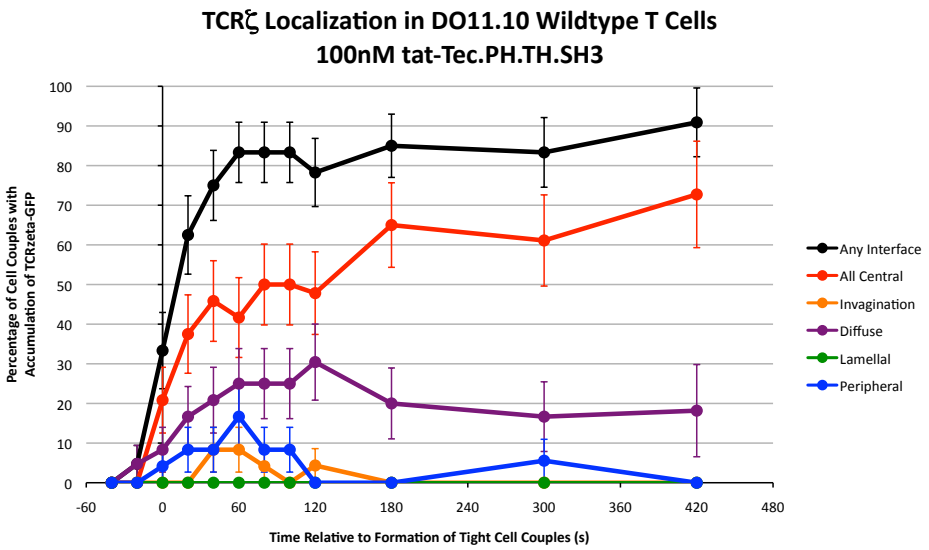

B.

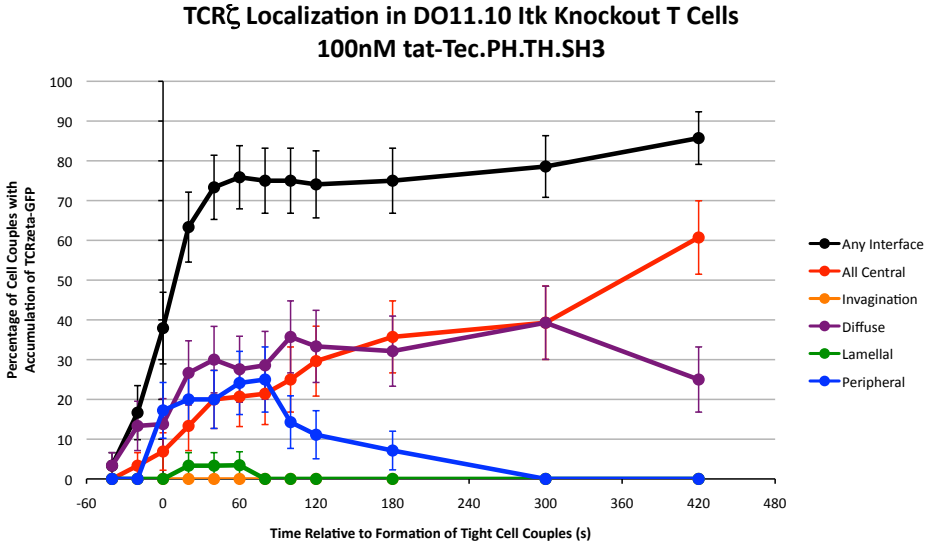

Figure 38: Spatiotemporal Localization of TCRζ.GFP in CD4$^+$ DO11.10 TCR Transgenic Wildtype or Itk$^{-/-}$ T Cells Treated with 100nM tat-Tec.PH.TH.SH3. Primed primary DO11.10 (A) wildtype or (B) Itk$^{-/-}$ T cells were transduced with TCRζ.GFP and stimulated with A20 B cell lymphoma APCs in the presence of 10μM OVA antigenic peptide and 100nM tat-Tec.PH.TH.SH3. Time indicated is relative to the formation of a tight coupling of the T cell with the APC. The graphs display the percentage of cell couples that displayed accumulation of signaling intermediates with the indicated patterns. 24 cell couples were analyzed for the wildtype T cells; 30 cell couples for the Itk$^{-/-}$ T cells. Error bars represent standard error.

A.

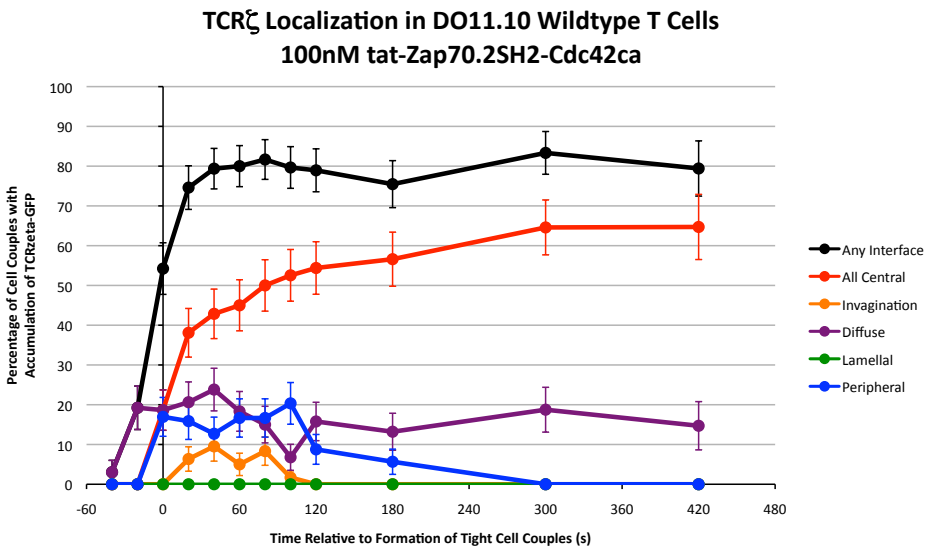

B.

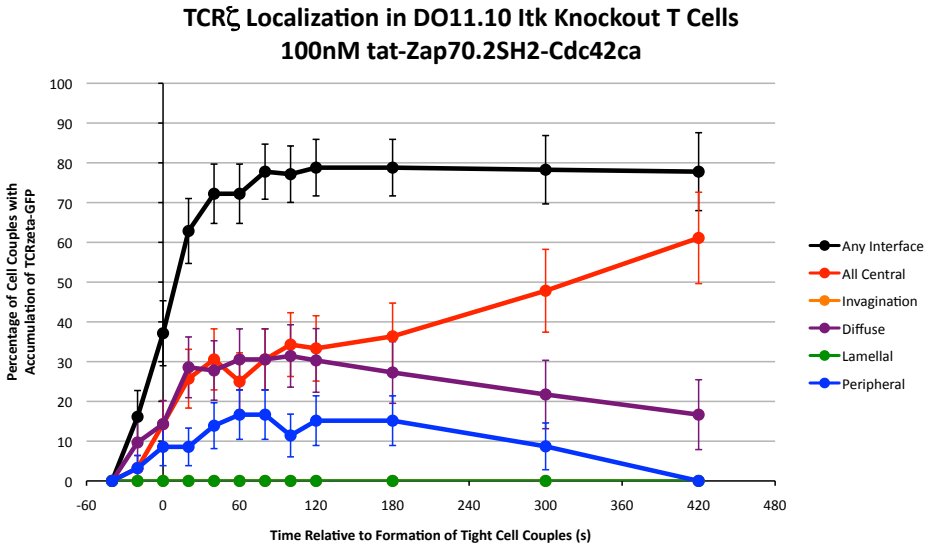

Figure 39: Spatiotemporal Localization of TCRζ.GFP in CD4$^+$ DO11.10 TCR Transgenic Wildtype or Itk$^{-/-}$ T Cells Treated with 100nM tat-Zap70.2SH2-Cdc42ca. Primed primary DO11.10 (A) wildtype or (B) Itk$^{-/-}$ T cells were transduced with TCRζ.GFP and stimulated with A20 B cell lymphoma APCs in the presence of 10μM OVA antigenic peptide and 100nM tat-Zap70.2SH2-Cdc42ca. Time indicated is relative to the formation of a tight coupling of the T cell with the APC. The graphs display the percentage of cell couples that displayed accumulation of signaling intermediates with the indicated patterns. 63 cell couples were analyzed for the wildtype T cells; 36 cell couples for the Itk$^{-/-}$ T cells. Error bars represent standard error.

A.

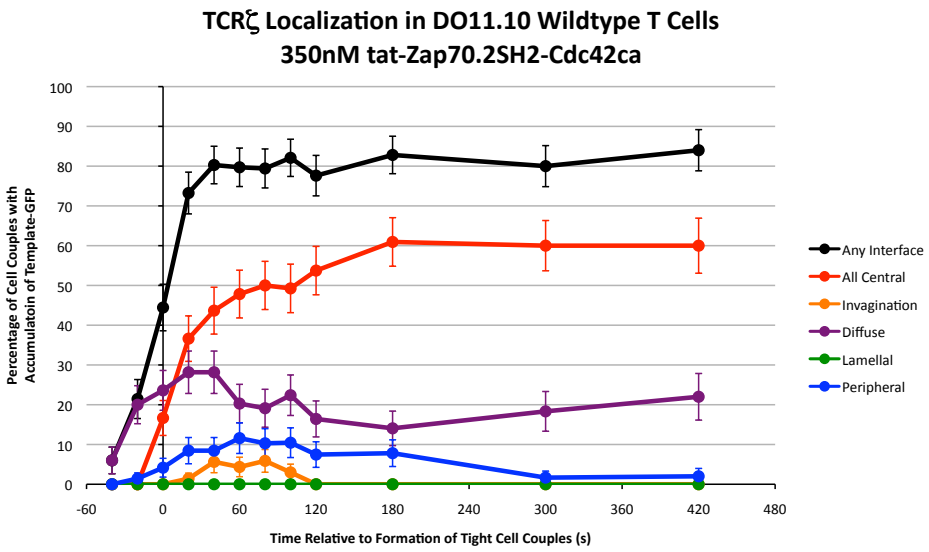

B.

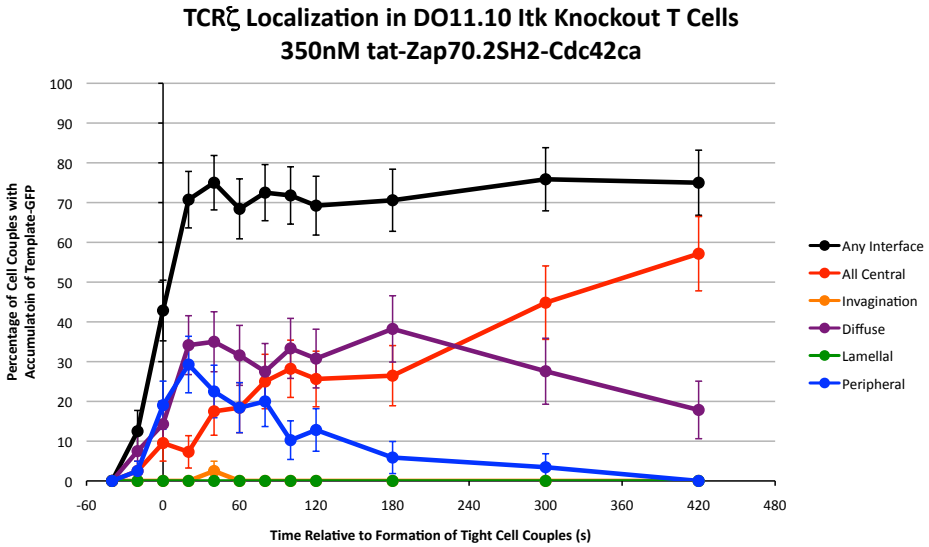

Figure 40: Spatiotemporal Localization of TCRζ.GFP in CD4$^+$ DO11.10 TCR Transgenic Wildtype or Itk$^{-/-}$ T Cells Treated with 350nM tat-Zap70.2SH2-Cdc42ca. Primed primary DO11.10 (A) wildtype or (B) Itk$^{-/-}$ T cells were transduced with TCRζ.GFP and stimulated with A20 B cell lymphoma APCs in the presence of 10μM OVA antigenic peptide and 350nM tat-Zap70.2SH2-Cdc42ca. Time indicated is relative to the formation of a tight coupling of the T cell with the APC. The graphs display the percentage of cell couples that displayed accumulation of signaling intermediates with the indicated patterns. 72 cell couples were analyzed for the wildtype T cells; 42 cell couples for the Itk$^{-/-}$ T cells. Error bars represent standard error.

A.

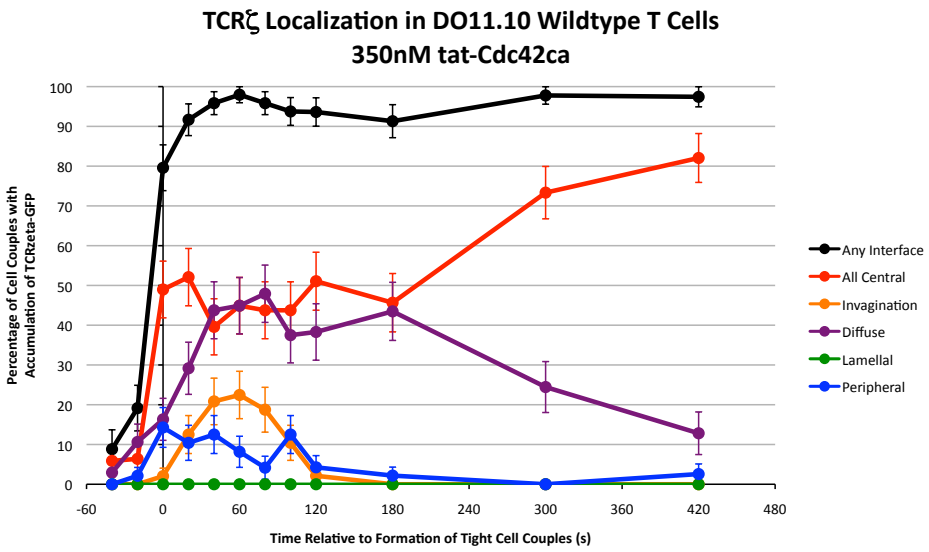

B.

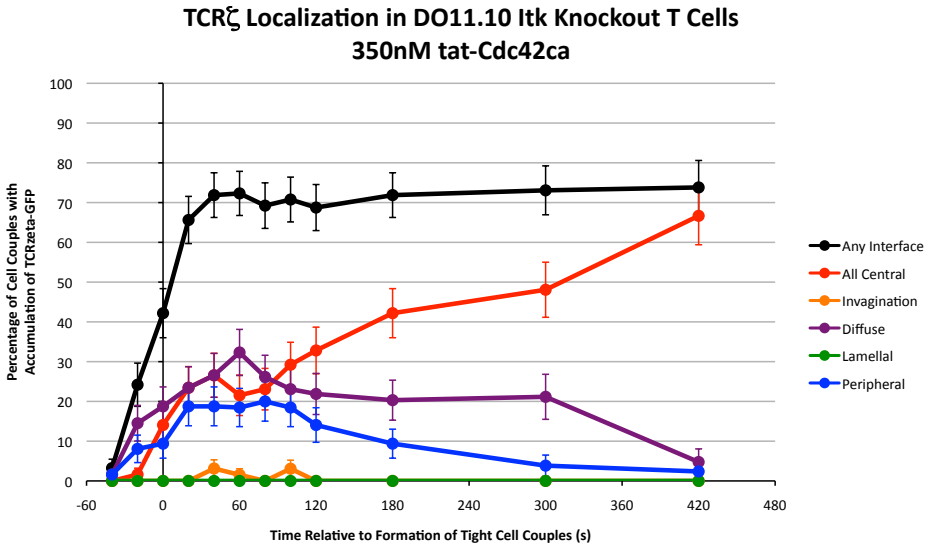

Figure 41: Spatiotemporal Localization of TCRζ.GFP in CD4$^+$ DO11.10 TCR Transgenic Wildtype or Itk$^{-/-}$ T Cells Treated with 350nM tat-Cdc42ca. Primed primary DO11.10 (A) wildtype or (B) Itk$^{-/-}$ T cells were transduced with TCRζ.GFP and stimulated with A20 B cell lymphoma APCs in the presence of 10μM OVA antigenic peptide and 350nM tat-Cdc42ca. Time indicated is relative to the formation of a tight coupling of the T cell with the APC. The graphs display the percentage of cell couples that displayed accumulation of signaling intermediates with the indicated patterns. 49 cell couples were analyzed for the wildtype T cells; 65 cell couples for the Itk$^{-/-}$ T cells. Error bars represent standard error.

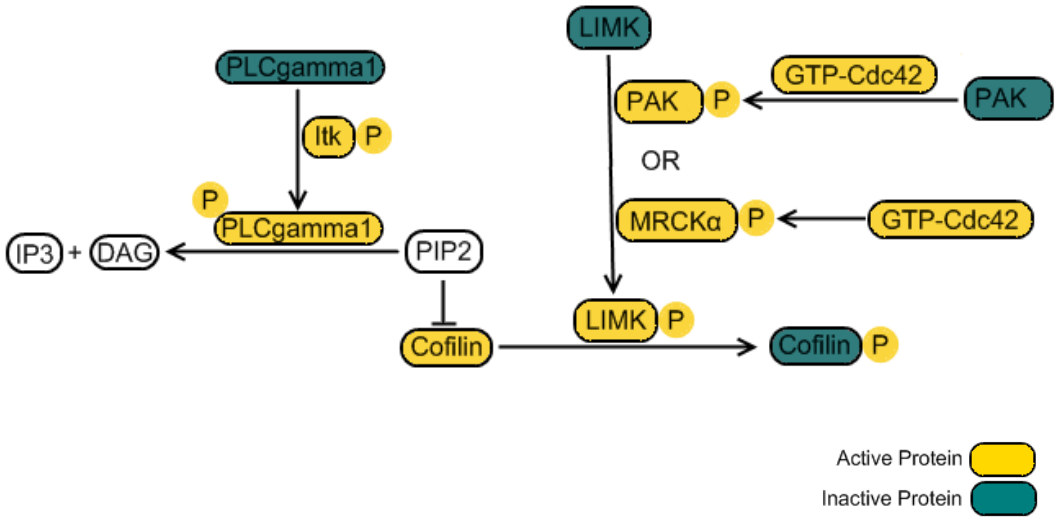

Figure 42: **Schematic Representing Two Mechanisms Regulating Cofilin Activity**. Itk and Cdc42 can both regulate the activity of Cofilin. Cofilin is active in its unphosphorylated state, and becomes inactive when phosphorylated by LIM kinases (LIMK) at Serine 3. LIM Kinases are activated by phosphorylation at Threonine 508 by either p21 activated kinases (PAK) or Myotonic Dystrophy Kinase-Related Cdc42-Binding Kinase α (MRCKα). PAK and MRCKα are activated through interactions with GTP-bound Cdc42. When bound by Cdc42, PAK undergoes a conformational change, allowing for autophosphorylation and activation. The role of Cdc42 in MRCKα activation is not clear. Itk regulates Cofilin activity through activation of PLCγ1, which clears $PI_{(4,5)}P_2$ from the membrane by hydrolyzing it into diacylglycerol (DAG) and inositol triphosphate (IP_3). $PI_{(4,5)}P_2$ binds to unphosphorylated Cofilin, acting as a negative regulator through sequesteration. Upon hydrolysis, $PI_{(4,5)}P_2$ releases Cofilin, allowing it to engage with Actin.

A.

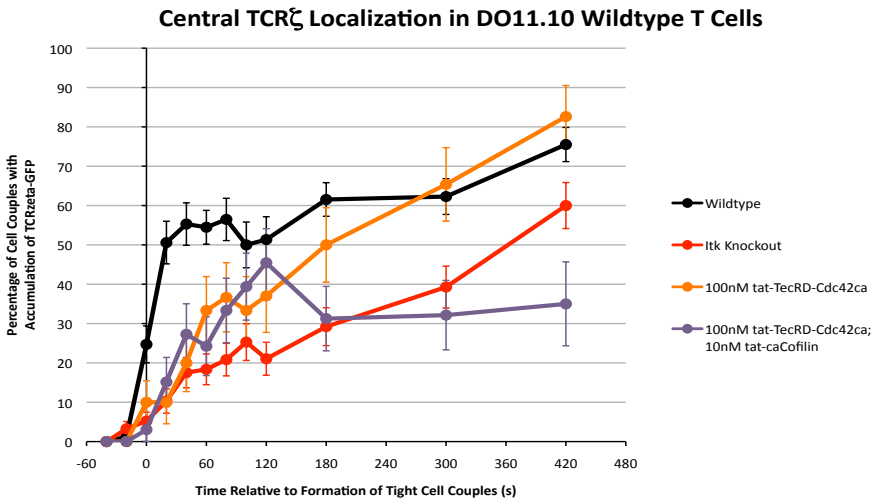

B.

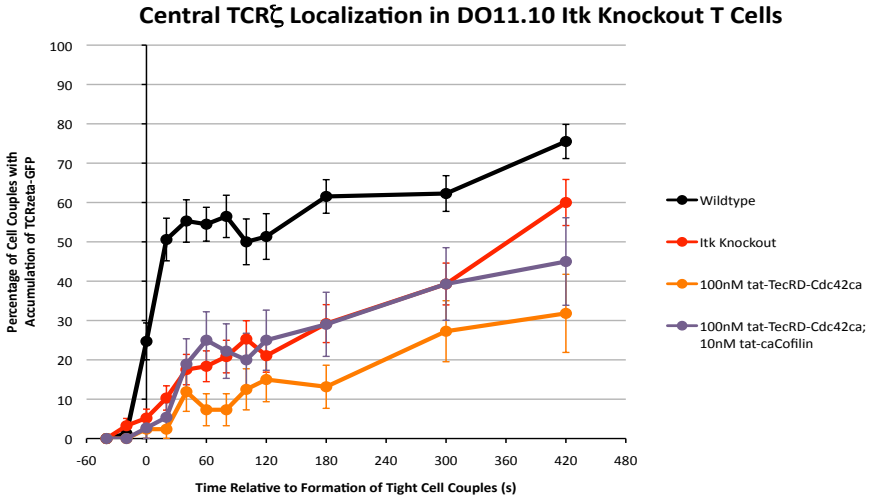

Figure 43: Central Localization of TCRζ in CD4$^+$ DO11.10 TCR Transgenic Wildtype or Itk$^{-/-}$ T Cells Treated with tat-caCofilin. Primed primary DO11.10 (A) wildtype or (B) Itk$^{-/-}$ T cells were transduced with GFP.Actin and stimulated with A20 B cell lymphoma APCs in the presence of 10μM OVA antigenic peptide and tat- proteins as indicated in the legend. TecRD indicates the Tec.PH.TH.SH3 recruitment domain. Time indicated is relative to the formation of a tight coupling of the T cell with the APC. The graphs display the percentage of cell couples that displayed accumulation of signaling intermediates with the indicated patterns. A total of 295 cell couples were analyzed for the wildtype T cells; 311 cell couples for the Itk$^{-/-}$ T cells. Error bars represent standard error.

A.

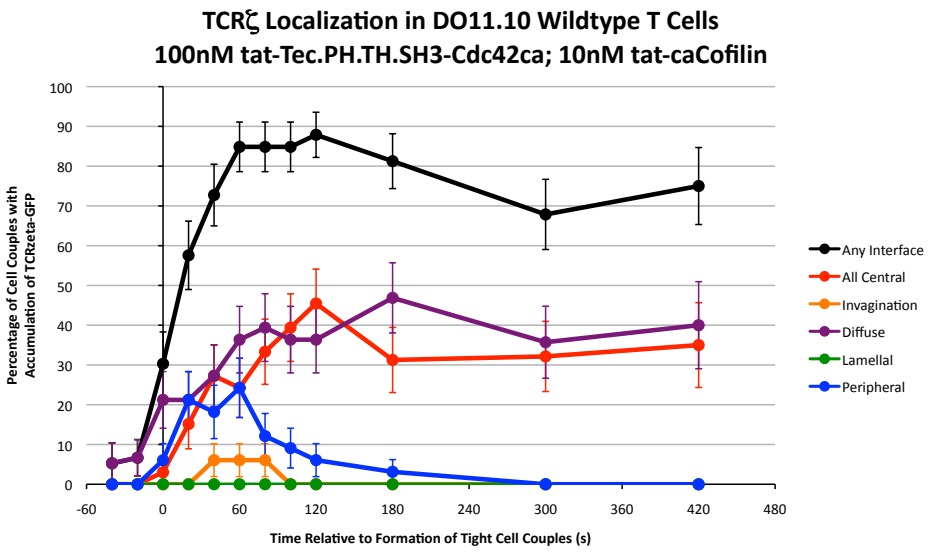

B.

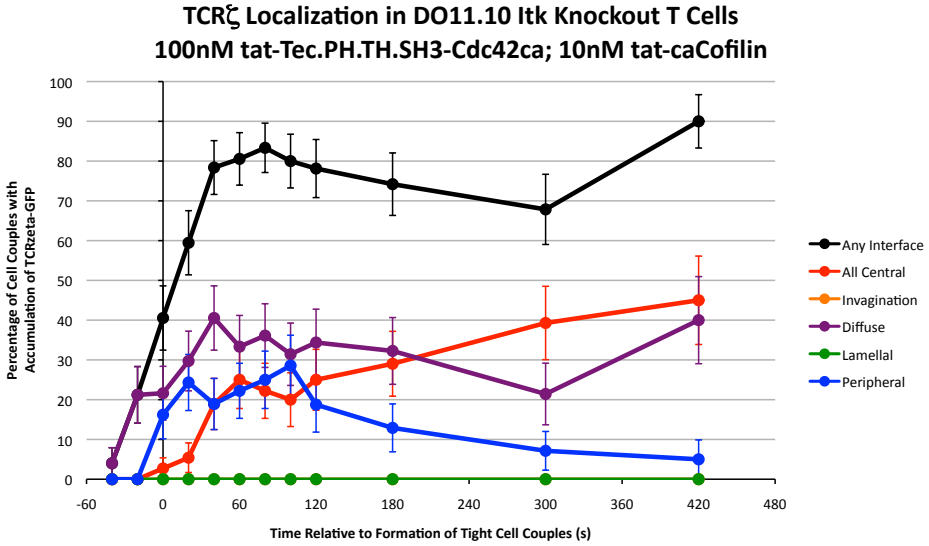

Figure 44: Spatiotemporal Localization of TCRζ.GFP in CD4^{+} DO11.10 TCR Transgenic Wildtype or Itk$^{-/-}$ T Cells Treated with 100nM tat-Tec.PH.TH.SH3 and 10nM tat-caCofilin. Primed primary DO11.10 (A) wildtype or (B) Itk$^{-/-}$ T cells were transduced with TCRζ.GFP and stimulated with A20 B cell lymphoma APCs in the presence of 10μM OVA antigenic peptide and 100nM tat-Tec.PH.TH.SH3 and 10nM tat-caCofilin. Time indicated is relative to the formation of a tight coupling of the T cell with the APC. The graphs display the percentage of cell couples that displayed accumulation of signaling intermediates with the indicated patterns. 37 cell couples were analyzed for the wildtype T cells; 33 cell couples for the Itk$^{-/-}$ T cells. Error bars represent standard error.

A.

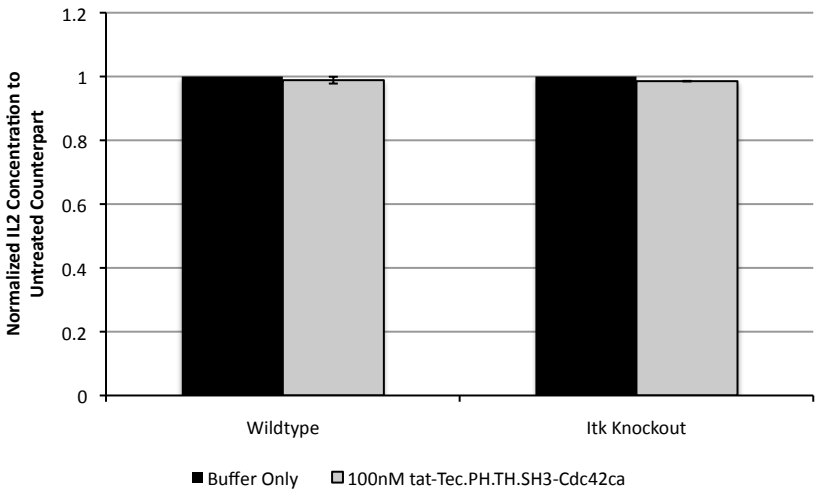

B.

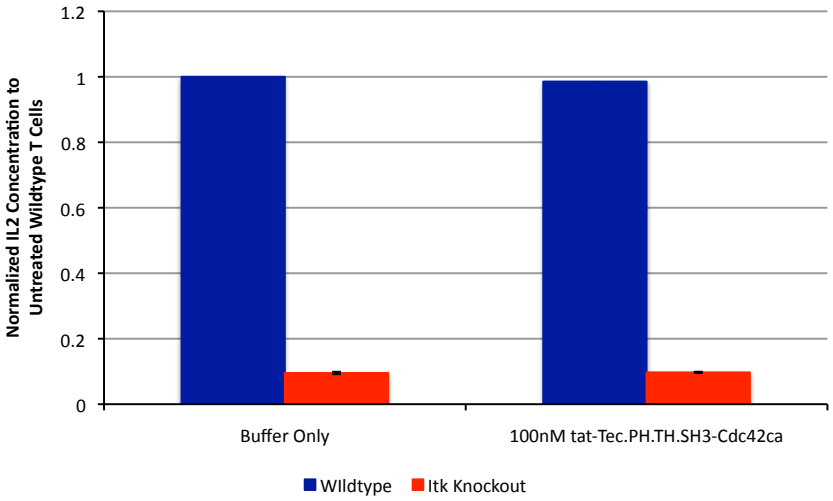

Figure 45: Relative IL2 Secretion by tat-Tec.PH.TH.SH3-Cdc24ca Treated and Untreated Wildtype and Itk$^{-/-}$ T Cells. Primed primary DO11.10 wildtype or Itk$^{-/-}$ T cells were cultured for 16 hours with 1:2 (T cell:APC) A20 B cell lymphoma APCs in the presence of 10μM OVA antigenic peptide. Parallel cultures included 100nM tat-Tec.PH.TH.SH3-Cdc42 (treated) or were left untreated. IL2 levels in the culture supernatant were measured by ELISA using the BD Biosciences BD OptEIA kit (catalog number 555148). To allow for comparison between data sets, samples were internally normalized either against (A) comparable untreated T cells (treated wildtype : untreated wildtype; or treated Itk$^{-/-}$: untreated Itk$^{-/-}$) or (B) untreated wildtype. The graph represents the mean of two independently collected and analyzed sample sets. Error bars, barely visible but present, represent standard error.

A.

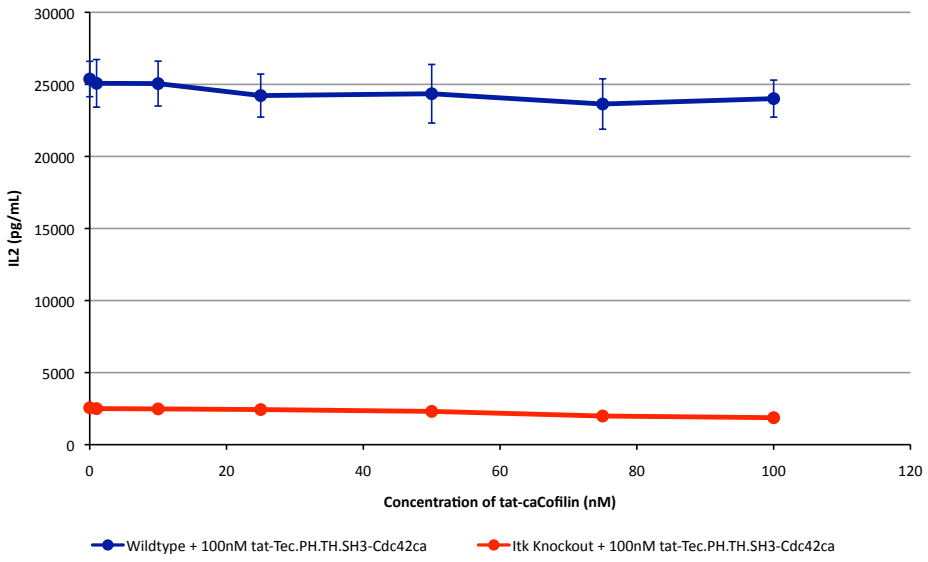

B.

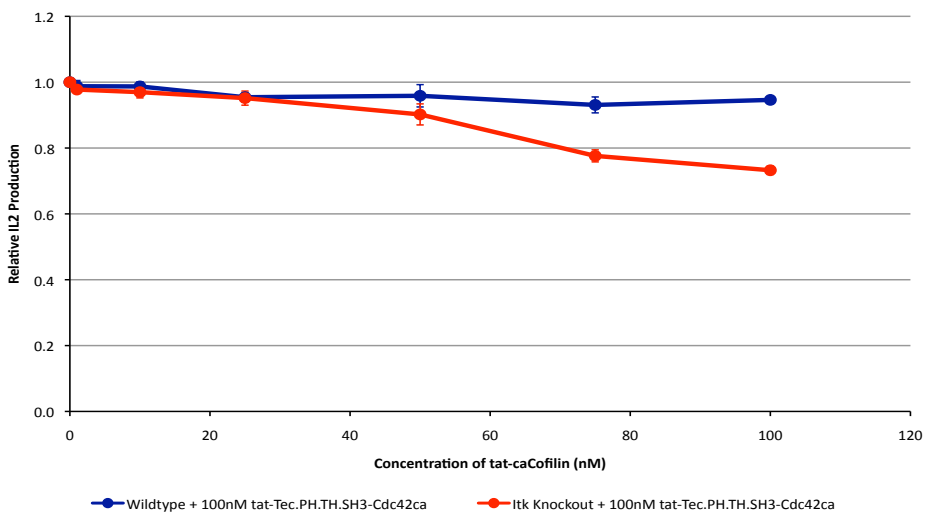

Figure 46: IL2 Secretion by tat-caCofilin Treated T Cells. Primed primary DO11.10 wildtype or Itk$^{-/-}$ T cells were cultured for 16 hours with 1:2 (T cell:APC) A20 B cell lymphoma APCs in the presence of 10μM OVA antigenic peptide, 100nM tat-Tec.PH.TH.SH3-Cdc42, and 0-100nM tat-caCofilin. IL2 levels in the culture supernatant were measured by ELISA using the BD Biosciences BD OptEIA kit (catalog number 555148). The top panel (A) displays the supernatant IL2 concentration, while the data in the bottom panel (B) is normalized to cultures containing no tat-caCofilin. The graphs represent the mean of three independently treated samples from a single mouse. Error bars represent standard error.

A.

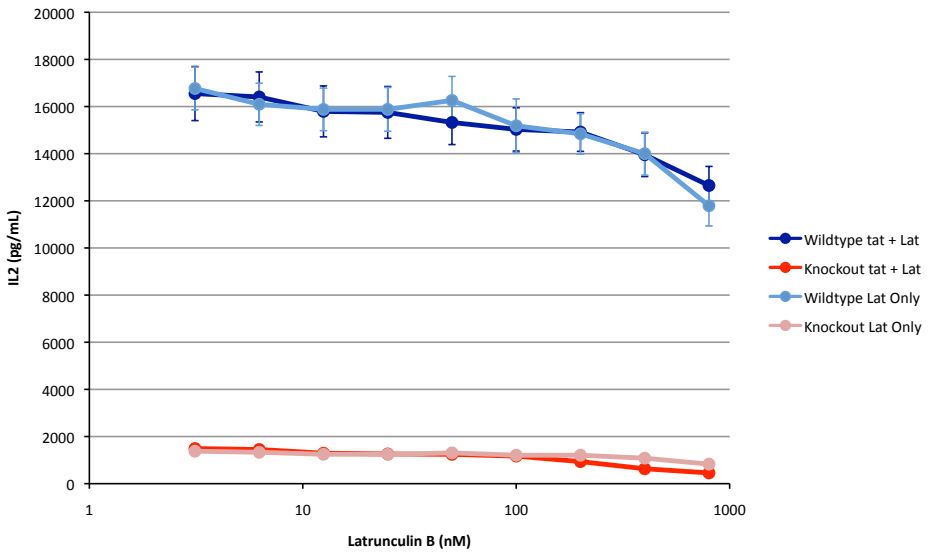

B.

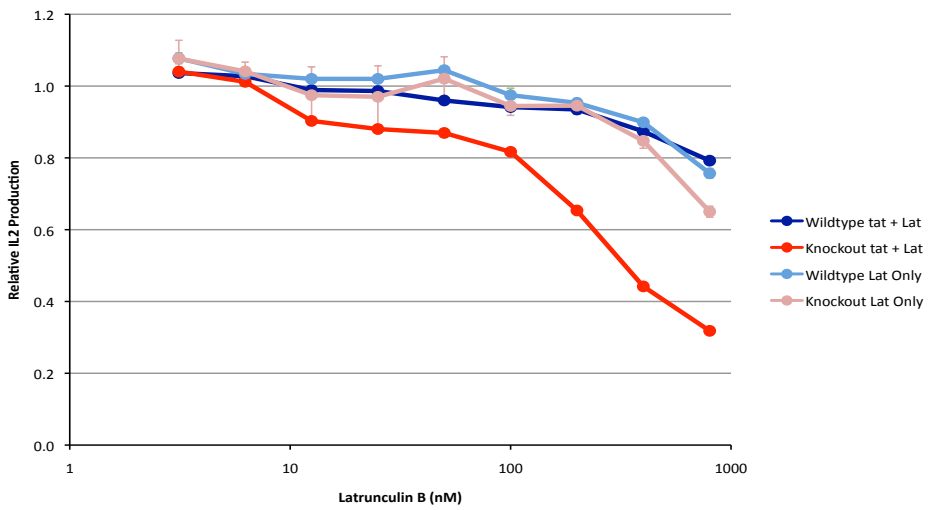

Figure 47: IL2 Secretion by Latrunculin B Treated T Cells. Primed primary DO11.10 wildtype or Itk$^{-/-}$ T cells were cultured for 16 hours with 1:2 (T cell:APC) A20 B cell lymphoma APCs in the presence of 10μM OVA antigenic peptide, 0-800nM Latrunculin B (Lat), and 100nM or 0nM tat-Tec.PH.TH.SH3-Cdc42 (tat). IL2 levels in the culture supernatant were measured by ELISA using the BD Biosciences BD OptEIA kit (catalog number 555148). The top panel (A) displays the supernatant IL2 concentration, while the data in the bottom panel (B) is normalized to cultures containing no Latrunculin B. The graphs represent the mean of three independently treated samples from a single mouse. Error bars represent standard error.

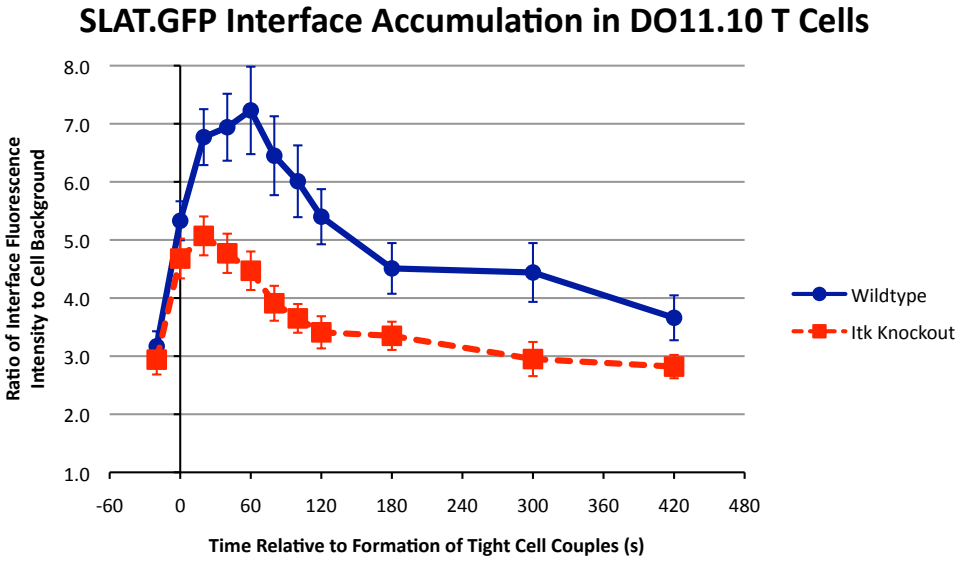

Figure 48: Interface Accumulation of GFP.SLAT in CD4^{+} DO11.10 TCR Transgenic Wildtype or Itk$^{-/-}$ T Cells. Primed primary DO11.10 wildtype or Itk$^{-/-}$ T cells were transduced with GFP.SLAT and stimulated with A20 B cell lymphoma APCs in the presence of 10μM OVA antigenic peptide. Time indicated is relative to the formation of a tight coupling of the T cell with the APC. The graphs display the ratio of the fluorescence intensity at the T cell / APC interface to the cell background. 32 wildtype and 25 Itk$^{-/-}$ cell couples were analyzed. Error bars represent standard error.

A.

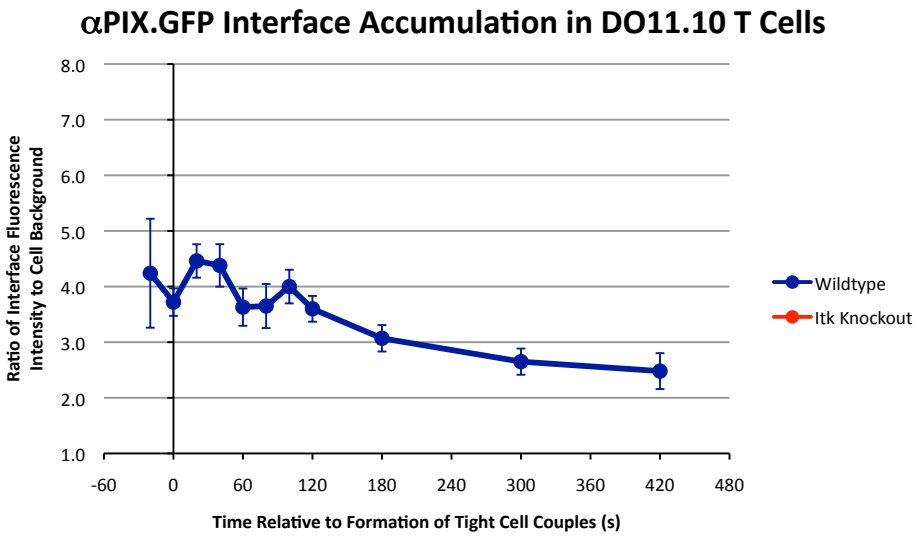

B.

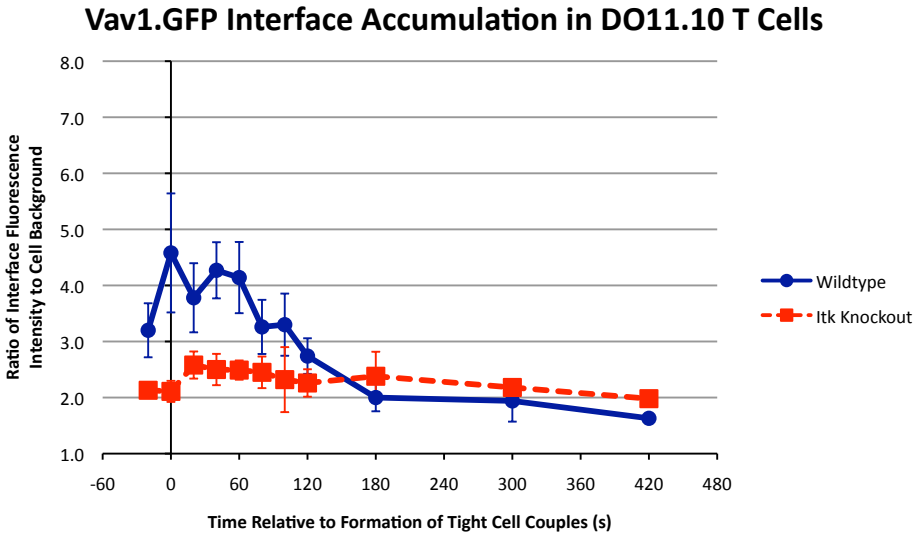

Figure 49: Interface Accumulation of αPIX.GFP and Vav1.GFP in CD4$^+$ DO11.10 TCR Transgenic Wildtype or Itk$^{-/-}$ T Cells. Primed primary DO11.10 wildtype or Itk$^{-/-}$ T cells were transduced with (A) αPIX.GFP or (B) Vav1.GFP and stimulated with A20 B cell lymphoma APCs in the presence of 10μM OVA antigenic peptide. Time indicated is relative to the formation of a tight coupling of the T cell with the APC. The graphs display the ratio of the fluorescence intensity at the T cell / APC interface to the cell background. 22 wildtype and 0 Itk$^{-/-}$ cell couples were analyzed for the αPIX.GFP construct; 6 wildtype and 7 Itk$^{-/-}$ cell couples for the Vav1.GFP. Error bars represent standard error.

A.

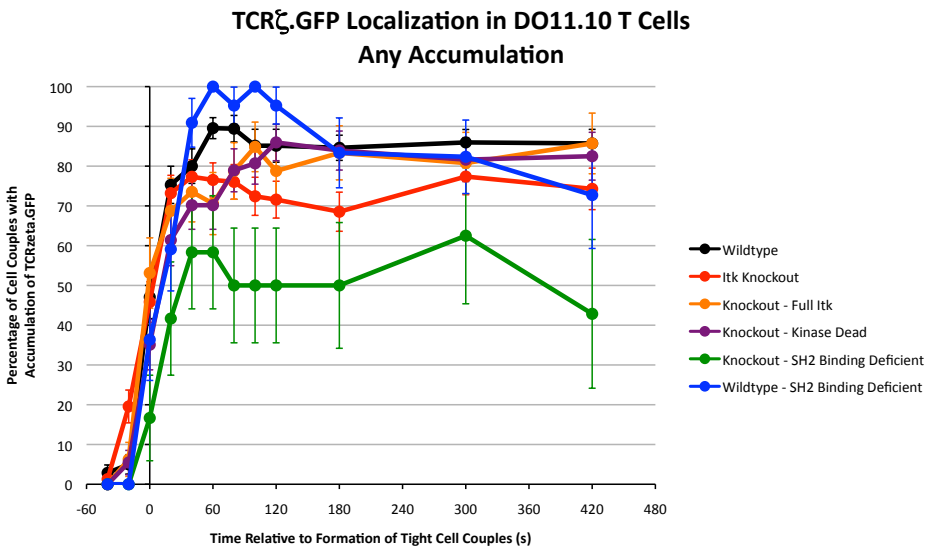

B.

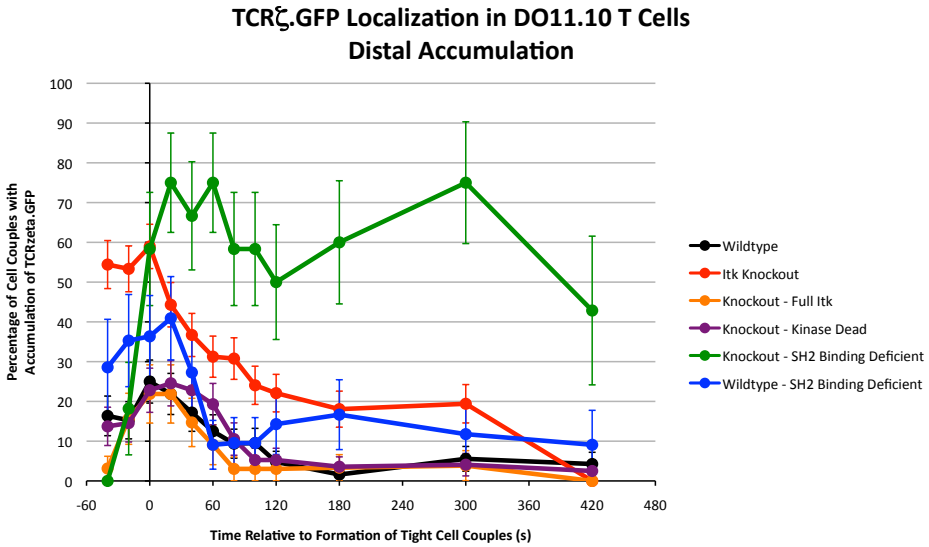

Figure 50: Localization of TCRζ in CD4^{+} DO11.10 TCR Transgenic Itk$^{-/-}$ T Cells Reconstituted with Itk Isoforms. Primed primary DO11.10 Itk$^{-/-}$ T cells were transduced with GFP.TCRζ and either wildtype (Full Itk), K390R (Kinase Dead), or R265K (SH2 Binding Deficient) Itk. These cells were stimulated with A20 B cell lymphoma APCs in the presence of 10μM OVA antigenic peptide. The graphs display the percentage of cell couples that presented (A) any accumulation at the interface or (B) recruitment to the distal pole. 34 wildtype, 57 K390R, 12 R265K reconstituted Itk$^{-/-}$ T cell couples were analyzed. 22 R265K expressed wildtype cell couples were analyzed. Error bars represent standard error.

A.

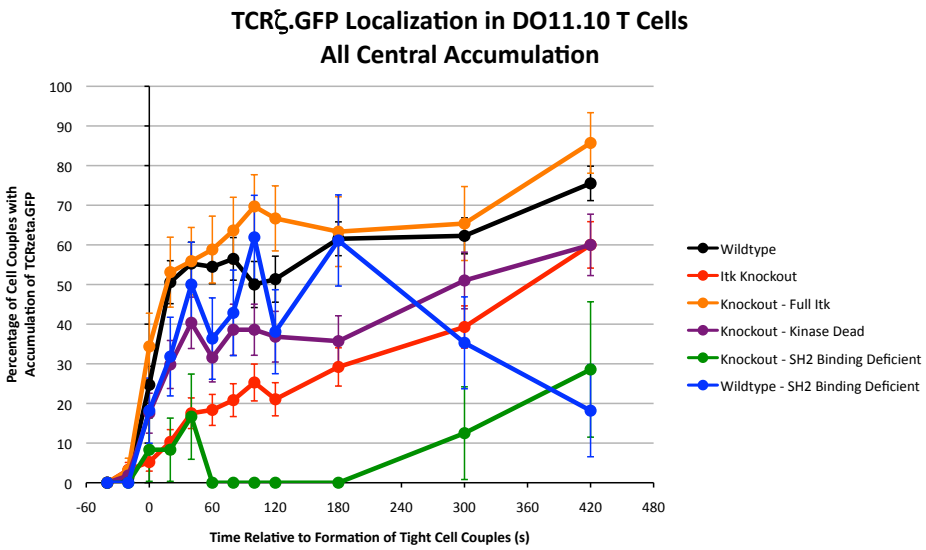

B.

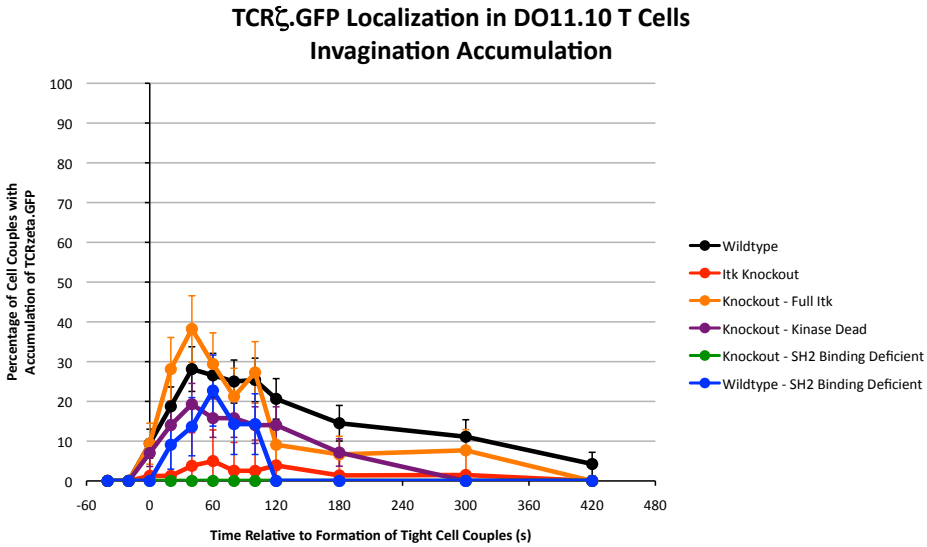

Figure 51: Localization of TCRζ in CD4^{+} DO11.10 TCR Transgenic Itk$^{-/-}$ T Cells Reconstituted with Itk Isoforms. Primed primary DO11.10 Itk$^{-/-}$ T cells were transduced with GFP.TCRζ and either wildtype (Full Itk), K390R (Kinase Dead), or R265K (SH2 Binding Deficient) Itk. These cells were stimulated with A20 B cell lymphoma APCs in the presence of 10μM OVA antigenic peptide. The graphs display the percentage of cell couples that presented (A) central accumulation at the interface or (B) recruitment to the invagination. 34 wildtype, 57 K390R, 12 R265K reconstituted Itk$^{-/-}$ T cell couples were analyzed. 22 R265K expressed wildtype cell couples were analyzed. Error bars represent standard error.

A.

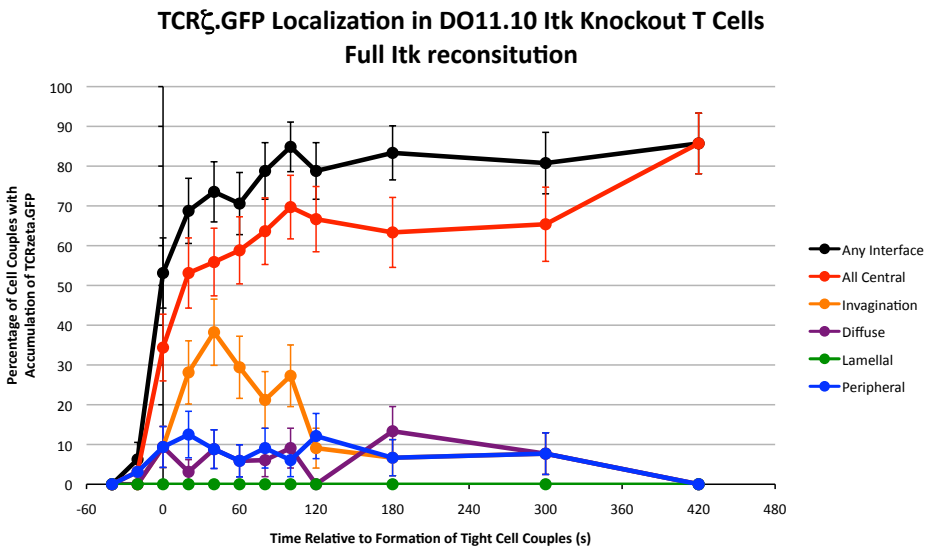

B.

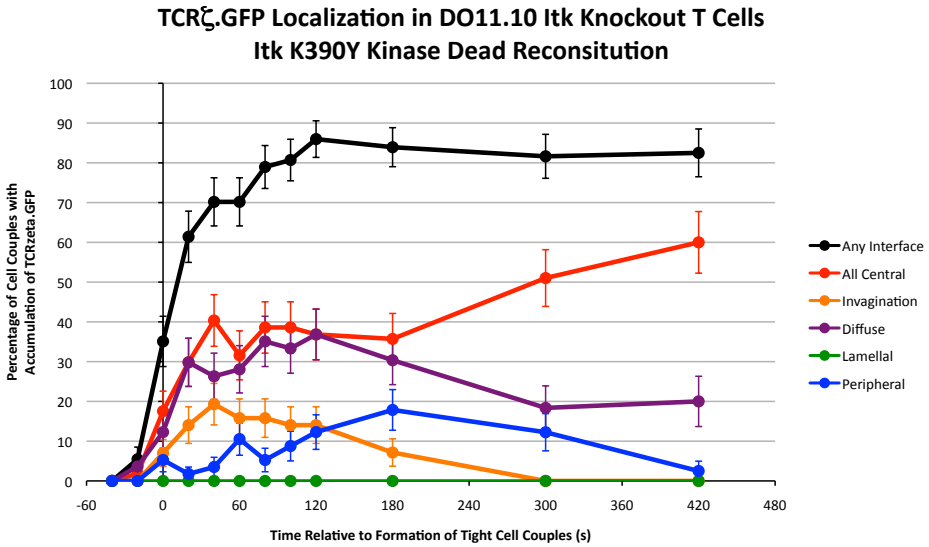

Figure 52: Localization of TCRζ in CD4$^+$ DO11.10 TCR Transgenic Itk$^{-/-}$ T Cells Reconstituted with Wildtype or Kinase Dead Itk. Primed primary DO11.10 Itk$^{-/-}$ T cells were transduced with GFP.TCRζ and either (A) wildtype (Full Itk) or (B) K390R (Kinase Dead). These cells were stimulated with A20 B cell lymphoma APCs in the presence of 10μM OVA antigenic peptide. Time indicated is relative to the formation of a tight coupling of the T cell with the APC. The graphs display the percentage of cell couples that displayed accumulation of signaling intermediates with the indicated patterns. 34 cell couples were analyzed for the wildtype reconstituted Itk$^{-/-}$ T cells; 57 cell couples for the Kinase Dead Itk reconstituted Itk$^{-/-}$ T cells. Error bars represent standard error.

A.

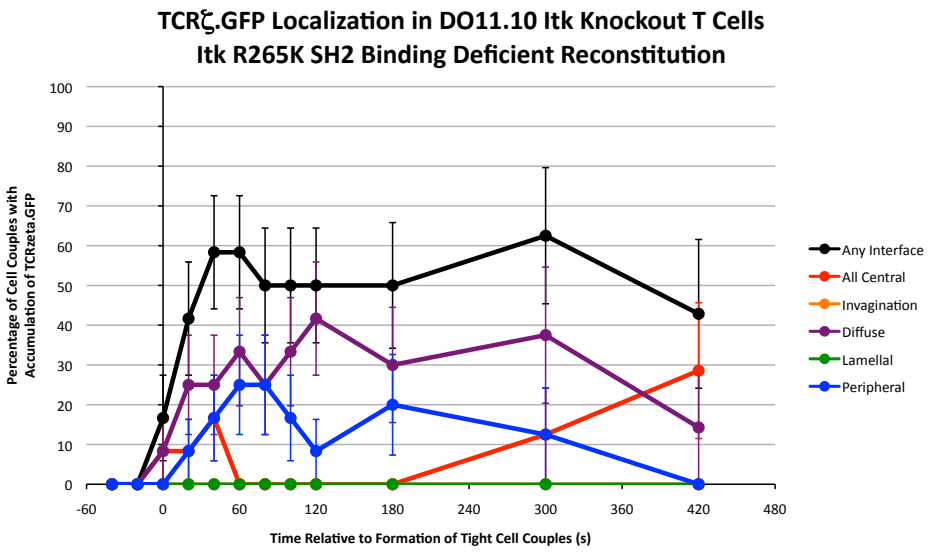

B.

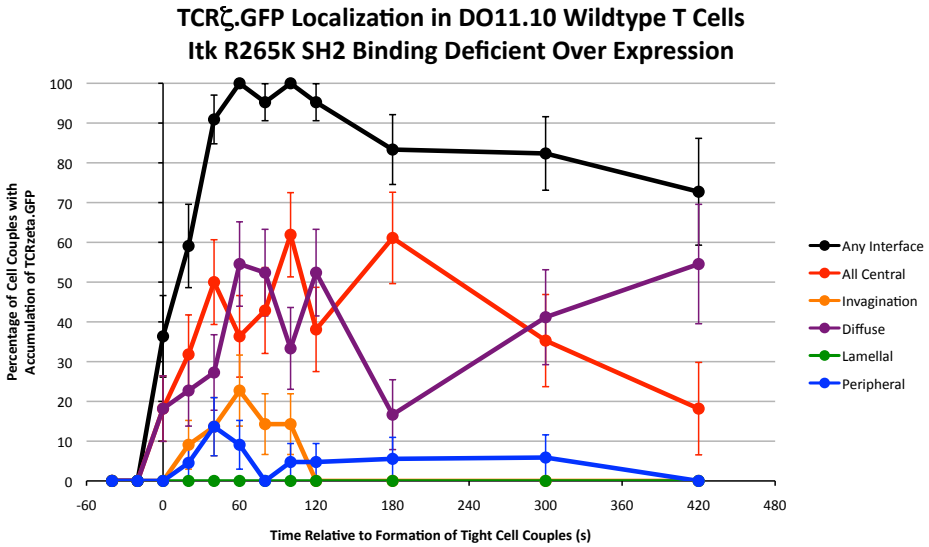

Figure 53: Localization of TCRζ in $CD4^+$ DO11.10 TCR Transgenic T Cells with R265K Itk. (A) Wildtype or (B) $Itk^{-/-}$ primed primary DO11.10 $Itk^{-/-}$ T cells were transduced with GFP.TCRζ and R265K Itk(SH2 binding deficient). These cells were stimulated with A20 B cell lymphoma APCs in the presence of 10μM OVA antigenic peptide. Time indicated is relative to the formation of a tight coupling of the T cell with the APC. The graphs display the percentage of cell couples that displayed accumulation of signaling intermediates with the indicated patterns. 22 cell couples were analyzed for the wildtype T cells; 12 cell couples for the $Itk^{-/-}$ T cells. Error bars represent standard error.

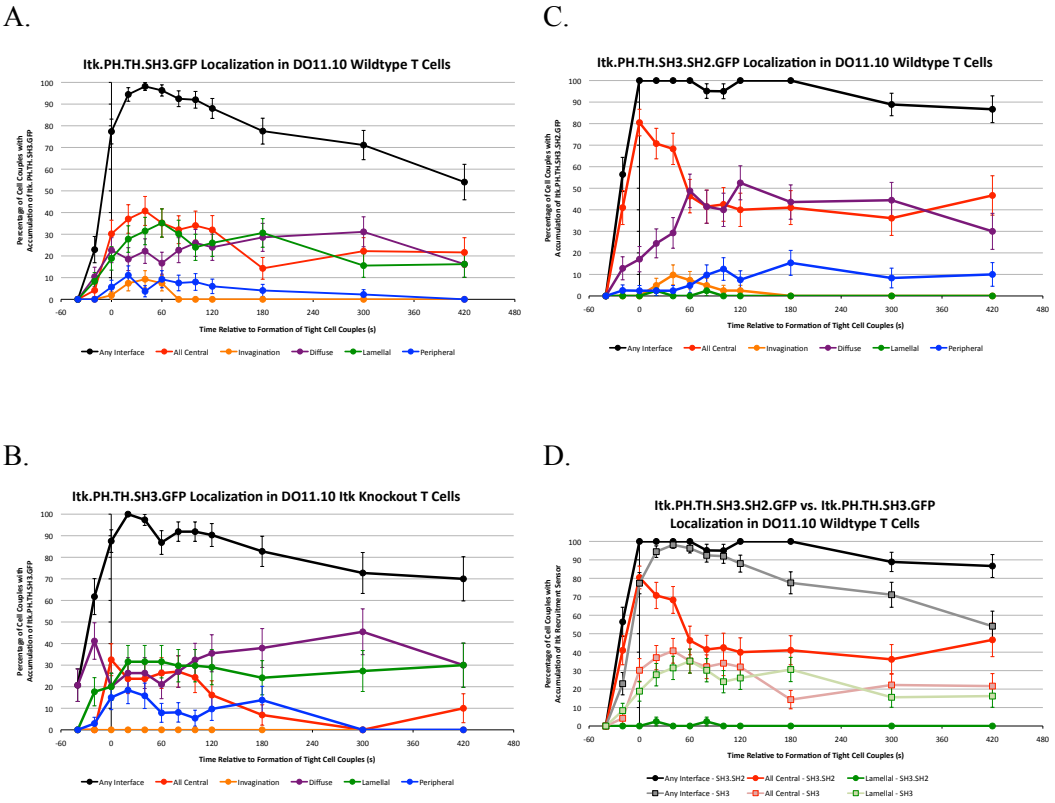

Figure 54: Spatiotemporal Localization of Itk.PH.TH.SH3.GFP in CD4^{+} DO11.10 TCR Transgenic Wildtype or Itk$^{-/-}$ T Cells. Primed primary DO11.10 (A and C) wildtype or (B) Itk$^{-/-}$ T cells were transduced with (A and B) Itk.PH.TH.SH3.GFP or (C) Itk.PH.TH.SH3.SH2.GFP and stimulated with A20 B cell lymphoma APCs in the presence of 10μM OVA antigenic peptide. (D) Shows the comparison of the Itk.PH.TH.SH3.GFP and Itk.PH.TH.SH3.SH2.GFP in wildtype T cells. Time indicated is relative to the formation of a tight coupling of the T cell with the APC. The graphs display the percentage of cell couples that displayed accumulation of signaling intermediates with the indicated patterns. 54 cell couples were analyzed for the wildtype T cells containing Itk.PH.TH.SH3.GFP; 40 cell couples for the Itk$^{-/-}$ T cells containing Itk.PH.TH.SH3.GFP; 41 cell couples for the wildtype T cells containing Itk.PH.TH.SH3.SH2.GFP. Error bars represent standard error.

A.

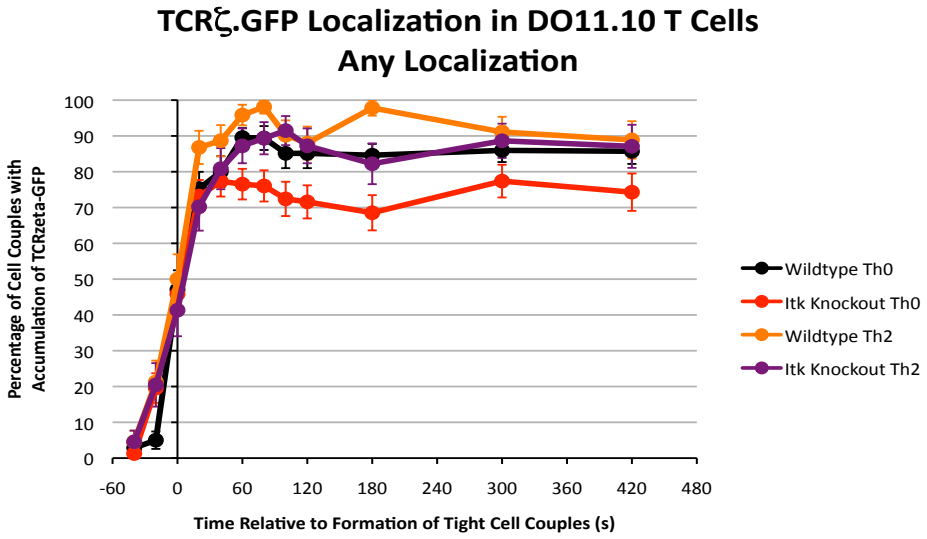

B.

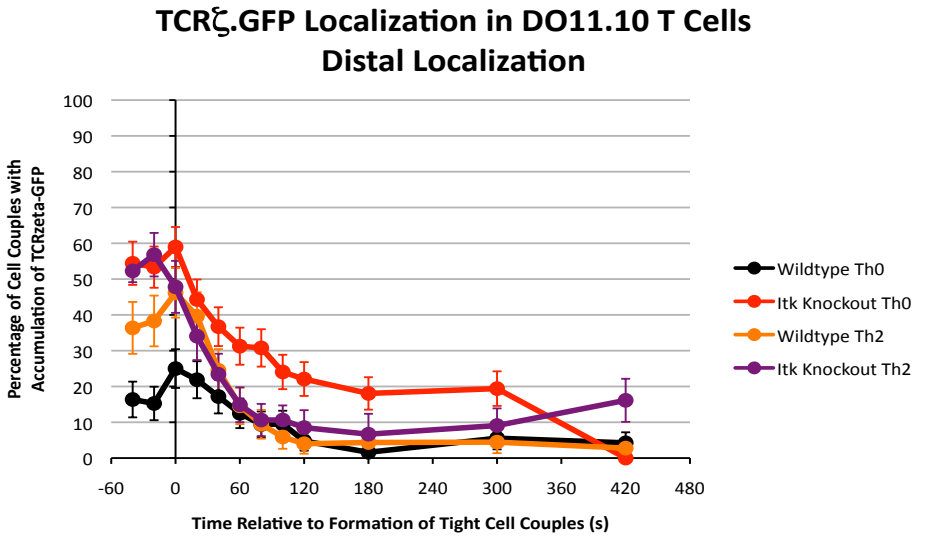

Figure 55: Localization of TCRζ in Th2 Polarized CD4^{+} DO11.10 TCR Transgenic Itk$^{-/-}$ or Wildtype T Cells. Wildtype and Itk$^{-/-}$ primary DO11.10 T cells were polarized under Th2 conditions or allowed to drift without any polarization stimuli (Th0). These primed cells were transduced with TCRζ.GFP and stimulated with A20 B cell lymphoma APCs in the presence of 10μM OVA antigenic peptide. Time indicated is relative to the formation of a tight coupling of the T cell with the APC. The graphs display the percentage of cell couples that displayed (A) any TCRζ accumulation at the interface or (B) recruitment to the distal pole. 134 wildtype and 98 Itk$^{-/-}$ Th0 T cells were analyzed; 53 wildtype and 47 Itk$^{-/-}$ for the Th2 polarized cells. Error bars represent standard error.

A.

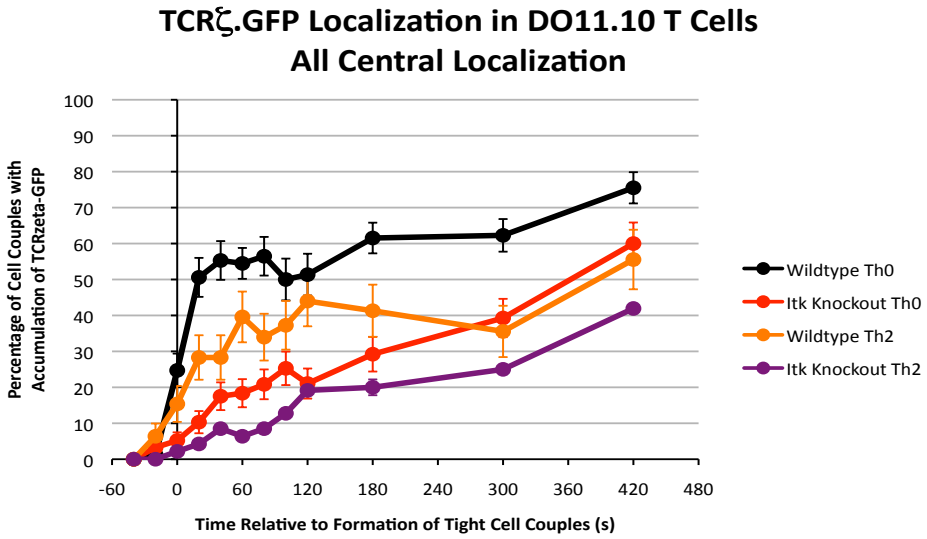

B.

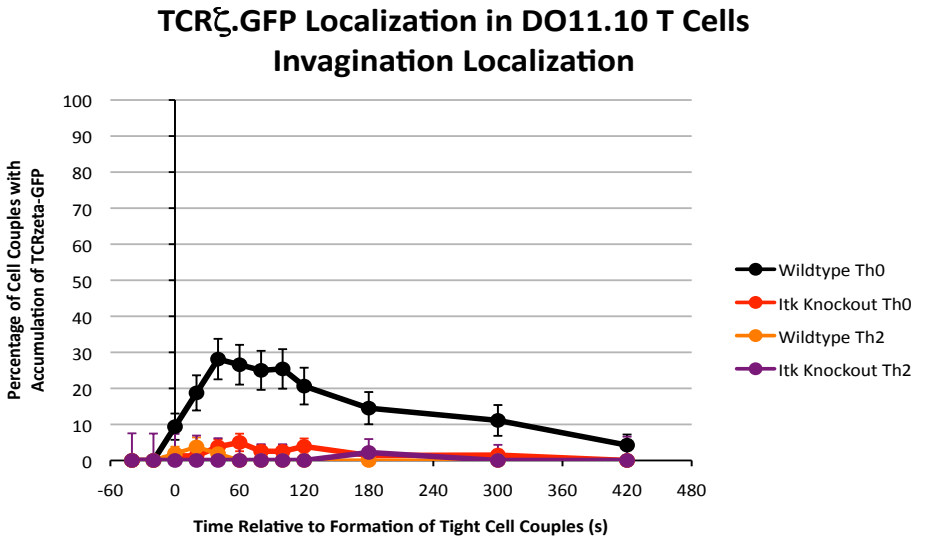

Figure 56: Localization of TCRζ in Th2 Polarized CD4^{+} DO11.10 TCR Transgenic Itk$^{-/-}$ or Wildtype T Cells. Wildtype and Itk$^{-/-}$ primary DO11.10 T cells were polarized under Th2 conditions or allowed to drift without any polarization stimuli (Th0). These primed cells were transduced with TCRζ.GFP and stimulated with A20 B cell lymphoma APCs in the presence of 10μM OVA antigenic peptide. Time indicated is relative to the formation of a tight coupling of the T cell with the APC. The graphs display the percentage of cell couples that displayed (A) central TCRζ accumulation at the interface or (B) recruitment to the invagination. 134 wildtype and 98 Itk$^{-/-}$ Th0 T cells were analyzed; 53 wildtype and 47 Itk$^{-/-}$ for the Th2 polarized cells. Error bars represent standard error.

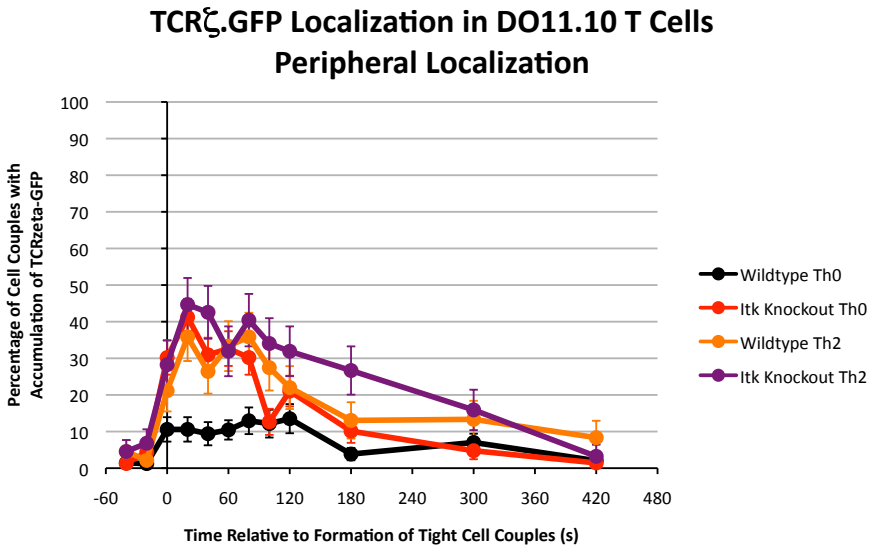

Figure 57: Peripheral Localization of TCRζ in Th2 Polarized CD4^{+} DO11.10 TCR Transgenic Itk$^{-/-}$ or Wildtype T Cells. Wildtype and Itk$^{-/-}$ primary DO11.10 T cells were polarized under Th2 conditions or allowed to drift without any polarization stimuli (Th0). These primed cells were transduced with TCRζ.GFP and stimulated with A20 B cell lymphoma APCs in the presence of 10μM OVA antigenic peptide. Time indicated is relative to the formation of a tight coupling of the T cell with the APC. The graph displays the percentage of cell couples that displayed peripheral TCRζ accumulation at the interface. 134 wildtype and 98 Itk$^{-/-}$ Th0 T cells were analyzed; 53 wildtype and 47 Itk$^{-/-}$ for the Th2 polarized cells. Error bars represent standard error.

A.

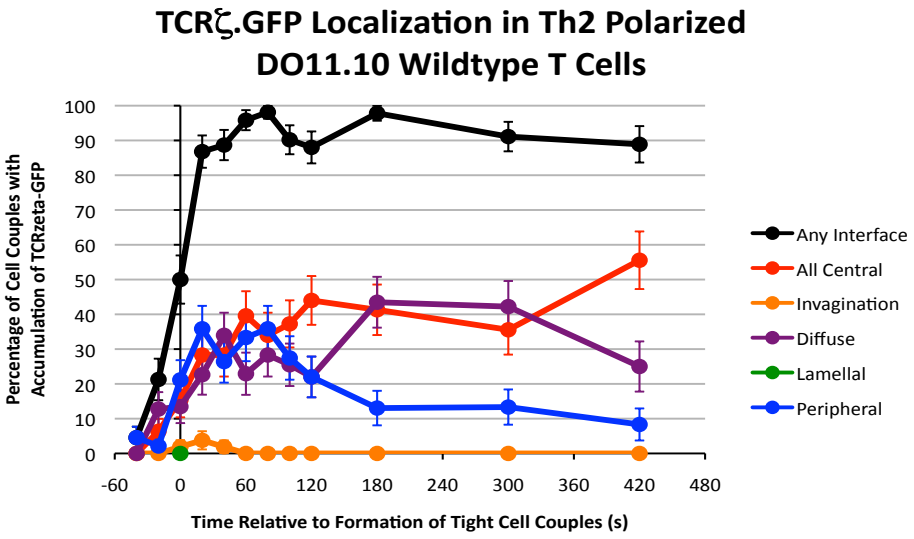

B.

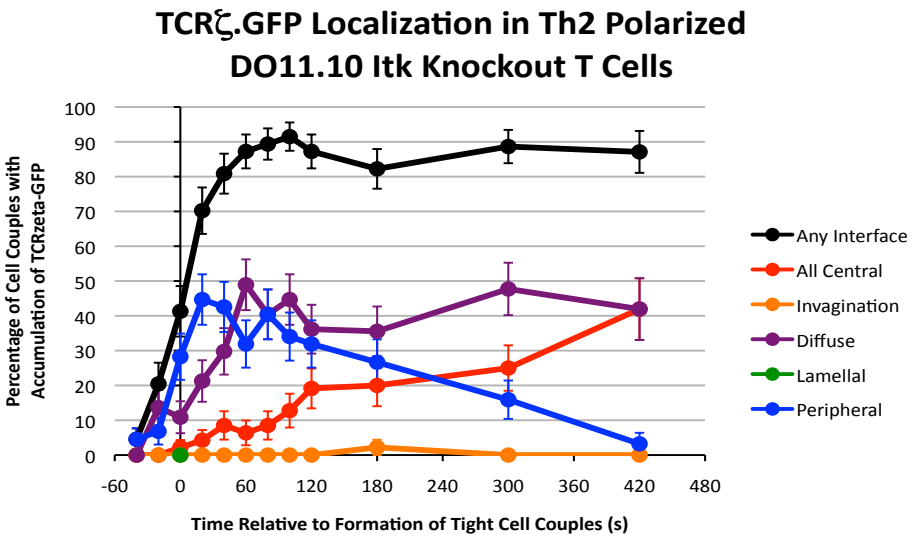

Figure 58: Spatiotemporal Localization of TCRζ.GFP in Th2 Polarized CD4^{+} DO11.10 TCR Transgenic Wildtype or Itk$^{-/-}$ T Cells. Primed primary DO11.10 (A) wildtype or (B) Itk$^{-/-}$ T cells were polarized under Th2 conditions. The cells were transduced with TCRζ.GFP and stimulated with A20 B cell lymphoma APCs in the presence of 10μM OVA antigenic peptide. Time indicated is relative to the formation of a tight coupling of the T cell with the APC. The graphs display the percentage of cell couples that displayed accumulation of signaling intermediates with the indicated patterns. 53 cell couples were analyzed for the wildtype T cells; 47 cell couples for the Itk$^{-/-}$ T cells. Error bars represent standard error.

CHAPTER IV

DISCUSSION

Overall Conclusions

In this thesis project, a systems-level approach was taken towards understanding the role Itk in T cell activation. While others have reported that $Itk^{-/-}$ T cells have deficiencies in the recruitment of individual molecules such as Vav1, this is the first large scale analysis where the spatial localization of multiple proteins were individually tracked in live cells within seconds of the T cells forming cell couples with APCs. Through quantitative analysis of the spatiotemporal patterning of 14 different receptors and signaling intermediates in both wildtype and $Itk^{-/-}$ T cells, it was found that Itk is a key regulator in the recruitment of signaling proteins to the center of the immunological synapse. Moreover, it was found that the greatest interruption in the organization of the $Itk^{-/-}$ synapse occurred within the first twenty seconds following cell couple formation, during the establishment of spatial segregation. Correlatively, Itk was strongly recruited exclusively to the center of the interface immediately upon wildtype T cell engagement with the APC, further supporting the role of Itk in this process. As the center of the immunological synapse has been identified as a site of active signaling, the failure of $Itk^{-/-}$ T cells to efficiently recruit signaling components to the center of the interface may be a contributing factor towards the hyporesponsiveness of these cells.

In contrast with a previous reports (52, 88), it was found here that $Itk^{-/-}$ T cells localized both activate Cdc42 and Vav1 to the immunological synapse. One possibility for the discrepancy may be the choice of TCR transgenic T cells. The study here used the DO11.10 TCR transgene while the previous studies used the AND transgene or Jurkat T cells. While it would be interesting to examine $Itk^{-/-}$ AND T cells directly using the system outlined in this thesis, an alternate approach would be to use decreasing peptide concentrations to determine if overall signal strength affects Itk mediated Cdc42 activation or Vav1 localization in the DO11.10 model. Another possible explanation for the conflicting observations might reside in that the previous studies used fixed cells while the study presented here followed T cells in real time. One advantage to using live cell imaging is that it is easy to distinguish the difference between a T cell that forms a productive cell couple with an APC versus a T cell that is simply adjacent to an APC cell. In contrast, the fixed cell samples were prepared by centrifuging the T cells and APCs together, incubating at 37°C for 5 or 10 minutes ((52) and (88) respectively), and then adding the fixative agent. Even if the cells were vigorously resuspended, this process would have formed cell-cell conjugates independent of T cell activation. As the $Itk^{-/-}$ AND T cells were reported to have decreased coupling frequency compared to the wildtype T cells, a higher percentage of the cell couples analyzed in the $Itk^{-/-}$ sample may have resulted from this experimental artifact and not from T cell activation. Further studies will need to be conducted to more completely examine the role of Itk in Cdc42 activation and Vav1 localization.

Data presented here identify a new actin polymerization phenotype, dubbed the actin burst, where wildtype T cells experience a sharp and transient increase in actin

immediately at the cell-cell interface. While others have previously reported that $Itk^{-/-}$ T cells recruit less actin to the synapse, these studies were conducted with fixed cell couples and the reduction in actin polymerization was concluded to be a generalized defect (87, 88). It was found here that the reduction in actin seen in $Itk^{-/-}$ cells predominantly occurs within the first two minutes of T cell stimulation with differences after five minutes being relatively small. The data also suggests two regulatory mechanisms of actin at the interface; the first being the Itk dependent actin burst with the second being an Itk independent basal level of actin localization at the synapse. Itk is therefore not a general regulator of actin polarization in the T cell, but plays a specific role in generating the actin burst.

Central localization of GTP bound Cdc42 was shown to play an important role in the generation of the actin burst. While wildtype T cells displayed a significant pool of centrally localized activated Cdc42, Itk deficient T cells instead showed a lack of central accumulation with the activated Cdc42 being enriched at the periphery of the interface. Reconstituting this central pool by targeting a constitutively active Cdc42 (Cdc42ca) to the center of the T cell / APC interface via the Tec PH.TH.SH3 recruitment domains restored the actin burst in $Itk^{-/-}$ T cells. The Cdc42ca had to be spatially targeted, however, as increasing Cdc42ca at the synapse without spatial consideration (via the Zap70.2SH2 domain) or increasing the total cellular level of Cdc42ca was not able to restore the actin burst. This is the first time that it has been shown that the spatial regulation of a signaling intermediate, and not the cellular levels of the activated protein, plays the important role in biological function. Additionally, this data further supports

the hypothesis that the center of the immunological synapse is an important site of active signaling and a key regulator of T cell activation.

Through a screen of four GEFs, SLAT was determined to be a likely candidate for Itk mediated activity of Cdc42 at the center of the T cell / APC interface. SLAT and Itk showed similar initial recruitment to the center of the interface and the early central localization of SLAT was severely reduced in the absence of Itk. Itk acting on SLAT would be consistent with the literature as, like $Itk^{-/-}$ cells, $SLAT^{-/-}$ T cells demonstrate impaired TCR-induced proliferation and IL2 production, inhibited release of Ca^{2+} from intracellular stores, reduced actin polymerization at the T cell / APC interface, and an impaired Th2 response (119, 120). This hypothesis will have to be further tested by selectively knocking down SLAT expression in wildtype T cells and determining if there is a reduction in activated Cdc42 at the center of the interface and a corresponding decrease in the actin burst. One caveat to this model is that levels of activated Cdc42 were normal in $Itk^{-/-}$ T cells. There are two possible, non-competing explanations for this observation. The first is that SLAT activated Cdc42 may be a minor fraction of the total cellar levels of activated Cdc42. The second possibility is that $Itk^{-/-}$ T cells may have enhanced peripheral activation of Cdc42. Should the SLAT knockdown experiments coincide with the model, it would identify a novel mechanistic role for both Itk and SLAT in T cell activation.

Restoration of the actin burst by centrally targeted Cdc42ca was not able to restore recruitment of TCRζ to the center of the synapse in $Itk^{-/-}$ T cells. Instead, tat-Tec.PH.TH.SH3-Cdc42ca inhibited this process in both the knockout and wildtype T cells. Having both $Itk^{-/-}$ and wildtype T cells affected indicated that the effect was Itk

independent and Cdc42 dependent. The introduction of caCdc42 to the center of the interface was a brute force approach towards encouraging actin polymerization that likely lacked the corresponding up-regulation of actin regulatory mechanisms that would have been present during the physiological actin burst. Actin dynamics and turnover may not have been properly reconstituted, possibly creating a relatively rigid cytoskeletal network. One candidate protein for this regulation was cofilin. Cofilin increases actin turnover and is an important factor in actin dynamics at the immunological synapse (107-110). Importantly, Cdc42 acts upstream of cofilin promoting its inactivation, suggesting that the increased Cdc42ca may have decreased cytoskeletal dynamics by inhibiting cofilin. Reintroducing 10nM constitutively active cofilin was able to relieve the inhibition in central TCRζ recruitment in the $Itk^{-/-}$ T cells caused by the centrally targeted Cdc42, but not restore central TCRζ recruitment to unmanipulated wildtype levels. It's possible that different concentrations (1nM or 100nM) of constitutively active cofilin might be able to further restore central TCRζ localization in the knockout T cell. While originally planned, these experiments weren't conducted due to the limited availability of $Itk^{-/-}$ T cells and the unstable nature of the tat-caCofilin protein, which had to be isolated every week immediately prior to each experiment. Another possible way to restore central recruitment of TCRζ might be to titrate down the tat-Tec.PH.TH.SH3-Cdc42ca. 100nM of centrally targeted Cdc42ca may be well beyond the amount necessary to restore the actin burst and the excess Cdc42ca may be causing the inhibited central localization. Unfortunately, as with the tat-caCofilin, these are not trivial experiments as it would take, on average, four weeks to test each concentration. It's possible that even if the actin burst was completely restored with all the proper cytoskeletal dynamics in $Itk^{-/-}$

T cells, the recruitment of signaling proteins and receptors to the center of the T cell / APC interface may not be rescued. Itk is composed of a Tec-homology, SH3, and SH2 domain, all of which engage in multiple protein-protein interactions allowing for Itk to act as a scaffolding protein; Itk has been proposed to help stabilize the LAT / SLP-76 signalosome (121). A critical mechanism for central signaling may be the stability of these protein-protein complexes. In the absence of Itk, these multi-protein complexes may fall apart. As the role of Itk as an adaptor protein is intertwined with its ability to regulate actin, it will be exceedingly difficult to uncouple these two functions in future experiments.

In evaluating the role of the Itk SH2 and kinase domains it was found that the SH2 domain was critical for the recruitment of the TCRζ from the distal pole to the T cell / APC interface. Others have examined the Itk SH2 domain in actin polymerization though the reconstitution or over expression of R265A Itk (SH2 binding mutation) and have concluded that the SH2 domain is important for the regulation of actin polymerization (52, 87). While likely true, the data here suggests the possibility that decreased levels of TCRζ recruited to the site of activation may have been a contributing factor in the reduced actin polymerization. One interesting observation is that R265A reconstituted T cells showed a more severe phenotype than the unmanipulated $Itk^{-/-}$ cells. A possible explanation for this is that Tec and Rlk, both Itk homologues, may be able to compensate to a limited extent for the absence of Itk. In support of this, over expression either homologue has been shown rescue $Itk^{-/-}$ T cells (27). The R265A SH2 binding mutant may have acted as a dominant negative (either through increased affinity or simple out expression), preventing Tec and Rlk from acting in lieu of Itk. This

hypothesis could be tested by comparing the spatiotemporal localization of Tec.PH.TH.SH3.SH2-GFP in wildtype, $Itk^{-/-}$, and $Itk^{-/-}$ R265A reconstituted T cells. If Tec were compensating for Itk, one would expect that the Tec sensor would show more sustained localization in the $Itk^{-/-}$ T cell, similar to Itk in the wildtype cell, and return to being transient in the R265A reconstituted T cells.

In contrast to the R265A SH2 mutant, reconstitution of $Itk^{-/-}$ T cells with a kinase dead (K390R) Itk showed a partial restoration in the central localization of TCRζ, particularly with an immediate, if diminished, burst of central recruitment immediately upon cell couple formation. What's interesting about this is that reintroducing K390R Itk has been shown to restore actin recruitment to the T cell / APC interface (52); though it should be noted that the work was conducted with fixed cells, so it's unclear whether the kinetics of actin recruitment were restored. This suggests that while the kinase domain may not be important for actin at the interface, it may play an important role in the organization of the synapse. Two possible mechanisms may explain this observation. In the absence of the Itk kinase domain, PLCγ1 remains hypophoshporylated on a cellular level and calcium flux is impaired. A number of proteins involved in T cell activation, including WASP, cofilin, and ERM proteins are regulated by $PI_{(4,5)}P_2$ (122-124). A failure to hydrolyze $PI_{(4,5)}P_2$ and remove it from the membrane would interrupt the spatial regulation of $PI_{(4,5)}P_2$ binding proteins, prolonging their activation (WASP and ERM proteins) or inhibition (cofilin) at the T cell / APC interface. The other mechanism that could possibly perturb synaptic organization would be the failure to restore calcium flux. Intracellular calcium levels regulate cytoskeletal dynamics and integrin adhesion through the activation of the calcium dependent protease calpain. Upon activation, calpain

cleaves actin-binding proteins promoting the clustering of integrins and cytoskeletal reorganization (125, 126). Actin at the interface may be restored by the kinase dead Itk, the cytoskeleton dynamics may have been impaired preventing the restoration of the center of the immunological synapse. Further studies examining the role of the kinase domain in T cell signaling will need to be conducted as several pharmaceutical companies are actively pursuing Itk specific kinase inhibitors as agents for selectively inhibiting the Th2 mediated immune response (45-50). Together, the findings here suggest that the Itk SH2 and kinase domains each play much broader, multidimensional roles in T cell activation than simply influencing actin polymerization and calcium flux. Each plays significant roles in the organization of the immunological synapse, thereby synergistically contributing to Itk's defined role as an amplifier of T cell signaling.

One of the more extensively studied defects in $Itk^{-/-}$ T cells is that Th2 polarized cells are unable exert effector cytokine production upon restimulation (35). In agreement with previously published work (4, 17, 51), it was shown that Th2 T cells displayed reduced central TCRζ localization compared to Th0 cells. Additionally, the impaired interface organization observed in $Itk^{-/-}$ T cells acted synergistically with the Th2 defect to further promote disorganization at the interface. While certainly not conclusive, this suggests the possibility that the combined effects on inhibiting central localization may be a contributing factor in promoting the anergic state of the Th2 $Itk^{-/-}$ T cell.

This thesis demonstrates that Itk is a key regulator of the spatiotemporal organization at the T cell / APC interface. One consequence of this is the activation of Cdc42 at the center of the interface, possibly by SLAT, which results immediate and transient actin polarization at the interface. This actin burst likely further promotes

enhanced spatial segregation at the immunological synapse, enhancing T cell signaling through clustering of signaling intermediates. In addition to identifying a possible mechanistic explanation for how Itk both regulates the cytoskeleton and acts to amplify T cell signaling, this is the first time that it has been directly shown that spatial control of a protein (the activation of Cdc42) at the immunological synapse has direct physiological consequence.

REFERENCES

1. Monks CR, Freiberg BA, Kupfer H, Sciaky N, Kupfer A. Three-dimensional segregation of supramolecular activation clusters in T cells. Nature. 1998;395(6697):82-6.

2. Monks CR, Kupfer H, Tamir I, Barlow A, Kupfer A. Selective modulation of protein kinase C-theta during T-cell activation. Nature. 1997;385(6611):83-6.

3. Grakoui A, Bromley SK, Sumen C, Davis MM, Shaw AS, Allen PM, et al. The immunological synapse: a molecular machine controlling T cell activation. Science. 1999;285(5425):221-7.

4. Singleton KL, Roybal KT, Sun Y, Fu G, Gascoigne NR, van Oers NS, et al. Spatiotemporal patterning during T cell activation is highly diverse. Sci Signal. 2009;2(65):ra15. PMCID: 2694444.

5. Krogsgaard M, Li QJ, Sumen C, Huppa JB, Huse M, Davis MM. Agonist/endogenous peptide-MHC heterodimers drive T cell activation and sensitivity. Nature. 2005;434(7030):238-43.

6. Wulfing C, Sumen C, Sjaastad MD, Wu LC, Dustin ML, Davis MM. Costimulation and endogenous MHC ligands contribute to T cell recognition. Nat Immunol. 2002;3(1):42-7.

7. Li QJ, Dinner AR, Qi S, Irvine DJ, Huppa JB, Davis MM, et al. CD4 enhances T cell sensitivity to antigen by coordinating Lck accumulation at the immunological synapse. Nat Immunol. 2004;5(8):791-9.

8. Purtic B, Pitcher LA, van Oers NS, Wulfing C. T cell receptor (TCR) clustering in the immunological synapse integrates TCR and costimulatory signaling in selected T cells. Proc Natl Acad Sci U S A. 2005;102(8):2904-9. PMCID: 549456.

9. Varma R, Campi G, Yokosuka T, Saito T, Dustin ML. T cell receptor-proximal signals are sustained in peripheral microclusters and terminated in the central supramolecular activation cluster. Immunity. 2006;25(1):117-27. PMCID: 1626533.

10. Campi G, Varma R, Dustin ML. Actin and agonist MHC-peptide complex-dependent T cell receptor microclusters as scaffolds for signaling. J Exp Med. 2005;202(8):1031-6. PMCID: 1373686.

11. Yokosuka T, Sakata-Sogawa K, Kobayashi W, Hiroshima M, Hashimoto-Tane A, Tokunaga M, et al. Newly generated T cell receptor microclusters initiate and sustain T cell activation by recruitment of Zap70 and SLP-76. Nat Immunol. 2005;6(12):1253-62.

12. Tamm LK, McConnell HM. Supported phospholipid bilayers. Biophys J. 1985;47(1):105-13. PMCID: 1435076.

13. Singleton K, Parvaze N, Dama KR, Chen KS, Jennings P, Purtic B, et al. A large T cell invagination with CD2 enrichment resets receptor engagement in the immunological synapse. J Immunol. 2006;177(7):4402-13.

14. Ilani T, Vasiliver-Shamis G, Vardhana S, Bretscher A, Dustin ML. T cell antigen receptor signaling and immunological synapse stability require myosin IIA. Nat Immunol. 2009;10(5):531-9. PMCID: 2719775.

15. Srivastava S, Di L, Zhdanova O, Li Z, Vardhana S, Wan Q, et al. The class II phosphatidylinositol 3 kinase C2beta is required for the activation of the K+ channel KCa3.1 and CD4 T-cells. Mol Biol Cell. 2009;20(17):3783-91. PMCID: 2735477.

16. Tseng SY, Waite JC, Liu M, Vardhana S, Dustin ML. T cell-dendritic cell immunological synapses contain TCR-dependent CD28-CD80 clusters that recruit protein kinase C theta. J Immunol. 2008;181(7):4852-63. PMCID: 2556893.

17. Thauland TJ, Koguchi Y, Wetzel SA, Dustin ML, Parker DC. Th1 and Th2 cells form morphologically distinct immunological synapses. J Immunol. 2008;181(1):393-9. PMCID: 2441916.

18. Sims TN, Soos TJ, Xenias HS, Dubin-Thaler B, Hofman JM, Waite JC, et al. Opposing effects of PKCtheta and WASp on symmetry breaking and relocation of the immunological synapse. Cell. 2007;129(4):773-85.

19. Yokosuka T, Kobayashi W, Sakata-Sogawa K, Takamatsu M, Hashimoto-Tane A, Dustin ML, et al. Spatiotemporal regulation of T cell costimulation by TCR-CD28 microclusters and protein kinase C theta translocation. Immunity. 2008;29(4):589-601.

20. Douglass AD, Vale RD. Single-molecule microscopy reveals plasma membrane microdomains created by protein-protein networks that exclude or trap signaling molecules in T cells. Cell. 2005;121(6):937-50.

21. Green JM, Karpitskiy V, Kimzey SL, Shaw AS. Coordinate regulation of T cell activation by CD2 and CD28. J Immunol. 2000;164(7):3591-5.

22. Pentcheva-Hoang T, Egen JG, Wojnoonski K, Allison JP. B7-1 and B7-2 selectively recruit CTLA-4 and CD28 to the immunological synapse. Immunity. 2004;21(3):401-13.

23. Symposium Some Mathematical Questions in B, Goldstein B, Wofsy C, editors. Cell biology : 1992 Symposium on Some Mathematical Questions in Biology, November 15-19, 1992, Denver, Colorado 1994; Providence, R.I.: American Mathematical Society.

24. Naramura M, Jang IK, Kole H, Huang F, Haines D, Gu H. c-Cbl and Cbl-b regulate T cell responsiveness by promoting ligand-induced TCR down-modulation. Nat Immunol. 2002;3(12):1192-9.

25. Lucas JA, Miller AT, Atherly LO, Berg LJ. The role of Tec family kinases in T cell development and function. Immunol Rev. 2003;191:119-38.

26. Miller AT, Wilcox HM, Lai Z, Berg LJ. Signaling through Itk promotes T helper 2 differentiation via negative regulation of T-bet. Immunity. 2004;21(1):67-80.

27. Tomlinson MG, Kane LP, Su J, Kadlecek TA, Mollenauer MN, Weiss A. Expression and function of Tec, Itk, and Btk in lymphocytes: evidence for a unique role for Tec. Mol Cell Biol. 2004;24(6):2455-66. PMCID: 355844.

28. Hu Q, Davidson D, Schwartzberg PL, Macchiarini F, Lenardo MJ, Bluestone JA, et al. Identification of Rlk, a novel protein tyrosine kinase with predominant expression in the T cell lineage. J Biol Chem. 1995;270(4):1928-34.

29. Colgan J, Asmal M, Neagu M, Yu B, Schneidkraut J, Lee Y, et al. Cyclophilin A regulates TCR signal strength in CD4+ T cells via a proline-directed conformational switch in Itk. Immunity. 2004;21(2):189-201.

30. Schaeffer EM, Yap GS, Lewis CM, Czar MJ, McVicar DW, Cheever AW, et al. Mutation of Tec family kinases alters T helper cell differentiation. Nat Immunol. 2001;2(12):1183-8.

31. Miller AT, Berg LJ. Defective Fas ligand expression and activation-induced cell death in the absence of IL-2-inducible T cell kinase. J Immunol. 2002;168(5):2163-72.

32. Liao XC, Littman DR. Altered T cell receptor signaling and disrupted T cell development in mice lacking Itk. Immunity. 1995;3(6):757-69.

33. Schaeffer EM, Debnath J, Yap G, McVicar D, Liao XC, Littman DR, et al. Requirement for Tec kinases Rlk and Itk in T cell receptor signaling and immunity. Science. 1999;284(5414):638-41.

34. Liu KQ, Bunnell SC, Gurniak CB, Berg LJ. T cell receptor-initiated calcium release is uncoupled from capacitative calcium entry in Itk-deficient T cells. J Exp Med. 1998;187(10):1721-7. PMCID: 2212298.

35. Au-Yeung BB, Katzman SD, Fowell DJ. Cutting edge: Itk-dependent signals required for CD4+ T cells to exert, but not gain, Th2 effector function. J Immunol. 2006;176(7):3895-9.

36. Donnadieu E, Lang V, Bismuth G, Ellmeier W, Acuto O, Michel F, et al. Differential roles of Lck and Itk in T cell response to antigen recognition revealed by calcium imaging and electron microscopy. J Immunol. 2001;166(9):5540-9.

37. Gomez-Rodriguez J, Readinger JA, Viorritto IC, Mueller KL, Houghtling RA, Schwartzberg PL. Tec kinases, actin, and cell adhesion. Immunol Rev. 2007;218:45-64.

38. Fowell DJ, Shinkai K, Liao XC, Beebe AM, Coffman RL, Littman DR, et al. Impaired NFATc translocation and failure of Th2 development in Itk-deficient CD4+ T cells. Immunity. 1999;11(4):399-409.

39. Hu J, Sahu N, Walsh E, August A. Memory phenotype CD8+ T cells with innate function selectively develop in the absence of active Itk. Eur J Immunol. 2007;37(10):2892-9. PMCID: 2770953.

40. Mueller C, August A. Attenuation of immunological symptoms of allergic asthma in mice lacking the tyrosine kinase ITK. J Immunol. 2003;170(10):5056-63.

41. Ferrara TJ, August A, Ben-Jebria A. Modulation of tracheal smooth muscle responses in inducible T-cell kinase knockout mice. Pulm Pharmacol Ther. 2004;17(5):301-8.

42. Ferrara TJ, Mueller C, Sahu N, Ben-Jebria A, August A. Reduced airway hyperresponsiveness and tracheal responses during allergic asthma in mice lacking tyrosine kinase inducible T-cell kinase. J Allergy Clin Immunol. 2006;117(4):780-6.

43. Sahu N, Mueller C, Fischer A, August A. Differential sensitivity to Itk kinase signals for T helper 2 cytokine production and chemokine-mediated migration. J Immunol. 2008;180(6):3833-8.

44. Sahu N, Venegas AM, Jankovic D, Mitzner W, Gomez-Rodriguez J, Cannons JL, et al. Selective expression rather than specific function of Txk and Itk regulate Th1 and Th2 responses. J Immunol. 2008;181(9):6125-31.

45. Cook BN, Bentzien J, White A, Nemoto PA, Wang J, Man CC, et al. Discovery of potent inhibitors of interleukin-2 inducible T-cell kinase (ITK) through structure-based drug design. Bioorg Med Chem Lett. 2009;19(3):773-7.

46. Riether D, Zindell R, Kowalski JA, Cook BN, Bentzien J, Lombaert SD, et al. 5-Aminomethylbenzimidazoles as potent ITK antagonists. Bioorg Med Chem Lett. 2009;19(6):1588-91.

47. Das J, Liu C, Moquin RV, Lin J, Furch JA, Spergel SH, et al. Discovery and SAR of 2-amino-5-[(thiomethyl)aryl]thiazoles as potent and selective Itk inhibitors. Bioorg Med Chem Lett. 2006;16(9):2411-5.

48. Lin TA, McIntyre KW, Das J, Liu C, O'Day KD, Penhallow B, et al. Selective Itk inhibitors block T-cell activation and murine lung inflammation. Biochemistry. 2004;43(34):11056-62.

49. Kashem MA, Nelson RM, Yingling JD, Pullen SS, Prokopowicz AS, 3rd, Jones JW, et al. Three mechanistically distinct kinase assays compared: Measurement of intrinsic ATPase activity identified the most comprehensive set of ITK inhibitors. J Biomol Screen. 2007;12(1):70-83.

50. Snow RJ, Abeywardane A, Campbell S, Lord J, Kashem MA, Khine HH, et al. Hit-to-lead studies on benzimidazole inhibitors of ITK: discovery of a novel class of kinase inhibitors. Bioorg Med Chem Lett. 2007;17(13):3660-5.

51. Balamuth F, Leitenberg D, Unternaehrer J, Mellman I, Bottomly K. Distinct patterns of membrane microdomain partitioning in Th1 and th2 cells. Immunity. 2001;15(5):729-38.

52. Dombroski D, Houghtling RA, Labno CM, Precht P, Takesono A, Caplen NJ, et al. Kinase-independent functions for Itk in TCR-induced regulation of Vav and the actin cytoskeleton. J Immunol. 2005;174(3):1385-92.

53. Huck K, Feyen O, Niehues T, Ruschendorf F, Hubner N, Laws HJ, et al. Girls homozygous for an IL-2-inducible T cell kinase mutation that leads to protein deficiency develop fatal EBV-associated lymphoproliferation. J Clin Invest. 2009;119(5):1350-8. PMCID: 2673872.

54. Benson M, Mobini R, Barrenas F, Hallden C, Naluai AT, Sall T, et al. A haplotype in the inducible T-cell tyrosine kinase is a risk factor for seasonal allergic rhinitis. Allergy. 2009;64(9):1286-91.

55. Rameh LE, Arvidsson A, Carraway KL, 3rd, Couvillon AD, Rathbun G, Crompton A, et al. A comparative analysis of the phosphoinositide binding specificity of pleckstrin homology domains. J Biol Chem. 1997;272(35):22059-66.

56. Salim K, Bottomley MJ, Querfurth E, Zvelebil MJ, Gout I, Scaife R, et al. Distinct specificity in the recognition of phosphoinositides by the pleckstrin homology domains of dynamin and Bruton's tyrosine kinase. EMBO J. 1996;15(22):6241-50. PMCID: 452447.

57. Yang WC, Ching KA, Tsoukas CD, Berg LJ. Tec kinase signaling in T cells is regulated by phosphatidylinositol 3-kinase and the Tec pleckstrin homology domain. J Immunol. 2001;166(1):387-95.

58. Bunnell SC, Diehn M, Yaffe MB, Findell PR, Cantley LC, Berg LJ. Biochemical interactions integrating Itk with the T cell receptor-initiated signaling cascade. J Biol Chem. 2000;275(3):2219-30.

59. Ching KA, Kawakami Y, Kawakami T, Tsoukas CD. Emt/Itk associates with activated TCR complexes: role of the pleckstrin homology domain. J Immunol. 1999;163(11):6006-13.

60. Shan X, Czar MJ, Bunnell SC, Liu P, Liu Y, Schwartzberg PL, et al. Deficiency of PTEN in Jurkat T cells causes constitutive localization of Itk to the plasma membrane and hyperresponsiveness to CD3 stimulation. Mol Cell Biol. 2000;20(18):6945-57. PMCID: 88770.

61. Smith CI, Islam TC, Mattsson PT, Mohamed AJ, Nore BF, Vihinen M. The Tec family of cytoplasmic tyrosine kinases: mammalian Btk, Bmx, Itk, Tec, Txk and homologs in other species. Bioessays. 2001;23(5):436-46.

62. Andreotti AH, Bunnell SC, Feng S, Berg LJ, Schreiber SL. Regulatory intramolecular association in a tyrosine kinase of the Tec family. Nature. 1997;385(6611):93-7.

63. Joseph RE, Fulton DB, Andreotti AH. Mechanism and functional significance of Itk autophosphorylation. J Mol Biol. 2007;373(5):1281-92. PMCID: 2753204.

64. Brazin KN, Fulton DB, Andreotti AH. A specific intermolecular association between the regulatory domains of a Tec family kinase. J Mol Biol. 2000;302(3):607-23.

65. Mallis RJ, Brazin KN, Fulton DB, Andreotti AH. Structural characterization of a proline-driven conformational switch within the Itk SH2 domain. Nat Struct Biol. 2002;9(12):900-5.

66. Laederach A, Cradic KW, Fulton DB, Andreotti AH. Determinants of intra versus intermolecular self-association within the regulatory domains of Rlk and Itk. J Mol Biol. 2003;329(5):1011-20.

67. Breheny PJ, Laederach A, Fulton DB, Andreotti AH. Ligand specificity modulated by prolyl imide bond Cis/Trans isomerization in the Itk SH2 domain: a quantitative NMR study. J Am Chem Soc. 2003;125(51):15706-7.

68. Pletneva EV, Sundd M, Fulton DB, Andreotti AH. Molecular details of Itk activation by prolyl isomerization and phospholigand binding: the NMR structure of the Itk SH2 domain bound to a phosphopeptide. J Mol Biol. 2006;357(2):550-61.

69. Severin A, Joseph RE, Boyken S, Fulton DB, Andreotti AH. Proline isomerization preorganizes the Itk SH2 domain for binding to the Itk SH3 domain. J Mol Biol. 2009;387(3):726-43. PMCID: 2810249.

70. Nore BF, Mattsson PT, Antonsson P, Backesjo CM, Westlund A, Lennartsson J, et al. Identification of phosphorylation sites within the SH3 domains of Tec family tyrosine kinases. Biochim Biophys Acta. 2003;1645(2):123-32.

71. Wilcox HM, Berg LJ. Itk phosphorylation sites are required for functional activity in primary T cells. J Biol Chem. 2003;278(39):37112-21.

72. Gibson S, August A, Branch D, Dupont B, Mills GM. Functional LCK Is required for optimal CD28-mediated activation of the TEC family tyrosine kinase EMT/ITK. J Biol Chem. 1996;271(12):7079-83.

73. Zhang W, Sloan-Lancaster J, Kitchen J, Trible RP, Samelson LE. LAT: the ZAP-70 tyrosine kinase substrate that links T cell receptor to cellular activation. Cell. 1998;92(1):83-92.

74. Bubeck Wardenburg J, Fu C, Jackman JK, Flotow H, Wilkinson SE, Williams DH, et al. Phosphorylation of SLP-76 by the ZAP-70 protein-tyrosine kinase is required for T-cell receptor function. J Biol Chem. 1996;271(33):19641-4.

75. Heyeck SD, Wilcox HM, Bunnell SC, Berg LJ. Lck phosphorylates the activation loop tyrosine of the Itk kinase domain and activates Itk kinase activity. J Biol Chem. 1997;272(40):25401-8.

76. Shan X, Wange RL. Itk/Emt/Tsk activation in response to CD3 cross-linking in Jurkat T cells requires ZAP-70 and Lat and is independent of membrane recruitment. J Biol Chem. 1999;274(41):29323-30.

77. Su YW, Zhang Y, Schweikert J, Koretzky GA, Reth M, Wienands J. Interaction of SLP adaptors with the SH2 domain of Tec family kinases. Eur J Immunol. 1999;29(11):3702-11.

78. Bogin Y, Ainey C, Beach D, Yablonski D. SLP-76 mediates and maintains activation of the Tec family kinase ITK via the T cell antigen receptor-induced association between SLP-76 and ITK. Proc Natl Acad Sci U S A. 2007;104(16):6638-43. PMCID: 1871838.

79. Smith-Garvin JE, Koretzky GA, Jordan MS. T cell activation. Annu Rev Immunol. 2009;27:591-619. PMCID: 2740335.

80. Reynolds LF, de Bettignies C, Norton T, Beeser A, Chernoff J, Tybulewicz VL. Vav1 transduces T cell receptor signals to the activation of the Ras/ERK pathway via LAT, Sos, and RasGRP1. J Biol Chem. 2004;279(18):18239-46.

81. Reynolds LF, Smyth LA, Norton T, Freshney N, Downward J, Kioussis D, et al. Vav1 transduces T cell receptor signals to the activation of phospholipase C-gamma1 via phosphoinositide 3-kinase-dependent and -independent pathways. J Exp Med. 2002;195(9):1103-14. PMCID: 2193701.

82. Genot E, Cantrell DA. Ras regulation and function in lymphocytes. Curr Opin Immunol. 2000;12(3):289-94.

83. Melowic HR, Stahelin RV, Blatner NR, Tian W, Hayashi K, Altman A, et al. Mechanism of diacylglycerol-induced membrane targeting and activation of protein kinase Ctheta. J Biol Chem. 2007;282(29):21467-76.

84. Oh-hora M, Rao A. Calcium signaling in lymphocytes. Curr Opin Immunol. 2008;20(3):250-8. PMCID: 2574011.

85. Parekh AB, Fleig A, Penner R. The store-operated calcium current I(CRAC): nonlinear activation by InsP3 and dissociation from calcium release. Cell. 1997;89(6):973-80.

86. Berg LJ, Finkelstein LD, Lucas JA, Schwartzberg PL. Tec family kinases in T lymphocyte development and function. Annu Rev Immunol. 2005;23:549-600.

87. Grasis JA, Browne CD, Tsoukas CD. Inducible T cell tyrosine kinase regulates actin-dependent cytoskeletal events induced by the T cell antigen receptor. J Immunol. 2003;170(8):3971-6.

88. Labno CM, Lewis CM, You D, Leung DW, Takesono A, Kamberos N, et al. Itk functions to control actin polymerization at the immune synapse through localized activation of Cdc42 and WASP. Curr Biol. 2003;13(18):1619-24.

89. Murphy KM, Heimberger AB, Loh DY. Induction by antigen of intrathymic apoptosis of CD4+CD8+TCRlo thymocytes in vivo. Science. 1990;250(4988):1720-3.

90. Costa GL, Benson JM, Seroogy CM, Achacoso P, Fathman CG, Nolan GP. Targeting rare populations of murine antigen-specific T lymphocytes by retroviral transduction for potential application in gene therapy for autoimmune disease. J Immunol. 2000;164(7):3581-90.

91. Carrizosa E, Gomez TS, Labno CM, Klos Dehring DA, Liu X, Freedman BD, et al. Hematopoietic lineage cell-specific protein 1 is recruited to the immunological synapse by IL-2-inducible T cell kinase and regulates phospholipase Cgamma1 Microcluster dynamics during T cell spreading. J Immunol. 2009;183(11):7352-61.

92. Perez-Villar JJ, Whitney GS, Sitnick MT, Dunn RJ, Venkatesan S, O'Day K, et al. Phosphorylation of the linker for activation of T-cells by Itk promotes recruitment of Vav. Biochemistry. 2002;41(34):10732-40.

93. Martin-Cofreces NB, Robles-Valero J, Cabrero JR, Mittelbrunn M, Gordon-Alonso M, Sung CH, et al. MTOC translocation modulates IS formation and controls sustained T cell signaling. J Cell Biol. 2008;182(5):951-62. PMCID: 2528574.

94. Kuhne MR, Lin J, Yablonski D, Mollenauer MN, Ehrlich LI, Huppa J, et al. Linker for activation of T cells, zeta-associated protein-70, and Src homology 2 domain-containing leukocyte protein-76 are required for TCR-induced microtubule-organizing center polarization. J Immunol. 2003;171(2):860-6.

95. Finkelstein LD, Schwartzberg PL. Tec kinases: shaping T-cell activation through actin. Trends Cell Biol. 2004;14(8):443-51.

96. Stowers L, Yelon D, Berg LJ, Chant J. Regulation of the polarization of T cells toward antigen-presenting cells by Ras-related GTPase CDC42. Proc Natl Acad Sci U S A. 1995;92(11):5027-31. PMCID: 41841.

97. Tskvitaria-Fuller I, Seth A, Mistry N, Gu H, Rosen MK, Wulfing C. Specific patterns of Cdc42 activity are related to distinct elements of T cell polarization. J Immunol. 2006;177(3):1708-20.

98. Soga N, Namba N, McAllister S, Cornelius L, Teitelbaum SL, Dowdy SF, et al. Rho family GTPases regulate VEGF-stimulated endothelial cell motility. Exp Cell Res. 2001;269(1):73-87.

99. Tskvitaria-Fuller I, Mistry N, Sun S, Wulfing C. Protein transduction as a means of effective manipulation of Cdc42 activity in primary T cells. J Immunol Methods. 2007;319(1-2):64-78. PMCID: 1847777.

100. Blanchard N, Di Bartolo V, Hivroz C. In the immune synapse, ZAP-70 controls T cell polarization and recruitment of signaling proteins but not formation of the synaptic pattern. Immunity. 2002;17(4):389-99.

101. Morgan MM, Labno CM, Van Seventer GA, Denny MF, Straus DB, Burkhardt JK. Superantigen-induced T cell:B cell conjugation is mediated by LFA-1 and requires signaling through Lck, but not ZAP-70. J Immunol. 2001;167(10):5708-18.

102. Krummel MF, Sjaastad MD, Wulfing C, Davis MM. Differential clustering of CD4 and CD3zeta during T cell recognition. Science. 2000;289(5483):1349-52.

103. Wulfing C, Davis MM. A receptor/cytoskeletal movement triggered by costimulation during T cell activation. Science. 1998;282(5397):2266-9.

104. Carlier MF, Laurent V, Santolini J, Melki R, Didry D, Xia GX, et al. Actin depolymerizing factor (ADF/cofilin) enhances the rate of filament turnover: implication in actin-based motility. J Cell Biol. 1997;136(6):1307-22. PMCID: 2132522.

105. Rosenblatt J, Agnew BJ, Abe H, Bamburg JR, Mitchison TJ. Xenopus actin depolymerizing factor/cofilin (XAC) is responsible for the turnover of actin filaments in Listeria monocytogenes tails. J Cell Biol. 1997;136(6):1323-32. PMCID: 2132508.

106. Lappalainen P, Drubin DG. Cofilin promotes rapid actin filament turnover in vivo. Nature. 1997;388(6637):78-82.

107. Samstag Y, Eckerskorn C, Wesselborg S, Henning S, Wallich R, Meuer SC. Costimulatory signals for human T-cell activation induce nuclear translocation of pp19/cofilin. Proc Natl Acad Sci U S A. 1994;91(10):4494-8. PMCID: 43812.

108. Samstag Y, Bader A, Meuer SC. A serine phosphatase is involved in CD2-mediated activation of human T lymphocytes and natural killer cells. J Immunol. 1991;147(3):788-94.

109. Ambach A, Saunus J, Konstandin M, Wesselborg S, Meuer SC, Samstag Y. The serine phosphatases PP1 and PP2A associate with and activate the actin-binding protein cofilin in human T lymphocytes. Eur J Immunol. 2000;30(12):3422-31.

110. Eibert SM, Lee KH, Pipkorn R, Sester U, Wabnitz GH, Giese T, et al. Cofilin peptide homologs interfere with immunological synapse formation and T cell activation. Proc Natl Acad Sci U S A. 2004;101(7):1957-62. PMCID: 357034.

111. Samstag Y, Eibert SM, Klemke M, Wabnitz GH. Actin cytoskeletal dynamics in T lymphocyte activation and migration. J Leukoc Biol. 2003;73(1):30-48.

112. Huang Y, Burkhardt JK. T-cell-receptor-dependent actin regulatory mechanisms. J Cell Sci. 2007;120(Pt 5):723-30.

113. Yonezawa N, Homma Y, Yahara I, Sakai H, Nishida E. A short sequence responsible for both phosphoinositide binding and actin binding activities of cofilin. J Biol Chem. 1991;266(26):17218-21.

114. Moriyama K, Iida K, Yahara I. Phosphorylation of Ser-3 of cofilin regulates its essential function on actin. Genes Cells. 1996;1(1):73-86.

115. Watanabe N, Higashida C. A Possible Role of Homeostasis Between Monomeric and Filamentous Actin in Filament Nucleation Revealed by Pharmacokinetic Modeling. 2009. p. 143-9.

116. Readinger JA, Mueller KL, Venegas AM, Horai R, Schwartzberg PL. Tec kinases regulate T-lymphocyte development and function: new insights into the roles of Itk and Rlk/Txk. Immunol Rev. 2009;228(1):93-114. PMCID: 2673963.

117. Lucas JA, Atherly LO, Berg LJ. The absence of Itk inhibits positive selection without changing lineage commitment. J Immunol. 2002;168(12):6142-51.

118. Mohrs M, Shinkai K, Mohrs K, Locksley RM. Analysis of type 2 immunity in vivo with a bicistronic IL-4 reporter. Immunity. 2001;15(2):303-11.

119. Becart S, Charvet C, Canonigo Balancio AJ, De Trez C, Tanaka Y, Duan W, et al. SLAT regulates Th1 and Th2 inflammatory responses by controlling Ca2+/NFAT signaling. J Clin Invest. 2007;117(8):2164-75. PMCID: 1924495.

120. Fanzo JC, Yang W, Jang SY, Gupta S, Chen Q, Siddiq A, et al. Loss of IRF-4-binding protein leads to the spontaneous development of systemic autoimmunity. J Clin Invest. 2006;116(3):703-14. PMCID: 1361345.

121. Jordan MS, Sadler J, Austin JE, Finkelstein LD, Singer AL, Schwartzberg PL, et al. Functional hierarchy of the N-terminal tyrosines of SLP-76. J Immunol. 2006;176(4):2430-8.

122. Higgs HN, Pollard TD. Activation by Cdc42 and PIP(2) of Wiskott-Aldrich syndrome protein (WASp) stimulates actin nucleation by Arp2/3 complex. J Cell Biol. 2000;150(6):1311-20. PMCID: 2150692.

123. Hao JJ, Liu Y, Kruhlak M, Debell KE, Rellahan BL, Shaw S. Phospholipase C-mediated hydrolysis of PIP2 releases ERM proteins from lymphocyte membrane. J Cell Biol. 2009;184(3):451-62. PMCID: 2646552.

124. van Rheenen J, Song X, van Roosmalen W, Cammer M, Chen X, Desmarais V, et al. EGF-induced PIP2 hydrolysis releases and activates cofilin locally in carcinoma cells. J Cell Biol. 2007;179(6):1247-59. PMCID: 2140025.

125. Morford LA, Forrest K, Logan B, Overstreet LK, Goebel J, Brooks WH, et al. Calpain II colocalizes with detergent-insoluble rafts on human and Jurkat T-cells. Biochem Biophys Res Commun. 2002;295(2):540-6.

126. Stewart MP, McDowall A, Hogg N. LFA-1-mediated adhesion is regulated by cytoskeletal restraint and by a Ca2+-dependent protease, calpain. J Cell Biol. 1998;140(3):699-707. PMCID: 2140165.